ÇUKUROVA UNIVERSITY
INSTITUTE OF NATURAL AND APPLIED SCIENCES

PhD THESIS

Ertaç HÜRDOĞAN

AIR CONDITIONING WITH DESICCANT COOLING

DEPARTMENT OF MECHANICAL ENGINEERING

ADANA, 2010

ÇUKUROVA UNIVERSITY
INSTITUTE OF NATURAL AND APPLIED SCIENCES

AIR CONDITIONING WITH DESICCANT COOLING

Ertaç HÜRDOĞAN

PhD THESIS

DEPARTMENT OF MECHANICAL ENGINEERING

We certify that the thesis titled above was reviewed and approved for the award of degree of the Doctor of Philosophy by the board of jury on 01/11/2010.

……	…….	……...
Prof. Dr. Orhan BÜYÜKALACA	Prof. Dr. Tuncay YILMAZ	Prof. Dr. R. Tuğrul OĞULATA
SUPERVISOR	MEMBER	MEMBER

……	……
Prof. Dr. Kadir AYDIN	Prof. Dr. Ertuğrul BALTACIOĞLU
MEMBER	MEMBER

This PhD Thesis is written at the Department of Institute of Natural And Applied Sciences of Çukurova University.
Registration Number:

Prof. Dr. İlhami YEĞİNGİL
Director
Institute of Natural and Applied Sciences

ABSTRACT

PhD THESIS

AIR CONDITIONING WITH DESICCANT COOLING

Ertaç HÜRDOĞAN

ÇUKUROVA UNIVERSITY
INSTITUTE OF NATURAL AND APPLIED SCIENCES
DEPARTMENT OF MECHANICAL ENGINEERING

Supervisor :Prof. Dr. Orhan BÜYÜKALACA

Year: 2010, Pages: 156

Jury :Prof. Dr. Orhan BÜYÜKALACA
:Prof. Dr. Tuncay YILMAZ
:Prof. Dr. R.Tuğrul OĞULATA
:Prof. Dr. Kadir AYDIN
:Prof. Dr. Ertuğrul BALTACIOĞLU

In this study, a desiccant based air-conditioning system was designed, constructed and tested. In the system, the moisture of the fresh air was reduced passing it through a solid desiccant wheel and then its temperature was decreased by the "dry coil" of a vapor-compression cycle. To enhance the performance of the system, some technologies such as "pre-cooling with outdoor air", "waste cool recovery" and "pre-cooling of waste air with evaporative cooling" were utilized. Energy analyses of the system were performed by using the results obtained from the experiments. Design parameters and suitability of the system suggested were investigated for the health care facilities in which hygiene is crucially important.

Key Words: Air-conditioning, Dehumidification, Desiccant cooling, Hygiene

ÖZ

DOKTORA TEZİ

DESİSİF SOĞUTMA İLE İKLİMLENDİRME

Ertaç HÜRDOĞAN

ÇUKUROVA ÜNİVERSİTESİ
FEN BİLİMLERİ ENSTİTÜSÜ
MAKİNA MÜHENDİSLİĞİ ANABİLİM DALI

Danışman :Prof. Dr. Orhan BÜYÜKALACA
Yıl: 2010, Sayfa: 156
Jüri :Prof. Dr. Orhan BÜYÜKALACA
:Prof. Dr. Tuncay YILMAZ
:Prof. Dr. R.Tuğrul OĞULATA
:Prof. Dr. Kadir AYDIN
:Prof. Dr. Ertuğrul BALTACIOĞLU

Bu çalışmada, nem almalı bir iklimlendirme sistemi tasarlanıp kurulmuş ve test edilmiştir. Sistemde, iklimlendirilen mahale gönderilen taze hava, önce bir nem alıcı üzerinden geçirilerek nemi düşürülmekte ve daha sonra buhar sıkıştırmalı bir soğutma çevrimiyle soğutulan suyun kullanıldığı "kuru serpantin" üzerinden geçirilerek sıcaklığı düşürülmektedir. Sistemin performansını artırmak için, dış havayla ön soğutma, atık soğu geri kazanımı ve atık havanın buharlaştırmalı soğutma ile soğutulması gibi teknolojiler kullanılmaktadır. Yapılan deneylerden elde edilen sonuçlar kullanılarak sistemin enerji analizleri yapılmıştır. Ayrıca bu tür sistemlerin hastaneler gibi hijyenin önemli olduğu uygulamalar için yapılabilirliği, uygunluğu ve tasarım parametreleri araştırılmıştır.

Anahtar Kelimeler: İklimlendirme, Nem alma, Desisif soğutma, Hijyen

ACKNOWLEDGEMENTS

I am truly grateful to my research supervisor, Prof. Dr. Orhan BÜYÜKALACA, for his invaluable guidance and support throughout the preparation of this thesis and during my graduate education.

Thanks are extended to Prof. Dr. Tuncay YILMAZ for providing valuable research advice, continuous support, his understanding and motivation during my thesis.

I wish to express my gratitude to The State Meteorological Affairs General Directorate (DMİ) for providing meteorological data.

I also would like to thank The Scientific and Technological Research Council of Turkey (TÜBİTAK) for providing scholarship during my thesis studies.

I would like to express my special thanks to Advisory Committee Members, Prof. Dr. Tuğrul OĞULATA, Prof. Dr. Kadir AYDIN, Prof. Dr. Arif HEPBAŞLI Prof. Dr. Ertuğrul BALTACIOĞLU and Assoc. Prof. Dr. Hüseyin AKILLI, for their devotion of invaluable time throughout my research activities.

I would like to thank to all my research assistant friends especially Arif ÖZBEK, Ahmet FERTELLİ, İrfan UÇKAN at our Mechanical Engineering Department for their continuous support and motivation.

Another point that should be emphasized here is the continuous moral support, motivation, encouragement and patience of my wife Neslihan HÜRDOĞAN, my lovely daughter Yağmur HÜRDOĞAN, my father Mustafa HÜRDOĞAN and my mother Suzan HÜRDOĞAN throughout my scientific efforts.

TABLE OF CONTENTS **PAGE**

LIST OF TABLES **PAGE**

LIST OF FIGURES **PAGE**

NOMENCLATURE

c_p	: Specific heat (kJ/kg K)
$\dot{C}$	: Capacitance rate (kW/K)
COP	: Coefficient of performance
COP_e	: Coefficient of performance obtained from experiments
COP_m	: Coefficient of performance obtained from solar energy model
CR	: Compensation ratio
$\dot{E}_{tot}$	: Total energy input (kW)
F	: Surface area of collector (m^2)
F_d	: The ratio of additional dry bulb temperature increase to total dry bulb temperature increase (^oC)
F_r	: The ratio of additional dry bulb temperature decrease to total dry bulb temperature decrease (^oC)
h	: Enthalpy (kJ/kg)
h_g	: Specific enthalpy of the saturated water vapor (kJ/kg)
$\dot{m}$	: Mass flow rate (kg/s)
$\dot{q}$	: Total solar radiation (W/m^2)
$\dot{q}_t$	: Solar radiation on the inclined surface (W/m^2)
$\dot{Q}$	: Actual heat transfer rate (kW)
$\dot{Q}_{col}$	: The amount of heat transferred from collectors (kW)
$\dot{Q}_{CC}$	: Cooling capacity (kW)
$\dot{Q}_g$	: Heat gain from the fan motor (kW)
$\dot{Q}_l$	: Latent cooling load of air-conditioned room (kW)
$\dot{Q}_{max}$	: Maximum possible heat transfer rate (kW)
$\dot{Q}_{reg}$	: Energy consumption of regeneration heat (kW)
$\dot{Q}_{reg,solar}$	: Thermal energy transferred due to solar energy (kW)
$\dot{Q}_s$	: Sensible cooling load of air-conditioned room (kW)

$\dot{Q}_{tot}$: Total cooling load of air-conditioned room (kW)

SHR : Sensible heat ratio

T : Temperature (^{o}C)

V : Volt (V)

$\dot{V}$: Volumetric flow rate (m^3/h)

W : Humidity ratio (kg/kg air)

$\dot{W}$: Power consumption (kW)

ΔP : Differential pressure (Pa)

ΔW : Moisture removal (kg/kg air)

Greek Letter

η : Effectiveness

φ : Relative humidity

θ : Title angle

Subscripts

1, 2,…,17 : States described in Fig.1

a : Ambient

c : Cold air

C : Collector

com : Compressor

da : Daily average

dt : Daily total

EC : Evaporative cooler

en : Entrance

eh : Electric heaters

ex : Exit

fan : Fans

f : Fresh air

h : Hot air

HE	: Heat exchanger
i	: Inlet
min	: Minimum
o	: Outlet
oth	: Other electrical components
r	: Regeneration air
rm	: Air-conditioned room
w	: Water
wb	: Wet bulb
ws	: Waste air

1. INTRODUCTION

Rapid changes have been observed in air-conditioning technology in recent years. There are many reasons for this. Increased importance of energy due to rapid depletion of fossil resources and increasing energy demands are the main reasons. Another factor originated from the understanding of the harmful effect of Chlorofluorocarbons (CFCs) used in air-conditioning systems on the ozone layer. This led to utilizing in the existing systems some alternative refrigerants that are harmless to the ozone layer or at least less harmful than existing CFCs or application of alternative air-conditioning technologies that do not utilize refrigerants harmful to ozone layer. Some of the alternative technologies are not new. They have been known for many years, but not used widely today. Realizing the fact that air-conditioning is not a luxury, it is a necessity for comfort and as well as for manufacturing has brought more strict indoor air quality conditions in recent years. This also affected the air-conditioning technologies.

One of the alternative systems that is brought to agenda is the desiccant air-conditioning systems. In these systems, a desiccant removes moisture from the fresh air, which releases heat and increases the air temperature. The dry air is then cooled using either evaporative cooling or the cooling coils of a conventional vapor-compression refrigeration cycle. The adsorbed moisture in the desiccant is then removed (the desiccant is regenerated to its original dry state) using a secondary warm air flow.

Since the infections spread through the air depend on humidity in some medical institutions like hospitals, humidity control is very important (Arundel et al., 1986). In conventional systems commonly used for air conditioning, the air sent to the place being conditioned comes through coils, cooled by a cooling unit – generally by a vapor compressing cycle. While coming through coils, both the heat (sensible heat) and the humidity (latent heat) of air are reduced. Removing humid from the air is realized by the condensation of the water steam in the air, which meets cold coil. This process creates a suitable atmosphere in the air sent to the place, for reproduction of bacteries that can cause infections.

Desiccant based air-conditioning systems are a suitable way to improve indoor air quality due to its superior humidity control. These systems are viable alternatives for air-conditioning in health care facilities to reduce the airborne disease transmission. The substances used in desiccant air-conditioning systems (desiccants) for removing humidity, removes the bacteries (Escherichia coli, Enterococcus, Pseudomonas aeruginosa, Staphylococcus aureus, Coagulase negative Staphylococcus (epidermidis), Mycobacterium fortuitum, Candida albicans) that can cause illnesses and various infections in the air sent to the place being air conditioned about 35-70% (Kovak et al., 1997). However, the mechanism removing bacteries have not actually been made totally clear.

Most common illnesses spread through air are tuberculosis, splenic fever and legionnaires' disease (ORNL, 2000). At the present time, intensive studies are being carried out in order to find out the sources of infections seen in hospitals and take necessary precautions. The observation frequency of hospital infections are being declared as 8.4% and according to a research made in the United States of America, hospital infections comes fourth as a death cause after heart diseases, cancer and cerebral hemorrhage (Tr.Net Website, 2005). Hospital infections are also a serious problem in Turkey. In recent years, some baby deaths and fatal infections after operations have been reported in some health facilities. Another problem is the amount of time patients stay at the hospitals. The stay time is much longer in Turkey than in developed countries.

Studies carried out in Turkey concluded that, hospital infections increase the amount of time patients stay at the hospitals about 2 weeks and cause approximately 1500 $ extra cost per patient (Turkish Infection Website, 2005). The average amount of time a patient stays in hospital after operation is 2 days in the USA, 3 days in EU countries, and about 13-14 days in Turkey (MMO, 2003). That's why the time of using antibiotics in Turkey is 7 times more than EU countries, and 8 times more than the USA. One of the causes of these incidents is the bacteria spread through air. In order to make such infection problems spread through air minimum, desiccant systems are suggested to be used at hospital operations (ORNL, 2000).

The main reason for choosing desiccant air conditioning systems in hospital

operations is not lowering the first investment cost of air conditioning system or saving up energy, but bringing the quality to hygiene and inside air, which is very important for health and economy. However if a cheap energy source (solar energy, waste heat, etc.) is used, energy consumption of desiccant systems can be less than that of conventional systems.

Although desiccant air conditioning systems have started to become widespread in Europe and the USA in recent years, they are not known exactly in Turkey and there are not many application of it.

In this study, a desiccant based air-conditioning system was designed, constructed and tested. The moisture of the fresh air was reduced passing it through a solid desiccant wheel and then its temperature decreased by the “dry coil” of a vapor-compression cycle. To enhance the performance of the system, some technologies such as “pre-cooling with outdoor air”, “waste cool recovery” and “pre-cooling of waste air with evaporative cooling” were utilized. Design parameters and suitability of the system suggested was investigated for the health care facilities in which hygiene is crucially important. It was aimed to increase the use of desiccant systems in Turkey in which this type of systems never used and not well known.

2. LITERATURE REVIEW

Desiccant cooling technology is rapidly becoming established technology in most parts of the world. This growth has been brought about by the contribution of refrigerants used in conventional cooling systems to the depletion of the ozone layer. Also, the contribution towards global warming of refrigerants and fossil fuels used to generate electricity to power the refrigeration systems is very significant. Therefore, many researches have been carried out on desiccant cooling technology. Some selected studies are given below.

Jain et al. (1995) investigated different solid desiccant cycles (the ventilation cycle, the recirculation cycle, the wet surface heat exchangers cycle (WSHE) and the Dunkle cycle) for various outdoor conditions (dry-bulb temperature and wet-bulb temperature) of many cities in India. The study was aimed at evaluating the influence of the effectiveness of heat exchangers and evaporative coolers on the cooling coefficient of performance (COP) as well as on the air volumetric circulation rate in different climatic conditions. The authors found that the cycle using wet surface heat exchangers give higher performance (COP) than other cycles. It was also found that high heat exchanger effectiveness values (greater than 0.8) are desirable for better performance of the cycles not using WSHE.

Kovak and Heimann (1997) investigated desiccant-based air conditioning (DBAC) systems to determine their sanitizing effects on airborne microorganisms. Their study focused on the use of desiccant-based cooling as a mechanism to control bioaerosols. As noted by Hines et al. (1992), desiccant systems can enhance the quality of indoor air and reduce the level of microorganisms. Their study was designed to examine this theory in both field and laboratory conditions. The study consisted of two parts; to determine if bioaerosols are being reduced through field-operating DBAC systems and whether specific infectious microorganisms were being reduced through the system. Three separate field and laboratory investigations were performed on the DBAC systems during this study. They showed that the DBAC system reduced airborne levels of bacteria and fungi in nearly every test (% 93). Their study demonstrated that desiccant based cooling technology may be useful

in reducing airborne microbial contamination and should be considered for use in hospitals, health care, and clean room environment where airborne microorganisms are a significant problem.

Oliviera et al. (2000) modeled a new air-conditioning system using a liquid desiccant and needle impeller rotors. Experimental data obtained for different components, i.e., evaporators, absorber, were used in the model. System performance was quantified through the definition of thermal coefficient of performance. Simulation results showed the effect of different system parameters: ambient temperature, ambient humidity and heat exchanger efficiency. By performing several simulations for an open cycle (without air recirculation), it was found that system performance is very sensitive to changes in both indoor and outdoor conditions.

Joudi and Dhaidan (2001) evaluated the performance of solar assisted heating and desiccant cooling systems for a domestic two story residence located in Baghdad. They developed a computer simulation to assess the effects of various designs and operation conditions on the performance of the system and its components. The authors showed that the performance of the desiccant cooling system is greatly influenced by the effectiveness of the heat exchangers, evaporative cooler and also by the regeneration temperature, while the effect of dehumidifier performance is relatively small.

Dai et al. (2002) presented a comparative study of a standalone vapor compression system (VCS), the desiccant-associated VCS, and the desiccant and evaporative cooling associated VCS. The authors found that the desiccant-associated VCS have more cooling production than the VCS alone by 20–30%. It was also found that the electric power consumption and size of vapor compression system can be further reduced.

Halliday et al. (2002) investigated the potential in the UK for exploiting solar energy to drive desiccant cooling systems. The parametric energy studies were carried out using a solar desiccant computer model developed at the University of Leeds. They reported that it is feasible to use solar energy to power desiccant cooling systems within the UK.

Dai et al. (2002) investigated numerically a hybrid solar powered solid adsorption–desiccant cooling system with a 20 m^2 solar collection area for cooling grain. It was indicated that this kind of hybrid solar cooling system used for grain storage is acceptable from both technology and economic operation viewpoints. They also found that the COP of the system increases with an increase in ambient temperature and humidity has a linear relationship with the effectiveness of evaporative cooling, that is, the greater the effectiveness of the evaporative cooling, the better the system performance will be.

Cejudo et al. (2002) presented two methodologies for modeling a solid desiccant wheel: physical and neural network models. Experimental values are used to validate the physical model and to calculate the parameters of the neural network model. An important conclusion of this work was that special attention must be paid when calculating moisture content from measured values of dry bulb temperature and relative humidity.

Zhang and Niu (2003) proposed a novel desiccant cooling system, a pre-cooling Munters environmental control (PMEC) cycle in combination with chilled-ceiling panels. They provided a mathematical model of the system and used to predict the system performance under South-east China weather conditions using hour-by-hour calculations. Their result indicated that chilled-ceiling combined with desiccant cooling could save up to 40% of primary energy consumption, in comparison with a conventional constant volume all-air system.

Camargo et al. (2003) presented a thermoeconomic analysis method based on the first and second law of thermodynamics and applied to an evaporative cooling system coupled to an adsorption dehumidifier. The main objective is the use of a method called exergetic manufacturing cost (EMC) applied to a system that operates in three different conditions to minimize the operation costs. Basic parameters are the R/P ratio (reactivation air/process air) and the reactivation air temperature. They showed that the minimum reactivation temperature and the minimum R/P ratio corresponds to the smaller EMC. This result can be corroborated through an energetic analysis. It was noted that this case is also the one corresponding to smaller energy loss.

Zhang et al. (2003) presented a theoretical model to predict the heat and mass transfer process of the desiccant wheel. The mathematical model was validated using a real desiccant wheel, and the calculation results were in reasonable agreement with the experimental data. The model was expected for assisting of designing desiccant wheel more easily and expediently. They analyzed the temperature and humidity profiles in the wheel during both the dehumidification and the regeneration processes. It was showed that there exists a hump curve, which indicates the variation in the maximum humidity ratio, regarding air humidity ratio along the air channel in the regeneration process. The hump curve can play an important role for improving the studied desiccant wheel. The effects of velocity of regeneration air, inlet temperature of regeneration air and velocity of process air on the hump moving speed are also investigated. They found that the desiccant wheel can have a high effectiveness of dehumidification if the regeneration temperature and the regeneration air velocity are also high.

Subramanyam et al. (2004) studied a desiccant wheel integrated air-conditioner for low humidity air-conditioning to evaluate its performance and compare with those of conventional and reheat systems. They showed that the proposed system can deliver supply air at much lower dew point temperature compared to the conventional system with a marginal penalty on COP. It was also showed that system performance is better than the typical reheat system to provide the same low humidify levels.

Kanoğlu et al. (2004) developed a procedure for the energy and exergy analyses of open-cycle desiccant cooling systems and it was applied to an experimental unit operating in ventilation mode with natural zeolite as the desiccant. They presented energy-based performance parameters such as the coefficient of performance (COP) of the unit and the effectiveness of system components. Exergy destruction and exergy efficiency relations for the system and its components as well as the reversible COP of the system were derived. The energy and exergy formulations were applied to the experimental unit using the data collected during a typical operation of the unit. The unit has a COP of 0.35, a reverseble COP of 3.11, and an exergy efficiency of 11.1%. Desiccant wheel has the greatest percentage of

total exergy destruction with 33.8% followed by the heating system with 31.2%. Rotary regenerator and evaporative coolers account for the remaining exergy destructions. They showed that an exergy analysis can provide useful information with respect to the theoretical upper limit of the system performance, which cannot be obtained from an energy analysis alone.

Daou et al. (2004) recalled the principles underlying the operation of desiccant cooling systems and discussed their actual technological applications. Through a literature review, the feasibility of the desiccant cooling in different climates was proven and the advantages it can offer in terms energy and cost savings were underscored. Some commented examples were presented to illustrate how the desiccant cooling can be a perfective supplement to other cooling systems such as traditional vapour compression air conditioning system, the evaporative cooling, and the chilled-ceiling radiant cooling. They showed that the desiccant materials, when associated with evaporative cooling or chilled-ceiling radiant cooling, can render them applicable under a diversity of climatic conditions.

Subramanyam et al. (2004) studied the effects of design variables of a desiccant based air-conditioner, namely supply airflow rate, compressor pumping capacity (compressor speed) and desiccant wheel speed on its performance. They found that an optimum wheel speed of about 17.5 rph exists at which both moisture removal capacity and COP are maximum.

Ando et al. (2005) proposed and investigated experimentally 4-rotor desiccant cooling process equipped with a double stage dehumidification. Their experimental results showed that the amount of dehumidified water at the process without water spray evaporative cooler was actually larger than that of process with water spray evaporative cooler. This behavior was due to increase of humidity or relative humidity in the regeneration air as expected. However, temperature of supply air produced by the process with evaporator was rather lower than that of the other, resulting higher COP value. It was concluded that the evaporative cooler effectively worked at higher regeneration temperature and lower ambient humidity.

Çarpınlıoğlu and Yıldırım (2005) presented an approach utilized for the performance evaluation of a constructed desiccant cooling system (Yıldırım, 2002)

throughout the description of the conducted experimental study and the methodology followed. The analysis of the experimental data was directed to determine the functional relationships between system performance parameters (coefficient of performance (COP), cooling capacity (CC)) and the operation parameters (the rotational speeds of rotary regenerator and desiccant wheel, air mass flow rate in process and regeneration lines, and the regeneration temperature). The correlations of COP–CC were found a major function of mass flow rate of air almost independent of other operation parameters in their covered ranges. However the suggested approach needs verification with further experimental data out of the covered ranges of the operation parameters, together with the varied physical system constraints.

Camargo et al. (2005) presented an air conditioning system that couples a desiccant dehumidification equipment to indirect and direct evaporative coolers. They analyzed some operation parameters such as: reactivation temperature, R/P relationship (reactivation air flow/ process air flow) and the thermodynamic conditions of the entering air flow. They also presented an application of the system in different climate characteristics of several tropical and equatorial cities. An analysis of the results showed that the lesser R/P relationship and lesser reactivation temperature take to the best operation point. The analyses of the supply air condition showed that the system is able to provide human thermal comfort in humid climates, and it can be an alternative for the conventional air conditioning systems.

Zhang et al. (2006) compared silica gel (SG), calcium chloride (CaCl2) and composite desiccant (SG–CaCl2) applied to a corrugated paper (CP) based desiccant rotary wheel for their abilities to remove moisture from wet air. Their experimental data showed that the CP–SG–CaCl2 material could attain equilibrium much faster than the other samples and its hygroscopic capacity is much higher than that of CP–SG.

Elsayed et al. (2006) presented a theoretical investigation on the performance of air cycle refrigerator driving air conditioning system integrated desiccant system. They showed that the system performance is better than the conventional vapor compression air conditioning system with reheating coil. They also reported that the system has a potential to become a good alternative for the conventional vapor

compression air conditioning system with low environmental load, especially for applications need high outdoor air ratio and a precise control of indoor humidity.

Nia et al. (2006) performed a simulation of the combined heat and mass transfer processes that occur in a solid desiccant wheel using MATLAB and predicted the temperature and humidity states of the outlet air from a desiccant wheel and the optimum speed of the desiccant wheel at different conditions. The model was validated through comparison the simulated results with the published actual values of an experimental work. Their method is useful to study and modeling of solid desiccant dehumidification and cooling system. The authors found the maximum difference between the results from the proposed correlations and simulation results is ±2%, provided that the limited range of the variables are considered.

Jia et al. (2007) investigated a high performance rotary solid desiccant cooling system using a novel compound desiccant wheel. The unique feature of the desiccant wheel was that it can work well under a lower regeneration temperature and have a higher dehumidification capacity due to the contribution of the new compound desiccant materials. Their experimental results indicated that the new desiccant wheel under practical operation can remove more moisture from the process air by about 20-40% over the desiccant wheel employing regular silica gel and the new composite desiccant is more hygroscopic and more easily regenerated. Their simulation results also showed that the dehumidification coefficient of performance (COP) for the new wheel is greatly better than the conventional one. The system COP may reach 1.28, about 35% higher over the system using silica gel.

Hirunlabh et al. (2007) investigated the performance and energy saving of the desiccant air-conditioning system in Thailand. They showed that desiccant air-conditioning is only viable for large cooling capacities and central air-conditioned buildings.

Kabeel (2007) investigated the performance of a solar powered desiccant air conditioning system using a rotary honeycomb wheel, which is utilized for the regeneration and absorption processes, at different conditions of inlet air and radiation intensity. The researcher showed that the system was highly effective in the regeneration process for all flow rates compared with the absorption process.

Elsayed et al. (2008) analyzed theoretically the performance of air cycle refrigerator driving desiccant air conditioning system used to cool and dehumidify warehouse. Simulation analysis was carried out to calculate the system coefficient of performance (COP), cooling effects and the humidity change under different conditions. From the simulation result it was found that, the desiccant system has the ability to supply air to the dock area at very low humidity (less than 0.4 g/kg). The COP of system increases due to the exhaust heat recovery, and this enhancement can be more than 100%. COP of the system also depends on the rotating speed of the rotor, air velocity and rotor length. They showed that COP of the proposed system is greater than that of a conventional system under the same operating conditions.

Ge et al. (2008) investigated experimentally a one-rotor two-stage rotary desiccant cooling system (OTSDC), in which two-stage dehumidification process is realized by one desiccant wheel. Their system was proposed to reduce the volume of two-stage rotary desiccant cooling system (TSDC) with two desiccant wheels without reduction in system performance by using the novel configuration. They showed that realization of two-stage dehumidification process by one rotary wheel is feasible and compared to the performance of one-stage desiccant wheel cooling system (OSDC) and TSDC, the investigated OTSDC inherits the merits of two-stage dehumidification system: low regeneration temperature and high COP.

Khalid et al. (2009) presented the results of experimental and simulation study of a solar assisted pre-cooled hybrid desiccant cooling (PHDCS) system for air conditioning applications in Pakistan. They simulated this system on TRNSYS simulation program. Simulation case studies showed that system can achieve significant energy saving as compared to reheat vapor compression air condition system.

Ge et al. (2009) studied the performance of a desiccant cooling system with double stage dehumidification. They reported that the required regeneration temperature of the system is lower and coefficient of performance is higher than single stage desiccant cooling system.

Enteria et al. (2009) presented a new desiccant cooling system employing double cross-flow heat exchangers to increase the dehumidification performance at

lower thermal energy requirement and to maintain the supply air humidity content at the same level as that of the processed air. The new desiccant cooling cycle presented in the study showed the constant humidity content of the supply air in contrast when direct evaporative cooler is used as presented by Kodama et al. (2005), Carpinlioglu and Yıldırım (2005), Ando et al. (2005), Henning et al. (2007).

La et al. (2010) carried out a review study that presents and analyzes the status of rotary desiccant dehumidification and air conditioning in the following three aspects: the development of advanced desiccant materials, the optimization of system configuration and the utilization of solar energy and other low grade heat sources, such as solar energy, district heating, waste heat and bioenergy. Some key problems to further push forward the research and development of this technology were also summarized.

Panaras et al. (2010) developed a model for a desiccant air-conditioning system and experimentally validated on an actual installation. The model is rather simple and easy to implement and it is based on the description of the operation of the main subsystems of such an installation through specific efficiency factors. Analysis indicated that there is a specific regeneration temperature limit beyond which the system cannot satisfy the imposed cooling load, as the system capacity exceeds the load requirements.

Ge et al. (2010) evaluated the performances of a solar driven two-stage rotary desiccant cooling system and a conventional vapor compression system in two cities with different climates: Berlin and Shanghai. The objectives of their study are to compare the thermodynamic and economic performance of the two systems and to obtain useful data for practical application. Their results show that the desiccant cooling system is able to meet the cooling demand and provide comfortable supply air in both of the two regions. The required regeneration temperatures are 55 ^{o}C in Berlin and 85 ^{o}C in Shanghai. As compared to the vapor compression system, the desiccant cooling system has better supply air quality and consumes less electricity. The results of the economic analysis demonstrate that the dynamic investment payback periods are 4.7 years in Berlin and 7.2 years in Shanghai.

The literature search showed that different types of rotary desiccant cooling systems were studied both analytically and experimentally by several researchers. It was also seen that desiccant based air-conditioning systems are a suitable way to improve indoor air quality due to its superior humidity control and these systems are cost effective systems when a cheap heat source is used to regenerate the desiccant. In this study, a novel desiccant based air conditioning system was designed and tested experimentally to improve the indoor air quality and reduce energy consumption. In the system studied, a heat exchanger, which is not used in this type of systems, for pre-heating the regeneration air with exhaust air was used.

3. MATERIAL AND METHOD

3.1. Desiccant Air Conditioning Systems

Air conditioning is usually carried out using vapor compression systems. However, increased global warming and the environmental impact of chlorofluorocarbons (CFCs) and other similar refrigerants on the ozone layer, have stimulated interest in the development of "environmentally-friendly" air conditioning systems such as desiccant air conditioning (cooling) systems (Oliviera et al., 2000).

Desiccant cooling technology provides a tool for controlling humidity (moisture) levels for conditioned air spaces (DCTRG, 2000). Desiccant materials are those that attract moisture due to differences in vapor pressure. Most people are familiar with desiccants such as silica gel packages that are included with new electronics or textile products. Desiccants can be in the form of a solid or a liquid. These desiccants have been selected based on their ability to hold large quantities of water, their ability to be reactivated, and cost. In order to be effective, the desiccant must be capable of addressing the latent cooling load in a continuous process. In order to accomplish this, commercial desiccant systems consist of a process air path and a regeneration air path. The desiccant that is in the process air path has been prepared to have a lower vapor pressure than the air passing over it. Thus, the moisture in the air is transferred onto the desiccant material. As the desiccant vapor pressure increases due to the presence of the moisture that it has attracted, the desiccant material is transferred to a regeneration process. In the regeneration process, hot air is passed over the desiccant. The vapor pressure of the hot air is lower than the desiccant surface which forces the moisture to transfer from the desiccant surface into the hot air stream. The moist hot air is then exhausted from the system into the outdoor air. The desiccant material that has had the trapped moisture removed is now prepared to attract moisture as it is transferred back into the process air path. The dry process air leaving the desiccant is then passed over a conventional cooling coil which addresses the sensible cooling work required to meet the air specification of the conditioned space.

Desiccant technologies should be considered when:

- Moisture levels are high
  - Latent/total cooling load ratio is > 30%
  - High levels of outdoor air make-up required in building
  - High building occupancy
- Potential costs savings are significant
  - High electrical demand charges
  - Low natural gas rates
  - Low cost heat source available
  - Heat recovery options available
- Tight control over moisture levels is required
  - Hospital operating rooms
  - Avionics repair laboratories
  - Museums
  - Munitions storage
- Moisture is problematic to interior spaces such as:
  - Ice Arenas (fogging)
  - Hospitals (bacteria)
  - Hotels/Apartments (moisture damage)
  - Food Stores (freezer case moisture)
- Occupant comfort cannot be compromised (DCTRG, 2000).

3.2. Types of Desiccant Cooling Systems

The design and operation of a desiccant system are based on the desiccant material used to accomplish the dehumidification. Desiccant materials attract moisture through the process of either adsorption or absorption. Adsorption is the process of trapping moisture within the desiccant material similar to the way a sponge holds water through capillaries. Most adsorbents are solid materials. Absorption is the process of trapping moisture through a chemical process in which

the desiccant undergoes a chemical change. Most absorbents are liquids. Types of materials used as a basis for desiccant systems include the following materials:

- Silica Gel
- Lithium Chloride (Liquid or Dry)
- Lithium Bromide
- Activated Alumina
- Titanium Silicate
- Molecular Sieve

Commercially available desiccant systems are based on five configurations or technologies.

- Liquid Spray Towers
- Solid Packed Tower
- Rotating Horizontal Bed
- Multiple Vertical Bed
- Rotating Desiccant Wheel

3.3. Advantages of Desiccant Cooling Systems

Desiccant cooling systems have started to become widespread because of their ability to remove moisture from outdoor ventilation air while allowing conventional air-conditioning systems to deal primarily with control temperature (sensible cooling loads). Desiccant cooling is a new approach to space conditioning that offers solutions for many of the current economic, environmental, and regulatory issues being faced by facility managers. Indoor air quality is improved through higher ventilation rates, and achieving those fresh air make-up rates becomes more feasible with desiccant systems. At “low load conditions” outdoor air used for ventilation and re-circulated air from the building have to be dehumidified more than

they have to be cooled. Properly integrated desiccant cooling systems have become cost-effective additions to many building HVAC systems because of:

- The lower cost of dehumidification when low-sensible load, high-latent load conditions are met.
- The promotion of gas cooling for summer air-conditioning by utilities in the form of preferential gas cooling rates.
- High electric utility demand charges, which encourage a shift away from conventional, electrically driven air-conditioning (which requires a heavy daytime loading). Better control of humidity prevents moisture, mildew, and rot damage to building materials. Desiccant dehumidification is particularly attractive in applications where building exhaust air is readily available for an energy-recovery ventilator (ERV, or “passive” desiccant system) or where a source of waste heat from other building operations is available to regenerate an “active” desiccant system.
- Desiccant systems offer significant potential for energy savings and reduced consumption of fossil fuels. The electrical energy consumption is small, and the source of thermal energy can be diverse (i.e., solar, waste heat, natural gas).
- With desiccant systems the use of CFCs is eliminated (if used in conjunction with evaporative coolers) or reduced (if integrated with vapor compression units). CFCs contribute to depletion of the earth's ozone layer and some of them have already been banned completely, and some will be banned in coming years.
- Indoor air quality is improved because of higher ventilation and fresh air rates associated with desiccant systems. Such systems also offer lower humidity levels and the capability to remove airborne pollutants.
- With desiccant systems, air humidity and temperature are controlled separately, enabling better control of humidity (Pesaran et al., 1992).

3.4. Desiccant Cooling Applications

Desiccants can dry either liquids or gases, including ambient air, and are used in many air-conditioning applications, particularly when the

- Latent load is large in comparison to the sensible load. For example; air conditioning systems for supermarkets have a very low heat load since the display cases also cool the store. The remaining load is mostly moisture.
- Energy cost to regenerate the desiccant is low compared to the cost of energy to dehumidify the air by chilling it below its dew point and reheating it.
- Moisture control level for the space would require chilling the air to subfreezing dew points if compression refrigeration alone were used to dehumidify the air.
- Temperature control level for the space or process requires continuous delivery of air at subfreezing temperatures.
- Thermal energy is available and inexpensive, or when electrical energy is limited or costly. For example, use desiccant systems where electrical demand is high and available capacity is low, or where waste heat is available.
- Low humidity control levels are advantageous. For example, steel warehouses can be dehumidified rather than heated during the winter, saving energy and avoiding rust, but the dehumidification system must be operate at a low temperature and a low humidity control level.
- An air conditioning system must operate without high relative humidity in duct work and without condensed water in drain pans. For example, air distribution systems in buildings can harbor fungi, which create indoor air quality problems. Desiccant systems keep the air dry in the ductwork, preventing microbial growth.
- Desiccants can attract and hold more than simply water vapor; they can remove contaminants from airstreams to improve indoor air quality.

Desiccants have been used to remove organic vapors and, in special circumstances, to control microbiological contaminants. Hines et al. (1992) also confirmed their usefulness in removing vapors that can degrade indoor air quality. Desiccant materials can adsorb hydrocarbon vapors while they are collecting moisture from air. These sorption phenomena show promise of improving indoor air quality in typical building HVAC systems.

- Desiccants are also used in drying compressed air to low dew points. In this application, moisture can be removed from the desiccant without heat. De-sorption is accomplished using differences in vapor pressures compared to the total pressures of the compressed and ambient pressure airstreams.
- Finally, desiccants are used to dry the refrigerant circulating in air-conditioning and refrigeration systems. This reduces corrosion in refrigerant piping and prevents valves and capillaries from becoming clogged with ice crystals. In this application, the desiccant is not regenerated; it is discarded when it has adsorbed its limit of water vapor.

3.5. Description of Desiccant Cooling System Studied

Figure 3.1 shows the desiccant based air-conditioning system, which was designed and constructed in the Laboratory of Mechanical Engineering Department of Çukurova University. Since the system was considered for the health care facilities, 100 % fresh air was used. In the system, three separate air channels are used for fresh, waste and regeneration air streams. Fresh air channel was used to supply fresh air to the air-conditioned room. The waste air sucked from the air-conditioned room was sent to outside via waste air channel. Regeneration air channel was used to remove moisture of desiccant wheel. Various components (dehumidifier, heat exchangers, fans, heaters, temperature and relative humidity sensors) were located into these channels to control and adjust the conditions of the air streams.

Humidity of the fresh outside air (state 1) is absorbed by the desiccant material of the wheel. The fresh air leaves the process side of the desiccant wheel (state 2) hotter, and much drier than when entering the system. Sensible cooling of the fresh air is carried out (process 4-5) in a cooling coil, which is fed by chilled water from a chiller unit. However, the fresh air is passed through two recuperative type heat exchangers (heat exchangers 1 and 2) before coming to the cooling coil for cool recovery. In the recuperators, only sensible heat is removed from the fresh air, and therefore, humidity ratio of the air remains constant.

The desired blowing temperature of the fresh air (state 6) is obtained in the cooling coil. The surface temperature of the cooling coil is always kept higher than the dew point temperature of the fresh air entering into the cooling coil. Therefore, only sensible cooling is performed in the coil (dry-coil application). Moisture from the fresh air (latent cooling) is removed only in the desiccant wheel and there is no change in the humidity ratio of the fresh air after the desiccant wheel.

The air sucked from the indoor (state 7) into the waste air duct is evaporatively cooled before entering into heat exchanger 2 in order to increase the cool recovery. In heat exchanger 2, due to the heat transfer from the fresh air to the waste air, temperature of the fresh air decreases and that of the waste air increases (process 9-10). The waste air leaving the heat exchanger is rejected to the outdoors.

Hot regeneration air is used for removing moisture at the desiccant wheel. In this study, outside air is used for regeneration process. The reason of using ambient air is to eliminate the possibility of mixing of the fresh air with the waste air, which may contains harmful bacteria originating from the air-conditioned room. The regeneration air first comes to heat exchanger 1 in which heat transfer from the fresh air to the regeneration air takes place. Temperature of the regeneration air at the exit of the desiccant wheel (state 15) is generally higher than that of the regeneration air leaving heat exchanger 1 (state 12). Therefore, a rotary regenerator (heat exchanger 4) is used for heat recovery. The regeneration air leaving the desiccant wheel passes through the heat exchanger 4 (process 15-16), in which heat is transferred from the regeneration air that left the desiccant wheel (state 15) to the regeneration air left heat exchanger 1 (state 12). Although the temperature of the regeneration air is

increased in heat exchangers 1 and 4 (process 11-13), it is not high enough for dehumidification of the desiccant wheel. Therefore, temperature of the regeneration air should be increased to the desired temperature before entering into the desiccant wheel. Temperature can be increased economically, if a cheap thermal energy source such as solar energy, waste heat or geothermal energy is available. Utilization of such cheap heating energy is very important for the economic operation of desiccant systems. If these systems can be backed up by a cheap thermal energy source, operating cost can be decreased dramatically. In this study, the final temperature of the regeneration air is achieved with the help of electric heaters (process 13-14) to simulate the cheap heat source. Electric heaters are used for adjusting the limits of regeneration temperature accurately, for simplifying the system and also reducing the size of the system. The air removes the humidity of the desiccant wheel (process 14-15) and flows through heat exchanger 4 (process 15-16) before discharged to the outdoors.

Psychrometric diagram of the system considered for the design day of Adana for summer air conditioning is shown in Figure 3.2.

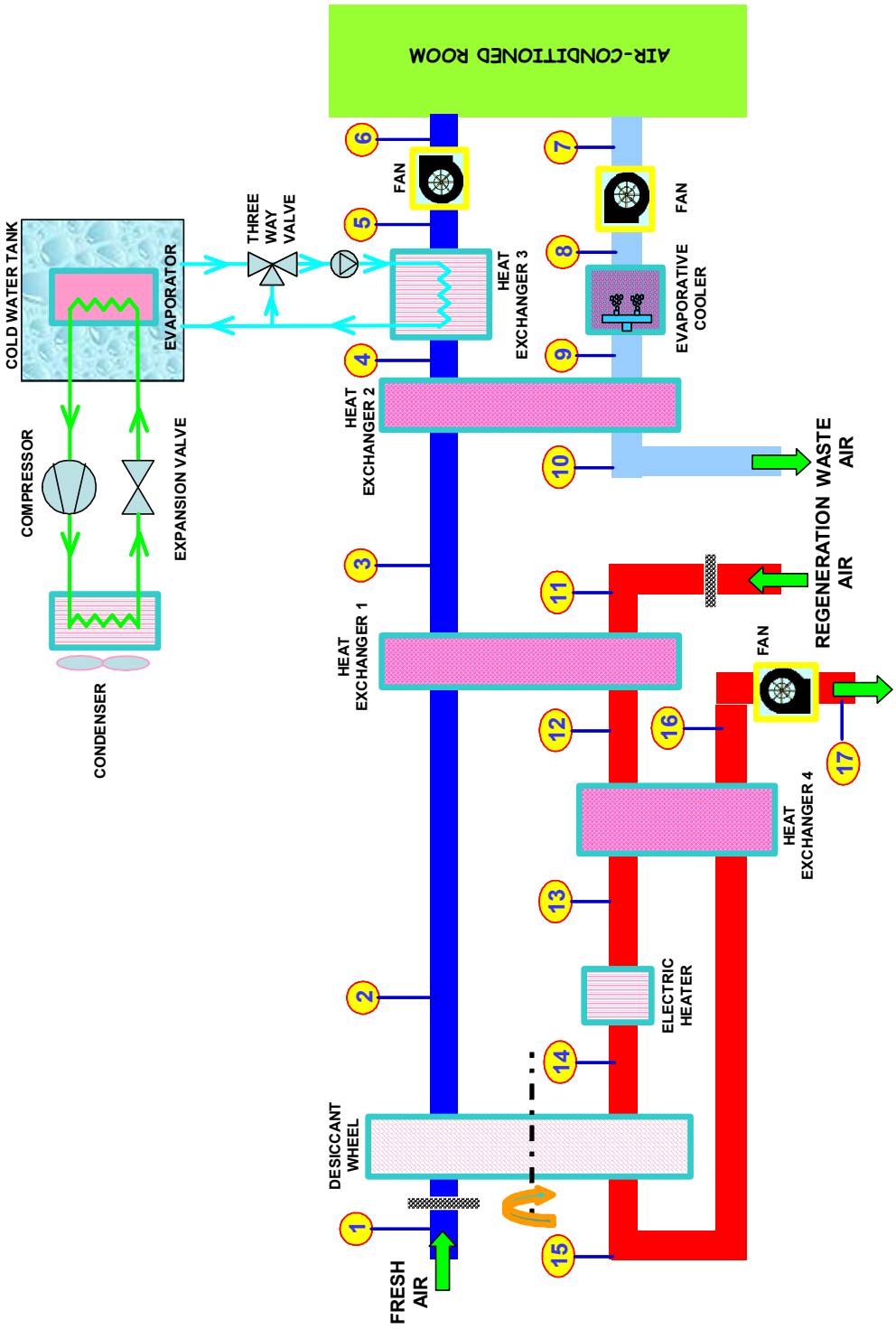

Figure 3.1. Schematic view of desiccant cooling system studied

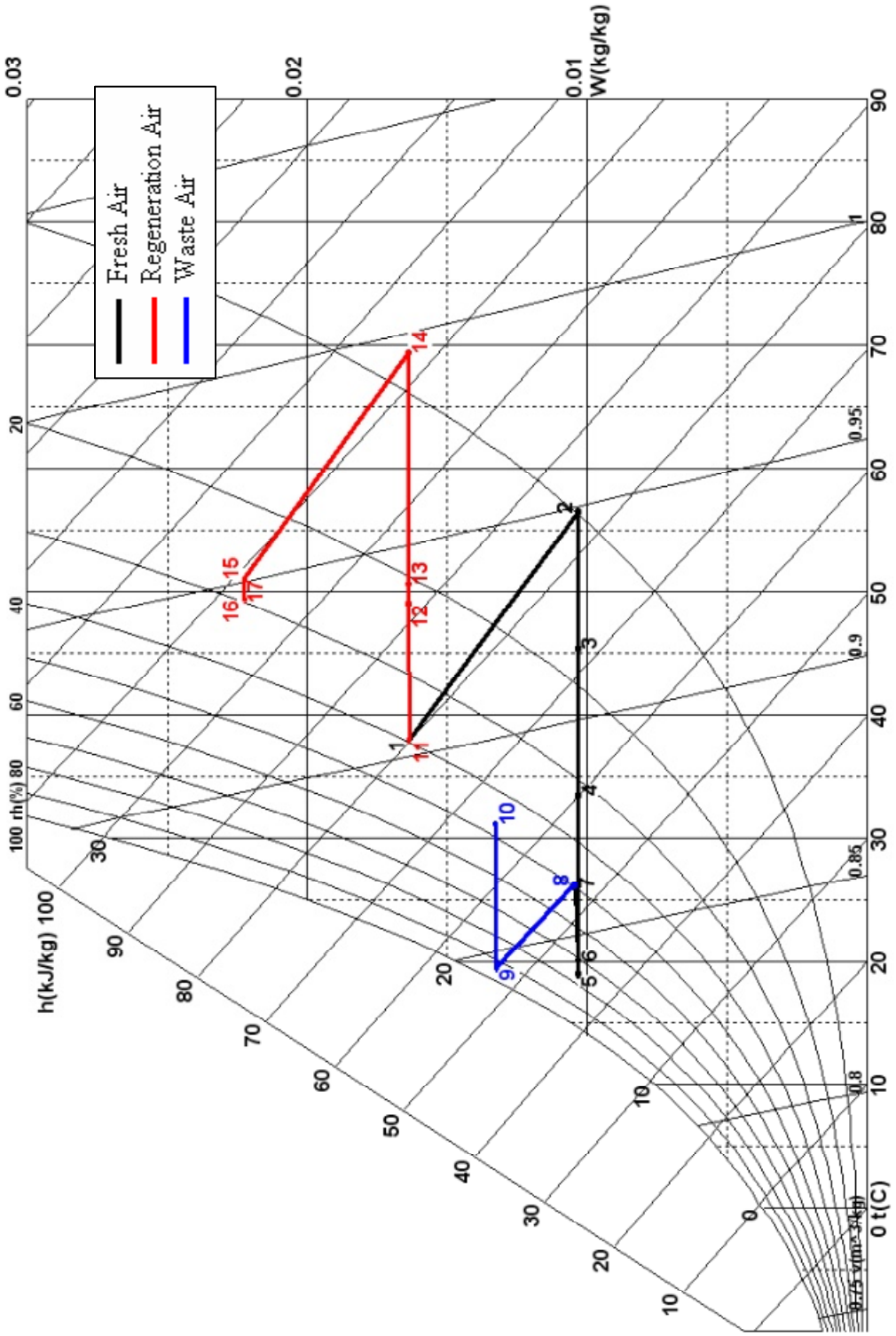

Figure 3.2. Psychrometric diagram of the system considered for the design day of Adana

3.6. Experimental Setup

3.6.1. Air Conditioned Room

In this study, a room that is located inside the Laboratory of Mechanical Engineering Department of Çukurova University was selected as the air-conditioned room. Dimensions of the room are 11.5 x 5.1 x 3.8 m. The walls of the room are not insulated. All the components such as the walls, windows, doors and roof are made of typical composite construction. Long sides of the room face to the West and the East. Only West side of the room faces to outside and other sides of the room face to the laboratory. The air conditioned room has 16.74 m^2 windows on the side.

Cooling load of the room was calculated using total equivalent temperature difference / time averaging method (TETD/TA). A MS-Excel worksheet was prepared for the calculations. Calculations were performed for 21st July, which is considered as the design day for Adana for summer air-conditioning. The outdoor design conditions for Adana are 38 ºC dry and 26 ºC wet-bulb temperature. The indoor conditions were selected as 26 ºC dry-bulb temperature and 50 % relative humidity according to ASHRAE comfort conditions (ASHRAE Fundamentals, 2001).

The results showed that the maximum cooling load of the room is 10.6 kW at 04.00 p.m. As a result of the psychrometric analysis, it was determined that the amount of fresh air which must be supplied to the room is approximately 4000 m^3/h (by considering the air requirement for hygienic applications).

3.6.2. Selection of Heat Exchangers

Desiccant wheel (rotor) is the most important component of the desiccant cooling system studied. First of all, performance data of desiccant wheel at different conditions which is given below were provided from the manufacturers.

- ✓ Different outdoor air conditions (temperature and relative humidity)

- ✓ Different regeneration air temperatures
- ✓ Different rotor diameters
- ✓ Different rotor depths
- ✓ Different rotor constructions (%75 process - %25 regeneration air flow or %50 process - %50 regeneration air flow)

Table 3.1 shows example performance data for different rotor diameters for outdoor design conditions of Adana. All of the performance data were evaluated in detail and desiccant wheel used in the study (Figure 3.3) was selected. The properties of desiccant wheel selected are given below:

- ✓ Rotor diameter : 965 mm
- ✓ Rotor depth : 200 mm
- ✓ Rotor air flow : %50 process air - %50 regeneration air
- ✓ Adsorbent : Silica gel
- ✓ Pressure drop : 290 Pa (at 4000 m^3/h)

Figure 3.3. Picture of the desiccant wheel used

Table 3.1. Some performance data of desiccant wheel at the outdoor design conditions for Adana (38 ^{o}C dry bulb temperature and 16.4 gr/kg humidity ratio)

Rotor Dia. (mm)	Rotor Entrance Condition (Process Air)		Rotor Exit Condition (Process Air)		Rotor Entrance Condition (Regeneration Air)		Rotor Exit Condition (Regeneration Air)		Pressure Drop (Pa)
	T_{db} (°C)	W (g/kg)	T_{db} (°C)	W (g/kg)	T_{db} (°C)	W (g/kg)	T_{db} (°C)	W (g/kg)	
550	38	16.4	44.8	14.2	60	16.4	53.3	18.6	963-996
			46.9	13.5	70		61.2	19.3	963-1011
			48.4	13.1	80		69.8	19.7	963-1026
			49.4	12.9	90		78.8	20.0	963-1041
			50.2	12.7	100		88.2	20.1	963-1056
770	38	16.4	47.9	13.2	60	16.4	50.2	19.6	460-475
			51.5	12.1	70		56.7	20.7	460-482
			54.3	11.3	80		63.9	21.5	460-490
			56.4	10.8	90		71.9	22.0	460-497
			58.0	10.5	100		80.4	22.3	460-504
965	38	16.4	49.6	12.6	60	16.4	48.5	20.2	287-297
			54.2	11.3	70		53.9	21.6	287-301
			58.2	10.2	80		60.0	22.6	287-306
			61.4	9.4	90		66.9	23.4	287-310
			63.9	8.9	100		74.5	23.9	287-315
1220	38	16.4	51.0	12.3	60	16.4	47.1	20.5	176-182
			56.5	10.7	70		51.7	22.1	176-185
			61.4	9.4	80		56.8	23.4	176-188
			65.8	8.3	90		62.4	24.5	176-191
			69.7	7.5	100		68.7	25.3	176-194

For the selection of recuperative type heat exchangers (heat exchanger 1 and 2) which is used in desiccant cooling system, air properties at the inlet of heat exchangers for the outdoor design conditions were calculated using a computer program written (explain in Section 3.8). Performance data for different heat exchanger dimensions and plate spacings were obtained from the manufacturers.

The performance data were evaluated in detail and recuperative type heat exchangers used in the system (Figure 3.4) were selected. The properties of heat exchangers 1 and 2 are given below:

- ✓ Dimensions : 600x600x600 mm
- ✓ Plate material : Epoxy coated aluminum
- ✓ Plate spacing : 1.5 mm

- ✓ Pressure drop : 250 Pa (at 4000 m^3/h)

Figure 3.4. Picture of the recuperative type heat exchanger used

Another important component of the desiccant cooling system is cooling coil (heat exchanger 3). This coil is used to decrease the process air temperature down to blowing temperature. Chilled water which is cooled by the vapor compression (refrigeration) unit is circulated inside the copper tubes and therefore the temperature of process air is decreased. Cooling capacity of the coil was determined according to the maximum cooling load of the air conditioned room. Cross sectional area of the ducts at the entrance and exit of the coil were taken into consideration and selection of coil was carried out. Properties of the cooling coil (Figure 3.5) are given below.

- ✓ Copper tube diameter : 1/2 inc
- ✓ Number of order : 5
- ✓ Number of tube : 18
- ✓ Distance between tubes : 32 mm (horizontal), 28 mm (vertical)
- ✓ Circuit : 9

- ✓ Dimension : 600x600x140 mm
- ✓ Pressure drop : 113 Pa (for Air), 18.7 kPa (for Water)

Figure 3.5. Picture of the cooling coil used

For the selection of rotary regenerator (heat exchanger 4), air properties at the inlet of rotary regenerator were calculated using a computer program written. Performance data for different rotor diameters, depths, well heights and materials were obtained from the manufacturers.

The performance data were evaluated in detail and rotary regenerator used (Figure 3.6) was selected. The properties of the regenerator are given below:

- ✓ Rotor material : 70μm aluminum
- ✓ Rotor diameter : 950 mm
- ✓ Rotor depth : 200 mm
- ✓ Well height : 1.5 mm
- ✓ Pressure drop : 260 Pa (at 4000 m^3/h)

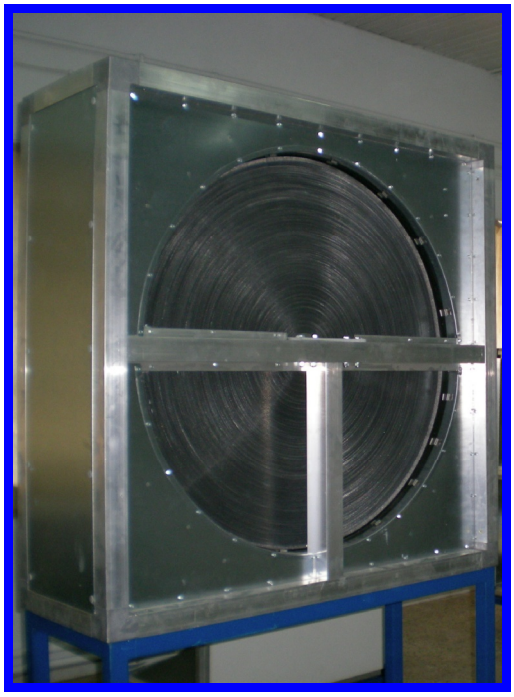

Figure 3.6. Picture of the rotary regenerator used

3.6.3. Selection of Fans

Three fans were used for the circulation of air in the fresh, waste and regeneration channels. The fans were selected using the determined air flow rate (4000 m^3/h) and pressure drop in each channel. Properties of the fans (Figure 3.7) are shown in Table 3.2.

Figure 3.7. Picture of the fans used

Table 3.2 Properties of the fans used

Fan	Model	Air Flow Rate (m^3/h)	Motor Power (HP)	Max. Motor Torque (rev/min)	Pressure Drop (Pa)
Fresh Air Fan	Nicotra (RDH 280R)	4000	4	3455	1500
Waste Air Fan	Nicotra (RDH 280R)	4000	1.5	3640	400
Regeneration Air Fan	Nicotra (RDH 280R)	4000	5.5	2220	1700

3.6.4. Refrigeration Unit

Chilled water, which is used to decrease the temperature of process air to blowing temperature, is cooled by refrigeration unit. Chilled water is circulated inside the copper tubes of cooling coil (heat exchanger 3) and therefore the temperature of process air is decreased. Figure 3.8 shows schematic view of refrigeration unit and cooling coil.

Availability, price and condenser / evaporator pressures were taken into account and it was decided to use R134a as refrigerant in the refrigeration unit. Cooling capacity of the refrigeration unit was determined as 18 kW according to the maximum cooling load of the air-conditioned room and results determined from computer program for the outdoor design conditions of Adana. Different compressor types and models were investigated in detail and the compressor used was selected. The properties of compressor are given below:

- ✓ Type : Semi-hermetic
- ✓ Displacement : 32.2 m^3/h
- ✓ Number of cylinders : 3
- ✓ Bore/Stroke : 55.6/50.8 mm
- ✓ Length/Width : 680/370 mm
- ✓ Max. High Pressure : 28 bar

- ✓ The rated power of electric motor driving : 7.5 HP (5.6 kW)
- ✓ Capacity : 18.2 kW (at evaporating/condensing temperatures of 5/50°C)

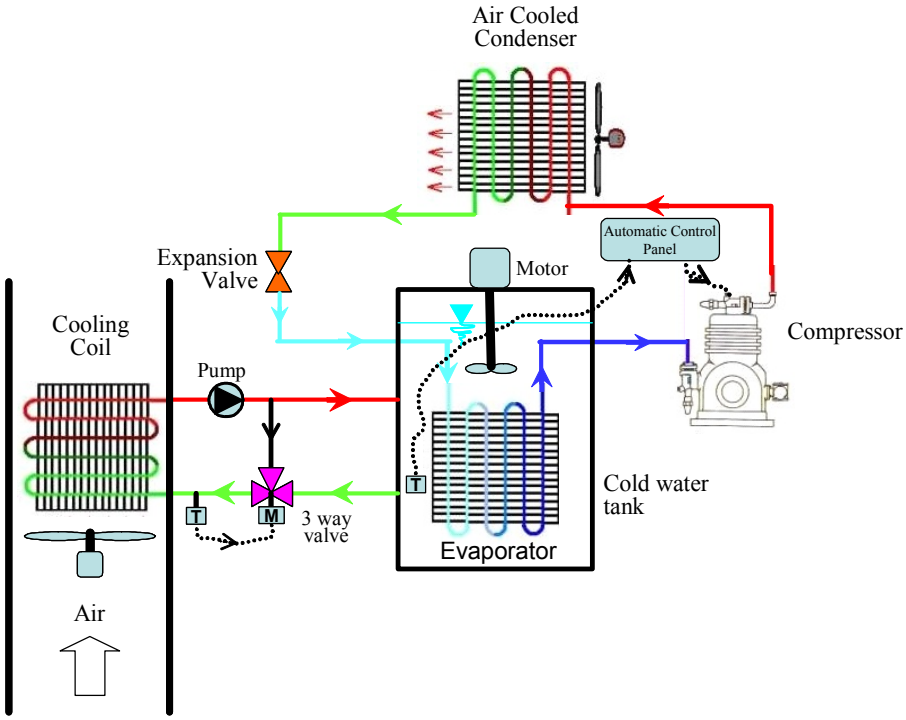

Figure 3.8. Schematic view of refrigeration unit and cooling coil

In the refrigeration unit, an air cooled condenser with 120 m^2 area and a tube type evaporator with 50 m tube length and 25 mm tube diameter were used. The evaporator was located inside the water tank. Tank volume is 315 l and dimensions are 90x70x50 cm. The tank was insulated with 60 mm stone wool to minimize the heat gain of the tank. A mixer was also located inside the tank to prevent the formation of temperature stratification in the tank.

3.6.5. Evaporative Cooler

Air which is sucked from the air-conditioned room is evaporatively cooled in a humidification unit (evaporative cooler) before entering into heat exchanger 2 in order to increase the saving. Fogging technology was used to humidify the air. The properties of spray nozzles used in evaporative cooler are given below.

- ✓ Hole diameter : 0.2 mm
- ✓ Spraying angle : 70^{o}
- ✓ Droplet diameter : 8 micron
- ✓ Flow rate : 0.071 lpm (at 60 bar)
- ✓ Working pressure : 30-100 bar

A pump that has ceramic pistons was used to pressurize the water into working pressure of the sprays. The flow rate of the pump is 1 lpm.

In the evaporative cooler, 15 nozzles were used to humidify the air. Nozzles were placed in 5 rows. Evaporative cooler was made in stages to make the tests at different capacities. In the first stage 6 nozzles, and in the second stage all the nozzles were used.

Deflectors were placed at the exit of the evaporative cooler to prevent the transport of the water droplets that are sprayed by the nozzles. Figure 3.9 shows the photographic view of evaporative cooler.

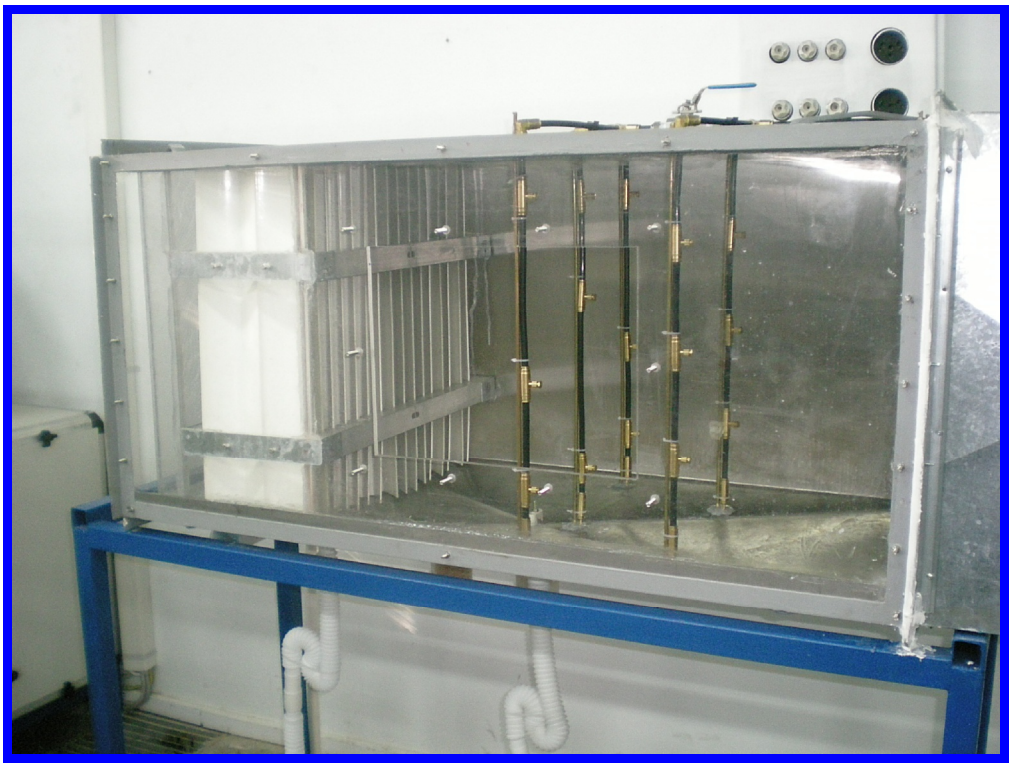

Figure 3.9. The photographic view of evaporative cooler

3.6.6. Electric Heater Unit

The final temperature of the regeneration air is achieved with the help of electric heaters (electric heater unit) to simulate the cheap heat source. Electric heaters were used for adjusting the limits of regeneration temperature accurately, for simplifying the system and also reducing the size of the system.

Electric heater unit consists of 24 U-shaped heating elements (each one is 2 kW). The heating elements were placed in 3 rows to obtain a uniform temperature distribution inside the unit. Figure 3.10 shows the photographic view of electric heater unit.

Figure 3.10. The photographic view of electric heater unit

After obtaining and manufacturing all the components needed, the system was assembled. Figure 3.11 shows the final photographic view of desiccant cooling system after the assembly stages.

Figure 3.11. The photographic view of desiccant cooling system

3.6.7. Measurement System

Temperature, relative humidity, flow rate, electric current and electrical potential difference were measured to carry out the analysis of the system and its components. Table 3.3 shows the parameters measured at different stages in the system. The points at which measurements were carried out are shown in Figure 3.1.

Dry bulb temperature of the air at states 1-17 (Figure 3.1) and temperature of the chilled water were measured using K-type thermocouples with an accuracy of 0.1 ^{o}C. An ice-bath is employed as the reference junction for all the thermocouples used. Arrangement employed in the temperature measurements is shown in Figure 3.12. Measuring junction (MJ) was placed into a measuring point to sense the temperature at that point. There are some desired properties from a measuring junction such as good electrical contact, low electrical resistance and high mechanical strength. Welding, soldering, brazing or twisting is some manufacturing processes for MJ. In this study welding method was used.

The other end of the thermocouple was replaced into a small oil-filled tube, which is placed into ice-water mixture to supply $0^{o}C$ reference junction (RJ). Copper wires were used to connect to measurement instrument.

Table 3.3. The parameters measured at different stages in the system

Measurement Point	**Measured Parameter**			
	Dry Bulb Temperature	**Relative Humidity**	**Flow Rate (Differential Pressure)**	**Dew Point Temperature**
1	√	√		
2	√		√	
3	√	√		
4	√			√
5	√			
6	√	√		
7	√	√	√	
8	√			
9	√	√		
10	√			
11	√	√		
12	√			
13	√			
14	√			
15	√		√	
16	√	√		
17	√			

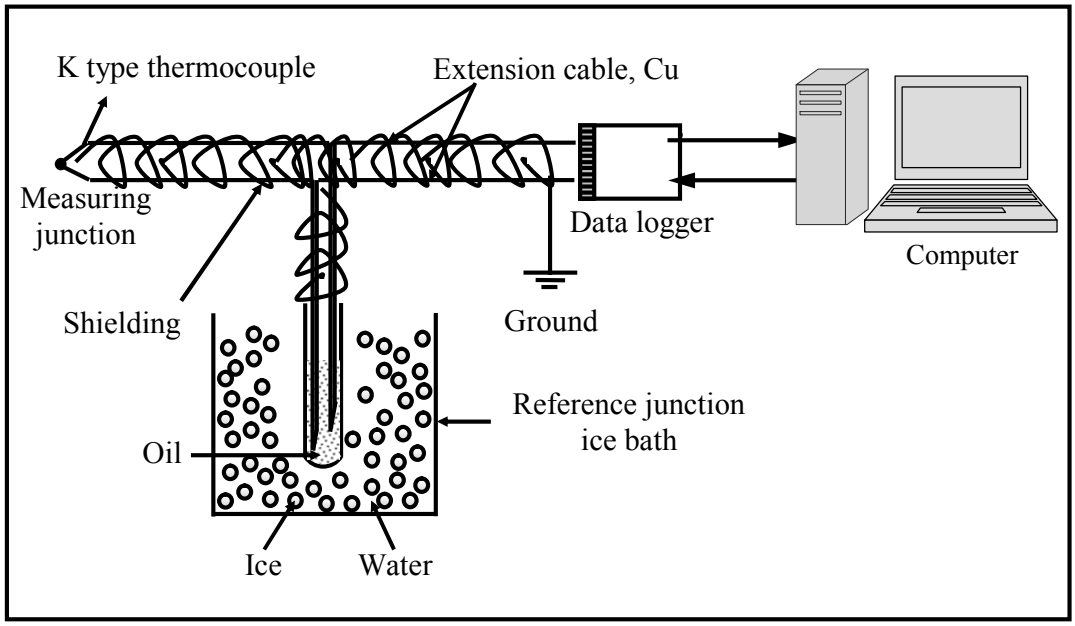

Figure 3.12. Schematic view of temperature measurement arrangement

The electromotor-force (emf) produced by the thermocouples is in the level of mV and measured by a data logger. The data stored in the computer in the form of mV was later converted to degree Celsius using the calibration curve (Fertelli, 2008) shown in Figure 3.13.

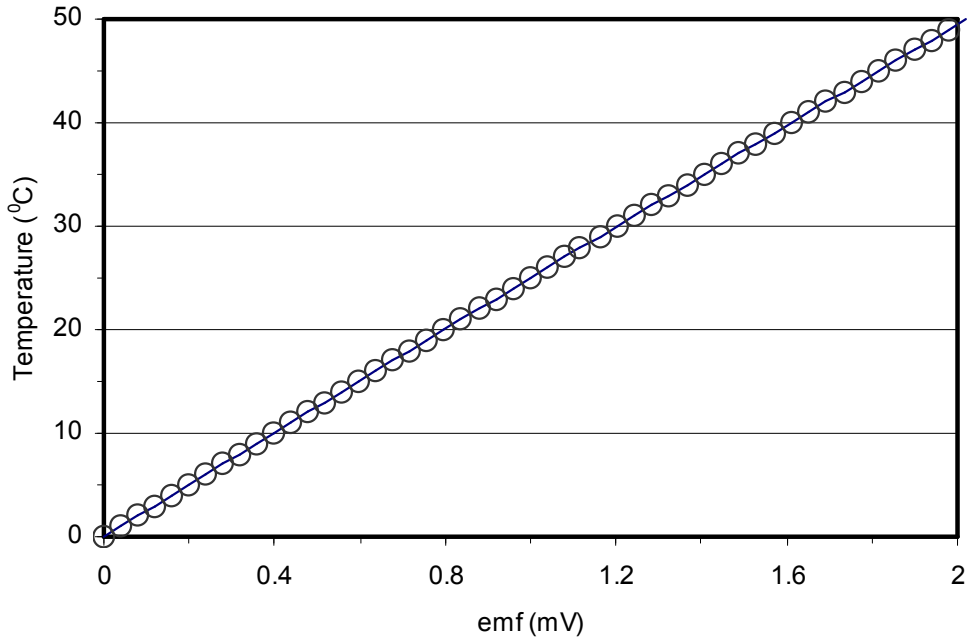

Figure 3.13. Calibration curve for the thermocouples used

An automatic control system that is explained in detail in Section 3.6.8.2.2 was designed to prevent the condensation at heat exchanger 3. Dew point temperature of the fresh air must be measured to make this control. For this purpose a dew point transmitter was used to measure the dew point temperature. The properties of the transmitter used are given below:

- ✓ Measuring range : 0-60 ^{o}C
- ✓ Working temperature : (-40) – 60 ^{o}C
- ✓ Accuracy : ± 0.2 ^{o}C
- ✓ Analog output : 0-10 V
- ✓ Supply voltage : 8-48V DC

In the system, relative humidity was measured using relative humidity transmitters. The properties of these transmitters are given below:

- ✓ Measuring range : 0-100 %RH
- ✓ Working temperature : (-40) – 60 ^{o}C
- ✓ Accuracy : ± 2% RH (0..90%), ± 3% RH (90..100%)
- ✓ Analog output : 0-10 V
- ✓ Supply voltage : 15 -35V DC

Flow rate of the air at each air channel (fresh, waste and regeneration air channels) was determined using averaging (blade type) pitot tubes and differential pressure transmitters. The properties of the differential pressure transmitters used are given below:

- ✓ Measuring range : 0-0.1” WC
- ✓ Working temperature : (-18) – 79 ^{o}C
- ✓ Accuracy : ± 1%FS
- ✓ Analog output : 0-5 V
- ✓ Supply voltage : 9 -30V DC

Total and static pressures were measured by averaging pitot tubes at different points in a considered air channel cross-section (stage 2, 7 and 15) and then air flow rate was calculated using these pressures. Measuring points at a cross-section of the channel were determined according to the method named as Log-Tchebycheff (Ernest, 1999). Figures 3.14-16 show the measuring points at each cross-section at which air flow rate were determined.

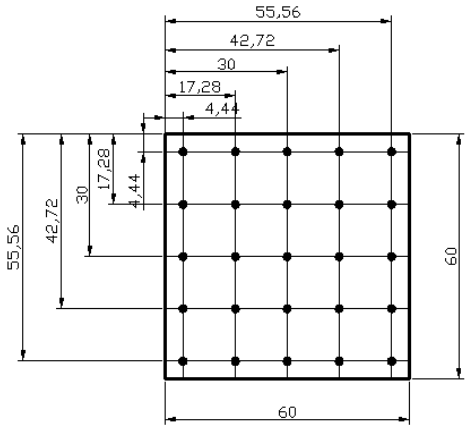

Figure 3.14. The locations of the measuring points at the cross section of the fresh air channel

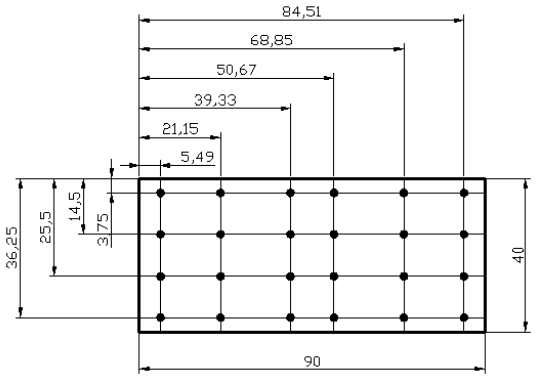

Figure 3.15. The locations of the measuring points at the cross section of the waste air channel

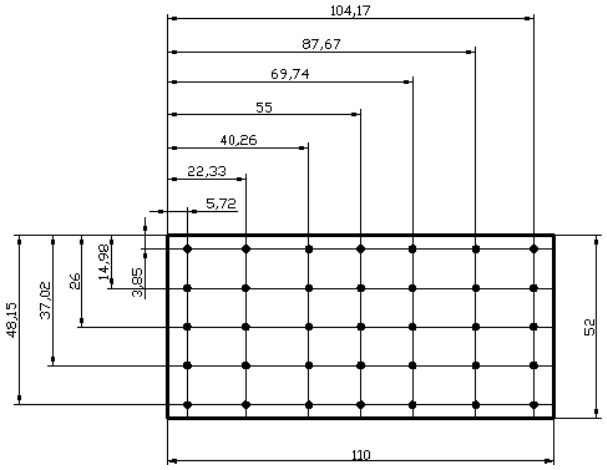

Figure 3.16. The locations of the measuring points at the cross section of the regeneration air channel

Electric current and electrical potential difference were measured to determine the power consumption of each electrical component in the experimental system. Monitoring modules were used to measure the electric current and electrical potential difference. The properties of these modules are given below:

- ✓ Measuring range : 0-250V AC (voltage module), 0-50A (ampere module)
- ✓ Working temperature : 0-50 ^{o}C
- ✓ Accuracy : ±1.5% (voltage module), ±0.5% (ampere module)
- ✓ Analog output : 0-10 V
- ✓ Supply voltage : 24V DC

Electrical signal outputs of the thermocouples, transmitters and modules were monitored and recorded with an interval of 30 second using a computer-controlled data acquisition system (Figure 3.17-18). The properties of data logger (Personal DAQ 3000+PDQ 30) are given below:

- ✓ Resolution : 16 bit
- ✓ Measuring range : ±10V, ±5V, ±2V, ±1V, ±0.5V, ±0.2V, ±0.1V
- ✓ Working temperature : (-30) - 70 ^{o}C
- ✓ Acquisition data buffer : 1 MSample

- ✓ Maximum sample rate : 1 MHz
- ✓ Over voltage protection : ±30V without damage
- ✓ Analog input channel : 64SE/32DE (with expansion module)
- ✓ Accuracy : ± 0.04 %
- ✓ Supply voltage : 6-16V DC

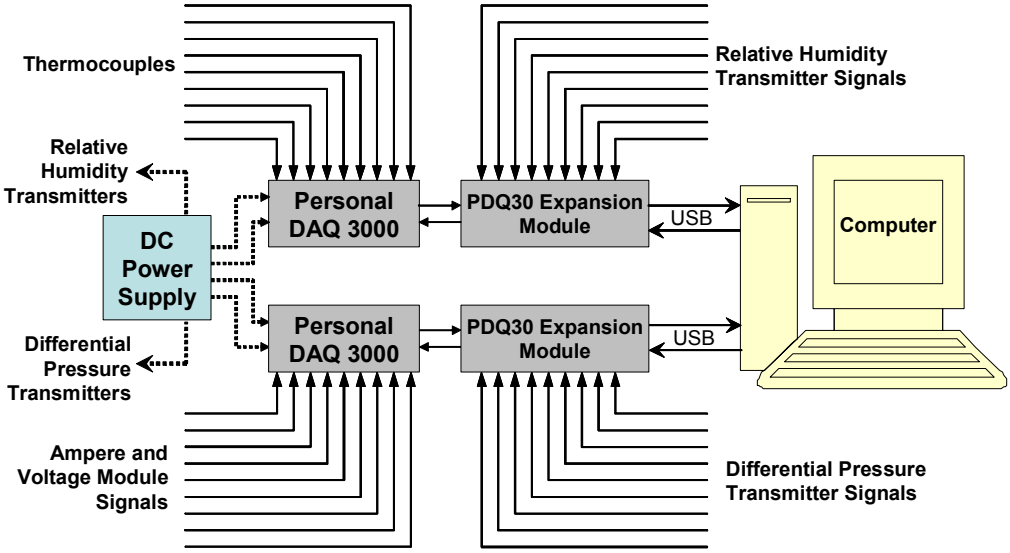

Figure 3.17. Schematic view of computer-controlled data acquisition system

Figure 3.18. The photographic view of computer-controlled data acquisition system

3.6.8. Automatic Control System

A Programmable Logic Controller (PLC) was used to control the operation of desiccant cooling system. Energy consumption of electric heaters (about ≅ 48 kW) is very high with respect to the other units. Therefore, two independent control panels were designed to control the operation of desiccant cooling system. First one was used only for the operation of the electric heaters (Figure 3.19a) and other one was used for the operation of all other components in the system (Figure 3.19b). Automatic controls used in the system are listed below:

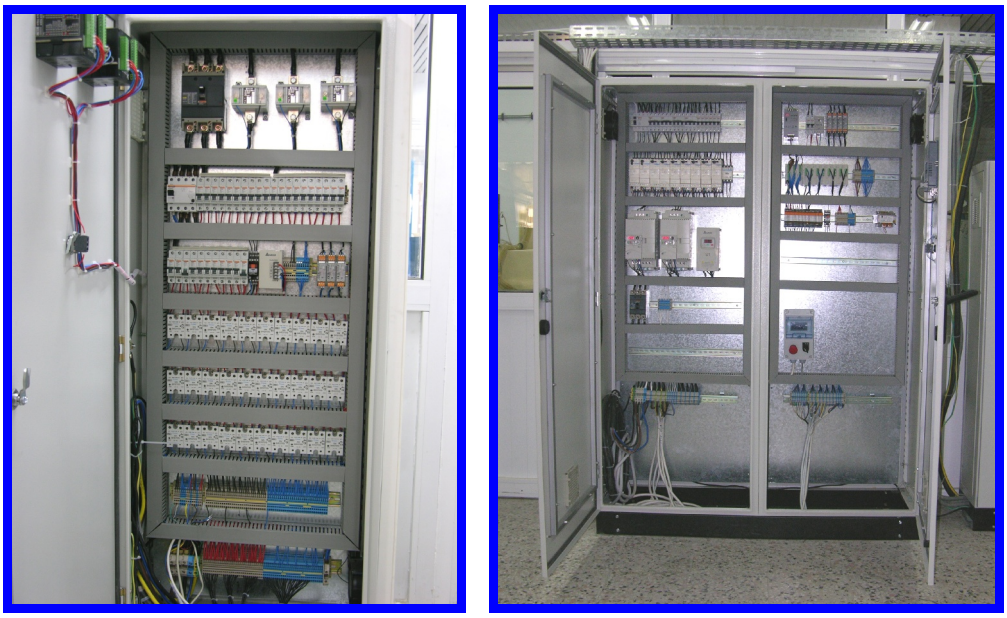

(a) ***(b)***

Figure 3.19. Control panel used for the operation of the electric heaters (a) and all other components in the system (b)

3.6.8.1. Control of the Electric Heaters

A control panel was designed to control and operate the electric heaters. An automatic control was used to protect the electric heaters. If there is no air flow or the air flow stops at the regeneration channel, electric heaters shut down. For this purpose, a pressure switch was installed to sense the flow inside the regeneration

channel. The damaging of electric heaters from the high temperature was prevented by this control. At this panel, another control was used to protect the desiccant wheel. If the desiccant wheel does not operate or stops, electric heaters also shut down.

3.6.8.1.(1). Control of the Humidity at the Conditioned Room

In the desiccant cooling systems, the amount of humidity adsorbed from the process air with desiccant wheel depends on the regeneration temperature. Humidity of the air-conditioned room is influenced by the humidity of process air leaving the desiccant wheel. In this system, the final temperature of the regeneration air (regeneration temperature) was achieved with the help of electric heaters. Therefore humidity of the air-conditioned room was controlled by the electric heaters. A transmitter measures the humidity of the air-conditioned room and transmits the data to the control system. According to the humidity measured at the room, electric heaters are switched either on or off by the control system.

3.6.8.1.(2). Control of the Upper Limit Value of the Regeneration Temperature

An automatic control was used to adjust the upper limit value of regeneration temperature with electric heaters. This control was designed to protect the desiccant wheel and to carry out experiments at different regeneration temperatures. The regeneration temperature was measured by a PT-100 sensor and transmits the data to the control panel. According to this temperature, electric heaters are switched either on or off by the control system.

3.6.8.2. Control of the Other Components Used in the System

Another control panel was designed to make the controls given below. In this panel, a touch screen was used to enter the set values.

3.6.8.2.(1). Control of the Air-Conditioned Room Temperature

Temperature of the air-conditioned room was controlled by adjusting of temperature of the chilled water that is circulated in the cooling coil. Temperature of the chilled water was adjusted by a three way valve. The desired temperature of air-conditioned room was set on the control panel. A PT 100 sensor measures the temperature of the air-conditioned room and transmits the data to a temperature controller unit, which is located in the control panel. The unit compares the actual room and set temperatures, and produces a control signal for the three way valve.

3.6.8.2.(2). Control of Condensation on the Cooling Coil

To prevent the condensation on the cooling coil, the temperature of the chilled water sent to the cooling coil must be higher than the dew point temperature of process air that enter the cooling coil. For this purpose, the dew point temperature of the air and the temperature of the chilled water were measured. A control system evaluates the signals come from the measuring devises and the temperature of the chilled water is adjusted by the three way valve.

The three way valve was used to control both the air-conditioned room temperature and condensation at cooling coil. It operates primarily according to the control of air-conditioned room temperature. However when the temperature of the water at the entrance of the cooling coil approaches to the dew point temperature of the process air at the entrance of the cooling coil, three way valve operates according to the condensation control. The value of difference between water and dew point temperature was set on the control panel.

3.6.8.2.(3). Control of the Air Flow Rate

Three centrifugal fans were used for the circulation of air in the fresh, waste and regeneration channels. Flow rates of the fresh, waste and regeneration air streams were adjusted precisely by the frequency controllers that drive the fan

motors. The desired frequency and consequently air flow rate was set on the control panel.

3.6.8.2.(4). Control of the Rotary Regenerator

Temperature of the regeneration air at the exit of the desiccant wheel is generally higher than that of the regeneration air leaving heat exchanger 1. Therefore, a rotary regenerator was used for heat recovery. An automatic control was designed to control the start up or shut down of the regenerator. According to this control, regenerator starts up when the temperature of the regeneration air at the exit of the desiccant wheel (state 15) is higher than the air temperature at the exit of the heat exchanger 1 (state 12). If the temperature of the regeneration air at state 15 is not higher than that of state 12, rotary regenerator is stopped.

3.6.8.2.(5). Control of the Refrigeration Unit

Chilled water that is used to decrease the temperature of the process air into blowing temperature was cooled by the refrigeration unit. Temperature of the water at the tank was controlled by automatic control system in the refrigeration unit. The desired temperature of the water was set on the control panel. The unit compares the actual water and set temperatures, and produces a control signal for compressor. Depending on the set temperature and the actual temperature, compressor is switched either on or off.

3.6.8.2.(6). Control of the Desiccant Wheel and Pumps

The desiccant wheel, and the circulation pumps used in the evaporative cooler and the cooling coil operate continuously. Therefore no control is needed for these components. They are energized from the control panel and it is possible to visualize from the panel that the components are switched on or off.

3.6.9. Calibration of the Measuring Devices

3.6.9.1. Calibration of the Humidity Transmitters

Relative humidity transmitters (H1, H3, H6, H7, H9, H16) were used to measure the humidity at states 1, 3, 6, 7, 9 and 16. Before the experiments, relative humidity transmitters were calibrated separately. Calibration of the transmitters was performed using a small scale air conditioning unit.

The base unit comprises a centrifugal fan with speed control, steam humidifier (boiler), electrical pre-heaters, direct expansion cooling coil, electrical heaters and orifice plate for an air flow measurement. Air cooling is provided by vapor compression refrigeration system with pressure, temperature and refrigerant flow measurement. Temperature of air is measured using precision dry and wet bulb thermometers.

The humidity transmitters were fitted into the discharge duct of the experimental unit. Amount of the steam, flow rate of the air and capacity of the pre and post heaters were adjusted to obtain required humidity at the discharge duct. Calibration process was carried out by reading output of the dry and wet thermometers and the humidity transmitters. This process was repeated for various values of the relative humidity. Figure 3.20 shows the variation of voltage (V, volt) with relative humidity (φ, %) for the humidity transmitter used at state 1 (H1). The curve, which was fitted (by using least square method) to the measured data, is also shown in Figure 3.20. The equation of the curve (Eqn. 3.1) is given below:

$$\varphi = 9.9035 * V + 4.7474 \quad (3.1)$$

Similar calibration curves were obtained for the humidity transmitters used at states 3, 6, 7, 9 and 16. Equations of these curves are given below:

$$\varphi = 9.9611 * V + 5.4064 \quad \text{(H3)} \quad (3.2)$$

$$\varphi = 9.9732 * V + 4.6724 \quad (H6) \tag{3.3}$$

$$\varphi = 9.7681 * V + 5.4811 \quad (H7) \tag{3.4}$$

$$\varphi = 9.7113 * V + 5.7163 \quad (H9) \tag{3.5}$$

$$\varphi = 9.7382 * V + 4.6299 \quad (H16) \tag{3.6}$$

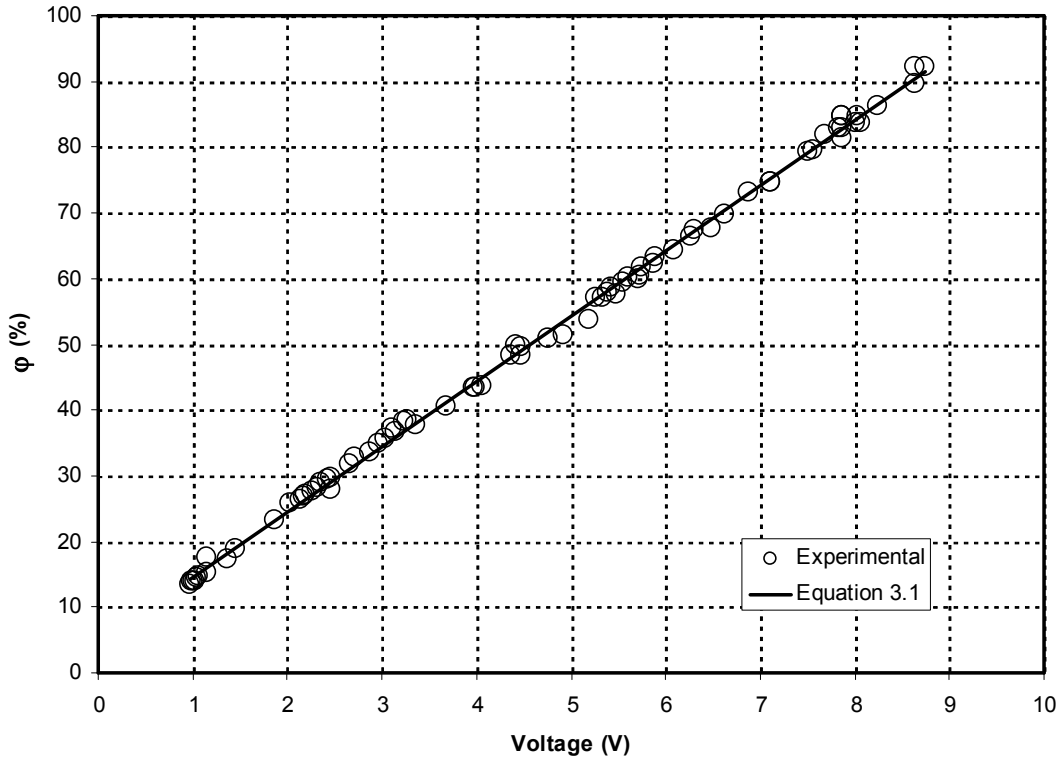

Figure 3.20. Calibration curve of humidity transmitter used at state 1 (H1)

3.6.9.2. Calibration of the Differential Pressure Transmitters

Differential pressure transmitters (P2, P7, P15) were used to determine the flow rate of the air at states 2, 7 and 15. Before the experiments, differential pressure transmitters were calibrated separately. Calibration of the transmitters was also

performed using a small scale air conditioning unit that is used for humidity transmitter calibration.

Differential pressure measuring was carried out with the help of pitot tube which static and total pressure can be measured separately. To carry out pressure measuring correctly, pitot tube must be located a place at which flow is fully developed. For this purpose, a pipe with 8 mm inner diameter was installed at the end of the discharge duct of the experimental unit and pitot tube was placed 3 m downstream length (40xD). Flow rate of the air was adjusted to obtain required pressure difference at the pipe. Calibration process was carried out by reading output of the Cussons Type 5 inclined manometer and the differential pressure transmitters. This process was repeated for various values of the pressure difference. Figure 3.21 shows the variation of voltage (V, volt) with differential pressure (ΔP, Pa) for the transmitter used at state 2 (P2). The curve which was fitted (by using least square method) to the measured data is also shown in Figure 3.21. The equation of the curve (Eqn. 3.7) is given below:

$$\Delta P = 4.856 * V - 0.096 \quad (3.7)$$

Similar calibration curves were obtained for the differential pressure transmitters used at states 7 and 15. Equations of these curves are given below:

$$\Delta P = 4.9045 * V - 0.1022 \quad (P7) \quad (3.8)$$

$$\Delta P = 4.8671 * V + 0.0431 \quad (P15) \quad (3.9)$$

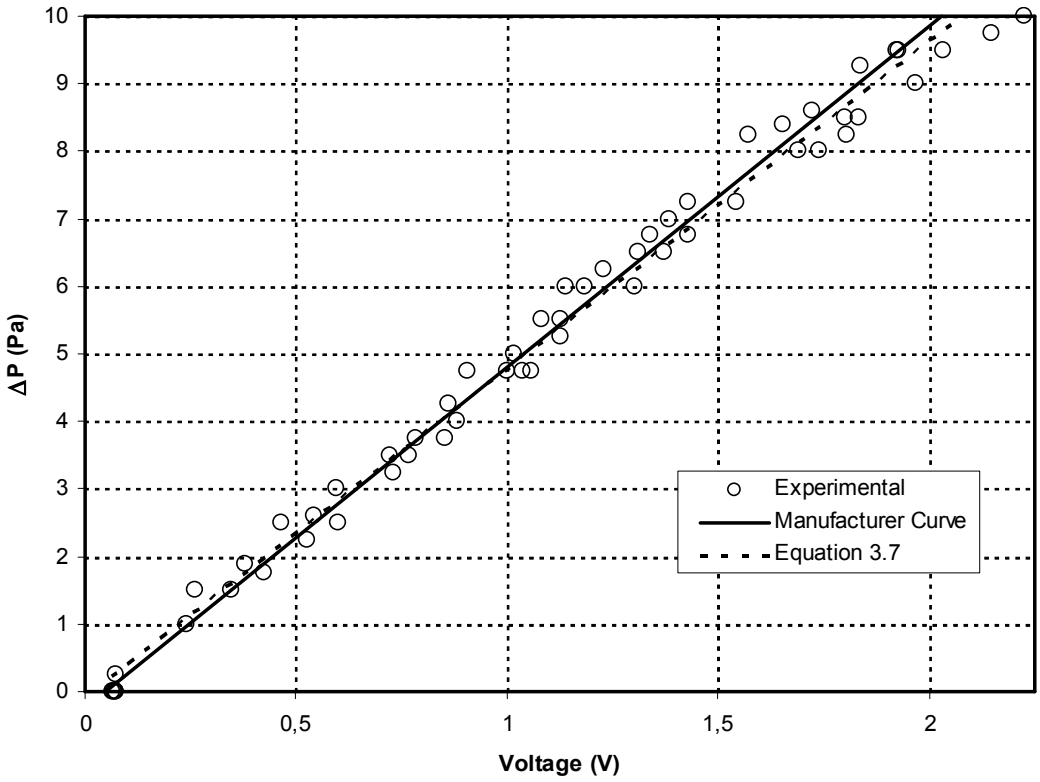

Figure 3.21. Calibration curve of differential pressure transmitter used at state 2 (P2)

3.7. Rotary Desiccant Wheel

The most important component of the desiccant cooling system is the desiccant wheel. Some of the publications and catalogs related with the desiccant wheels point out that dehumidification and removal of humidity operations (regeneration, reactivation) realize approximately at constant enthalpy (approximately at constant wet bulb temperature) (Jıa et al., 2006). These processes are represented with the curves (A→B) and (C→D) in Figure 3.22. However, dehumidification and regeneration processes do not occur at constant wet bulb temperature according to the data given by the rotary desiccant wheel manufactures. Actual increase in dry bulb temperature during dehumidification (A→B') is higher than that of the constant wet bulb case (A→B). This is due to fact that a chemical thermal energy arises during dehumidification process and the energy carried from the regeneration air by the matrix of the desiccant wheel (ASHRAE Systems and

Equipment Handbook, 2000). Because of this additional energy, dry bulb temperature further increases. The ratio of additional dry bulb temperature increase ($T_{B'} - T_B$) to total dry bulb temperature increase ($T_{B'} - T_A$) was defined as:

$$F_d = \frac{T_{B'} - T_B}{T_{B'} - T_A} \tag{3.10}$$

Similarly, dry bulb temperature decrease is higher than constant wet bulb temperature case during regeneration (C→D'), due to sensible heat transfer to the process air. The ratio of additional dry bulb temperature decrease ($T_{D'} - T_D$) to total dry bulb temperature decrease ($T_{D'} - T_C$) was also defined as:

$$F_r = \frac{T_{D'} - T_D}{T_{D'} - T_C} \tag{3.11}$$

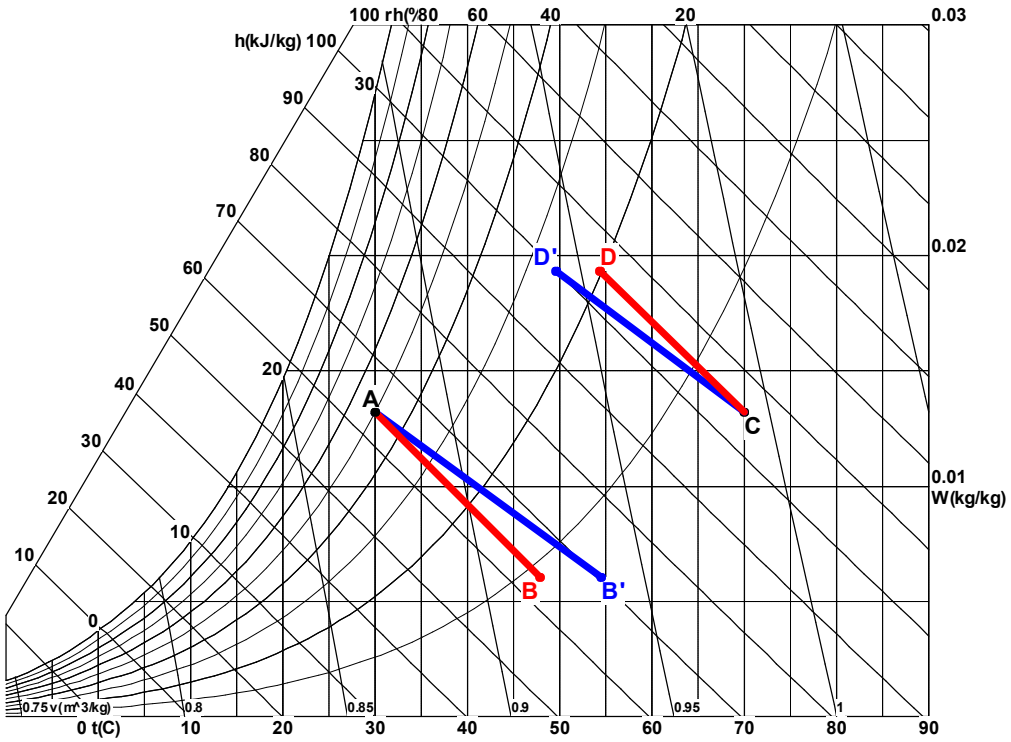

Figure 3.22. The process of dehumidification (A-B) and regeneration (C-D)

It is important to determine the values of F_d and F_r accurately to able to model the system using the computer program explained in Section 3.8. The performance data of the rotary desiccant wheel given by manufacturers were evaluated in detail and results are given in Section 4.1.

3.8. Description of Computer Program Written

Psychrometric analyses of desiccant cooling system were carried out using the design day parameters of Adana (38 ºC dry and 26 ºC wet bulb temperature). The preliminary design of the system was based on the results of these parameters.

However, an air-conditioning system operates in design values of outside environment only a few days and/or even a few hours in a season. Therefore, it is also very important to know the behavior of the system on the other days of the season and different hours in a day. In Adana, it is assumed that cooling season starts in the middle of May and ends in the middle of October. This corresponds nearly 3600 hours. Considering the variable outdoor conditions in a cooling season, analyses of the system should be made on an hourly basis.

When the number of the states (17 states) in the system considered, and number of the hours in a cooling season (3600 hours) are thought together, it is clear that analysis can not be carried out manually. Therefore, it was decided to develop a computer program for the hourly analysis of the system. FORTRAN programming language was selected for the programming. The parameters below were used as input for the program:

- Volumetric flow rate of the fresh air ($\dot{V}_f$)
- Volumetric flow rate of the waste air ($\dot{V}_{ws}$)
- Volumetric flow rate of the regeneration air ($\dot{V}_r$)
- Dry bulb temperature of the ambient air (T_a)
- Humidity ratio of the ambient air (W_a)
- Design dry bulb temperature of the air-conditioned room (T_{rm})

- Design relative humidity of the air-conditioned room (φ_{rm})
- Sensible heat ratio of the air-conditioned room (SHR)
- Total cooling load of the air-conditioned room ($\dot{Q}_{tot}$)
- Effectiveness of the heat exchangers (η_{HE})
- Effectiveness of evaporative cooler (η_{EC})
- Efficiency of the fans (η_{fan})
- Powers of the fans ($\dot{W}_{fan}$)

Using these inputs, the psychrometric features given below were calculated separately for each state on the system:

- Dry bulb temperature (^oC)
- Wet bulb temperature (^oC)
- Enthalpy (kJ/kg)
- Humidity ratio (kg/kg dry air)
- Relative humidity (%)
- Dew point temperature (^oC)
- Density (kg/m^3)
- Specific heat (kJ/kg K)

These psychrometric properties can be calculated using psychrometric equations given by ASHRAE (ASHRAE Fundamental Handbook, 2001). Prepared computer program for the analyses of the system is given in Appendix 1.

In the computer program, the dry bulb temperatures at state 3, 4, 10, 12, 13 and 16 (Figure 3.1) were calculated using the equations for the effectiveness of heat exchangers (η_{HE}) (Kreider ve Rabl, 1994):

$$\eta_{HE} = \frac{\dot{Q}}{\dot{Q}_{max}} \tag{3.12}$$

where $\dot{Q}$ is the amount of actual heat transfer and $\dot{Q}_{max}$ is the maximum possible heat transfer:

$$\dot{Q} = \dot{m} c_p (T_i - T_o) \tag{3.13}$$

$$\dot{Q}_{max} = \dot{C}_{min} (T_{hi} - T_{ci}) \tag{3.14}$$

$\dot{C}_{min}$ is the minimum of the capacitance rate of cold ($\dot{C}_c$) and hot ($\dot{C}_h$) air streams:

$$\dot{C}_h = \dot{m}_h c_{ph} \tag{3.15}$$

$$\dot{C}_c = \dot{m}_c c_{pc} \tag{3.16}$$

The dry bulb temperature at state 6 (blowing temperature) was calculated by psychrometric equations and equations (Aktacir, 2005) given below:

$$SHR = \frac{\dot{Q}_s}{\dot{Q}_{tot}} \tag{3.17}$$

$$\dot{Q}_{tot} = \dot{Q}_l + Q_s \tag{3.18}$$

$$\dot{Q}_l = \dot{m}_f \times h_g \times (W_7 - W_6) \tag{3.19}$$

$$\dot{Q}_s = \dot{m}_f \times c_p \times (T_7 - T_6) \tag{3.20}$$

$$\frac{W_7 - W_6}{T_7 - T_6} = \frac{c_p}{h_g} * \left(\frac{1}{SHR} - 1 \right) \tag{3.21}$$

The fans that circulate air in the system cause a temperature rise in air, because fan motors were located inside the air channels. This temperature rise (T_o-T_i) can be calculated using the equations (ASHRAE Fundamental Handbook, 2001) below:

$$\dot{Q}_g = \left(1 - \frac{\eta_{fan}}{100}\right) \times \dot{W}_{fan} \tag{3.22}$$

$$T_o - T_i = \left(\frac{\dot{Q}_g}{c_p \times \dot{m}}\right) \tag{3.23}$$

The dry bulb temperature at state 9 (exit of the evaporative cooler) was calculated using the humidifier efficiency (η_{EC}) (Kreider ve Rabl, 1994):

$$\eta_{EC} = \frac{T_i - T_o}{T_i - T_{wb,i}} \tag{3.24}$$

The equations which were used in the calculation of the amount of heat transfer that take place in heat exchanger 1, 2, 3 and 4 ($\dot{Q}_{2\rightarrow3}$ (heat that is transferred from the fresh air), $\dot{Q}_{3\rightarrow4}$ (heat that is transferred from the fresh air), $\dot{Q}_{4\rightarrow5}$ (heat that is transferred from the fresh air), $\dot{Q}_{15\rightarrow16}$ (heat that is transferred from the hot regeneration air) respectively) and the amount of heat that is given by the electric heater ($\dot{Q}_{14\rightarrow13}$) are presented in Table 3.4.

Table 3.4. Equations used for the calculation of heat transfer

	Calculated Parameter	***Equations Used***	***Equation Number***
Heat Exchanger 1	$\dot{Q}_{2\rightarrow3}$	$\dot{m}_f * (h_2 - h_3)$	3.25
Heat Exchanger 2	$\dot{Q}_{3\rightarrow4}$	$\dot{m}_f * (h_3 - h_4)$	3.26
Heat Exchanger 3	$\dot{Q}_{4\rightarrow5}$	$\dot{m}_f * (h_4 - h_5)$	3.27
Heat Exchanger 4	$\dot{Q}_{15\rightarrow16}$	$\dot{m}_r * (h_{15} - h_{16})$	3.28
Electric Heater	$\dot{Q}_{14\rightarrow13}$	$\dot{m}_r * (h_{14} - h_{13})$	3.29

3.9. Equations used for the Analysis of the Experimental Data

In the analysis of the experimental data, various calculations (effectiveness of the heat exchangers, moisture removal, cooling capacity, COP etc.) were carried out to determine the performance of the system and each component.

Amount of the moisture removed from the process air (moisture removal, ΔW) is defined as the difference between the humidity ratio at the inlet (W_1) and outlet (W_2) of the desiccant wheel:

$$\Delta W = \dot{m}_f (W_1 - W_2) \tag{3.30}$$

Cooling capacity of a desiccant cooling system $\dot{Q}_{CC}$ is obtained from:

$$\dot{Q}_{CC} = \dot{m}_f (h_6 - h_1) \tag{3.31}$$

where $\dot{m}_f$ is the mass flow rate of the fresh air stream and h is the enthalpy of the air.

The coefficient of performance (COP) of the system is defined as the ratio between the cooling capacity obtained and total energy input ($\dot{E}_{tot}$) to the system:

$$COP = \frac{\dot{Q}_{CC}}{\dot{E}_{tot}} \tag{3.32}$$

$\dot{E}_{tot}$ is the sum of energy consumption of regeneration heat ($\dot{Q}_{reg}$), fans ($\dot{W}_{fan}$), compressor of the refrigeration unit ($\dot{W}_{com}$) and other electrical components ($\dot{W}_{oth}$):

$$\dot{E}_{tot} = \dot{Q}_{reg} + \dot{W}_{fan} + \dot{W}_{com} + \dot{W}_{oth} \tag{3.33}$$

In this study, since electric heaters are used to simulate regeneration heat source, the heat input for the regeneration is almost same as power consumption of electric heaters ($\dot{W}_{eh}$) when the daily total values are considered ($\dot{Q}_{reg} = \dot{W}_{eh}$).

3.10. Uncertainty Analysis

Uncertainty analysis is needed to prove the accuracy of the experiments. An uncertainty analysis was performed using the method described by Holman (Holman, McGraw Hill, 1989). In the present study, the temperatures, relative humidities, flow rates, electric currents and electrical potential differences were measured with appropriate instruments explained previously. The total uncertainties of the measurements were estimated to be ±0.3 ^{o}C for the air and water temperatures, ±2.51% for the relative humidities, ±1.59% for power inputs to the electrical heaters, compressor and motor of the fans, dehumidifier, regenerator and circulating pump. The total uncertainty associated with mass flow rates of the air was found to be ±2.89%. The uncertainties associated with the calculated parameters moisture removal, cooling capacity and COP were found to be ±4.2%, ±6.3% and ±7.1%, respectively. The calculation procedure of uncertainties is given in Appendix 2.

3.11. Studies for Solar Energy

In the system, hot regeneration air, which is used for removing the humidity on the dehumidifier, was produced with the help of electric heaters. In desiccant based air-conditioning systems, hot air is generally achieved with the help of electric heaters or cheap energy sources (solar energy, waste heat, natural gas, and etc.). (Dai et al., 2002; Kabeel, 2007; Yutong and Hongxing, 2008). In the solar desiccant air conditioning systems, hot water is produced using solar collectors. Hot water is circulated inside the copper tubes of heat exchanger and therefore the temperature of the regeneration air is increased.

Applicability of the solar energy in desiccant based air- conditioning system studied was investigated using the model described in detail below. To benefit from

the solar energy in the system, the heat produced in regeneration air should be within an acceptable level. In the solar desiccant air conditioning systems, the amount of heat that is transferred from water to the air is largely depends on the outside air conditions. Therefore, it is necessary to analyze the system on the cooling season not only on the summer design day to evaluate the benefit of solar energy in the system studied. For this purpose, total solar radiation ($\dot{q}$), temperature (T_a) and relative humidity (φ_a) data measured by The State Meteorological Affairs (DMİ) during 21 years (1986-2006) for Adana were used to calculate the amount of temperature increase in the regeneration air temperature due to solar energy. In the calculations, meteorological data measured between 06:00-19:00 hours during May-October were used.

In the solar desiccant air conditioning systems, hot water is produced using solar collectors, and this hot water is send to the heat exchanger. Therefore the temperature of the regeneration air is increased (Figure 3.23).

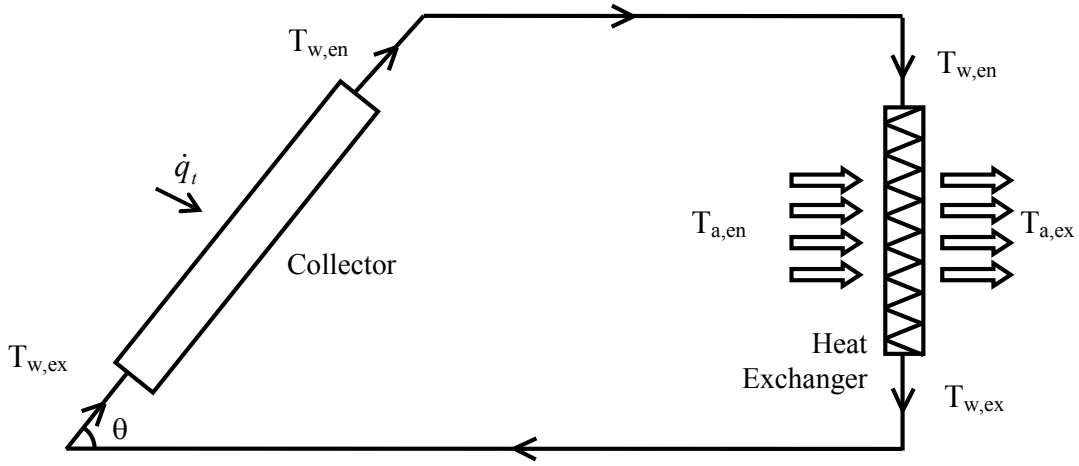

Figure 3.23. Schematic view of using solar energy in the system

Since the collectors in the solar energy systems are mounted with an angle, solar radiation on the inclined surface ($\dot{q}_t$) should be known for calculations. Although the solar radiation on the horizontal surface is measured, the solar radiation on the inclined surface cannot be measured except the experimental studies. $\dot{q}_t$ is determined with the help of various solar radiation models in which horizontal

surface data are used (Bulut, 2008). In this study, $\dot{q}_t$ was calculated using the model developed by Liu and Jordan (Liu and Jordan, 1960; 1961) and the solar radiation data on the horizontal surface measured by DMI.

It is recommended that in summer season, collectors used in the water heating system should be mounted with an angle (title angle, θ) that 15^o less than the latitude angle of current place (Ministry of Public Works and Settlements, 1984). Consequently, in calculations, θ was selected 22^o for Adana which has almost 37^o (36^o 59^o) latitude.

In the system, air temperature at the entrance of the heat exchanger (T_{13}, state 13 in Figure 3.1, $T_{a,en}$ at the model ($T_{13}=T_{a,en}$)) must be known to determine the amount of increase in the regeneration air temperature ($T_{a,ex}$ - $T_{a,en}$). The experiments which were carried out during cooling season of 2008, were evaluated in detail and it was found that temperature at the entrance of the heat exchanger (T_{13}) depends on the ambient temperature (T_{11}, state 11 in Figure 3.1, T_a at the model ($T_{11}=T_a$)) and ambient relative humidity (φ_{11}, state 11 in Figure 3.1, φ_a at the model ($\varphi_{11}=\varphi_a$)). Figure 3.24 shows the variation of daily average temperature difference with daily average outside relative humidity. Least-square method was applied to the data obtained from the experiments (R^2=0.86) and the equation given below was found for the calculations.

$$T_{13} = T_{11} - 0.0129 * \varphi_{11}^2 + 2.1143 * \varphi_{11} - 62.091 \qquad (3.33)$$

The temperature of the water at the entrance of the heat exchanger ($T_{w,\,en}$) depends on the efficiency of collector (η_C), surface area of collector (F), title angle (θ), solar radiation on the inclined surface ($\dot{q}_t$) and the water temperature at the exit of the heat exchanger ($T_{w,\,ex}$). However, water temperature at the exit of the heat exchanger depends on the temperature of the water and air at the entrance of the heat exchanger and the efficiency of heat exchanger (η_{HE}) used.

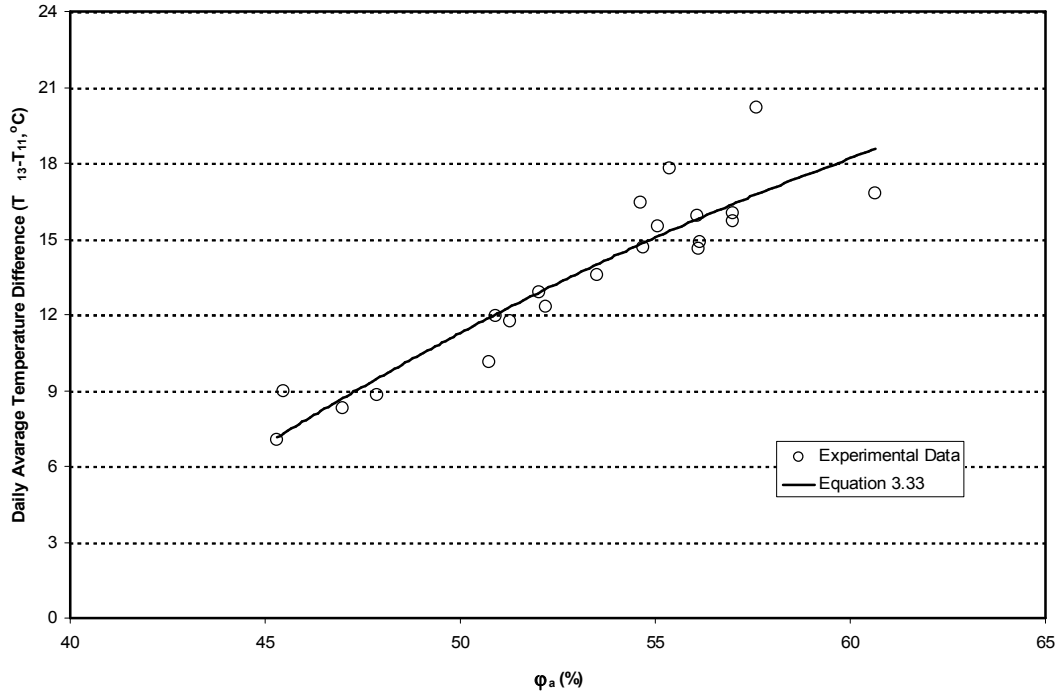

Figure 3.24. Variation of daily average temperature difference with daily average outside relative humidity

Efficiency of collector depends on ambient temperature (DMI data, T_a), total solar radiation (DMI data, $\dot{q}$) and mean water temperature ($T_{m,w}$) at the entrance and exit of the collector. In the calculations, it was assumed that selective surface collectors produced by well-known company (EZİNÇ Co.) were used. Least-square method was applied to the data provided from the manufacturer (Figure 3.25, R^2=0.98) and the equation given below was found for the efficiency.

$$\eta_C = -11.235 * \left(\frac{T_{m,w} - T_a}{\dot{q}} \right)^2 - 3{,}4165 * \left(\frac{T_{m,w} - T_a}{\dot{q}} \right) + 0{,}728 \qquad (3.34)$$

In the calculations, the amount of heat transferred from collectors ($\dot{Q}_{col}$) was determined using equation 3.35 and total surface area of the collectors was assumed to be 50 m^2.

$$\dot{Q}_{col} = \eta_c * F * \dot{q}_t \qquad (3.35)$$

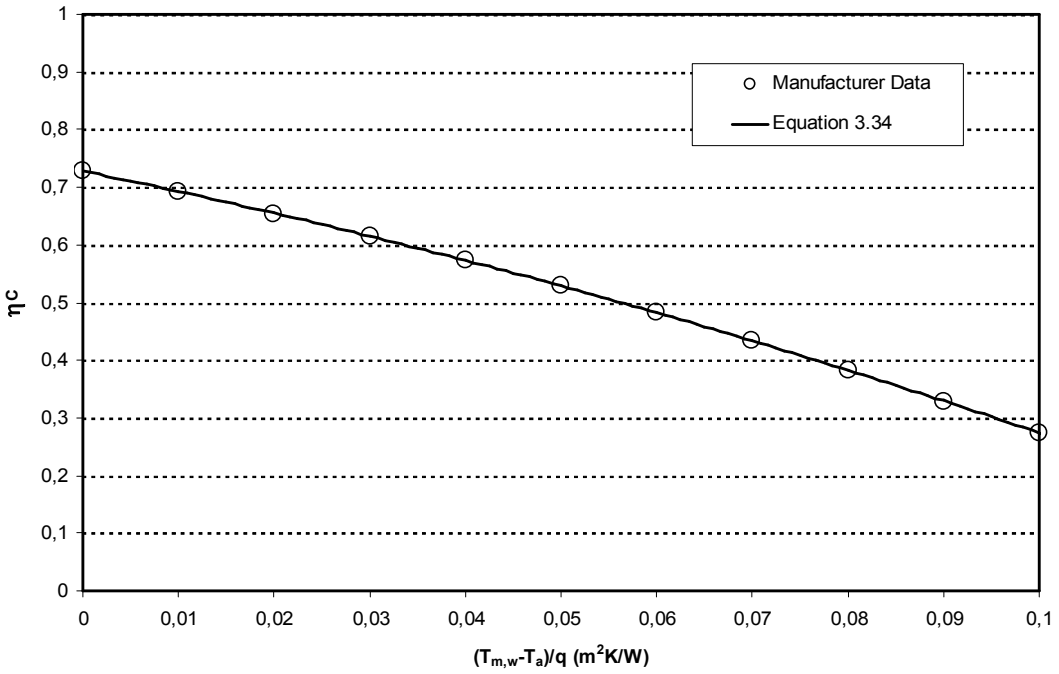

Figure 3.25. Performance data provided from the manufacturer

The equations that are given in section 3.8 for the heat exchangers were also used in the calculations and the efficiency of heat exchanger was assumed to be 60%. It was also assumed that the difference between the water temperature at the entrance and exit of the heat exchanger (ΔT) is 5 ^{o}C and flow rate of the air ($\dot{m}_f$) is 4000 m^3/h.

A computer program using FORTRAN programming language was written to determine the amount of increase in the regeneration air temperature due to solar energy. Prepared computer program for solar energy analyses is given in Appendix 3.

4. RESULTS AND DISCUSSION

In this chapter, the results obtained from the evaluation of the performance data of the rotary desiccant wheel given by manufacturers, the results obtained from the hourly analyses of the system using computer program and the results obtained from the solar energy analyses are given.

Two series of experiments were carried out in the system. The results obtained from the experiments are also given in this chapter. The comparison of two series of experiments was carried out and results are given below.

4.1. Results of the Studies for Rotary Desiccant Wheel

It is important to determine values of F_d and F_r explained in Section 3.7 to able to analyze the system using the computer program written (explained in Section 3.8). The performance data of the rotary desiccant wheel given by the manufacturers were evaluated in detail. It was found that F_d and F_r are functions of humidity ratio of the dehumidified (process) air, dry bulb temperature and humidity ratio of the regeneration air.

In the system studied, the humidity ratio of the process air and the regeneration air are equal, since the same ambient air was used as the process air and the regeneration air. Figure 4.1 shows variation of F_d values with the humidity ratio of the ambient air (W_a) for 70 ^oC regeneration temperature. In the figure, F_d values are plotted for different ambient air dry bulb temperatures (T_a) varying between 25 ^oC and 40 ^oC. As can be seen from the figure, F_d decreases smoothly with increasing humidity ratio of ambient air. Dry bulb temperature of the ambient air has no considerable influence on F_d. Similar results were obtained for different regeneration temperatures.

Figure 4.2 shows values of F_d and F_r, which were calculated for different regeneration temperatures (T_r) for dehumidification and humidity removal (regeneration) processes. As can be seen from the figure, F_d and F_r are almost the same for a given regeneration temperature. Therefore, the dehumidification and

humidity removal data were handled together in order to obtain equations required for the computer modeling.

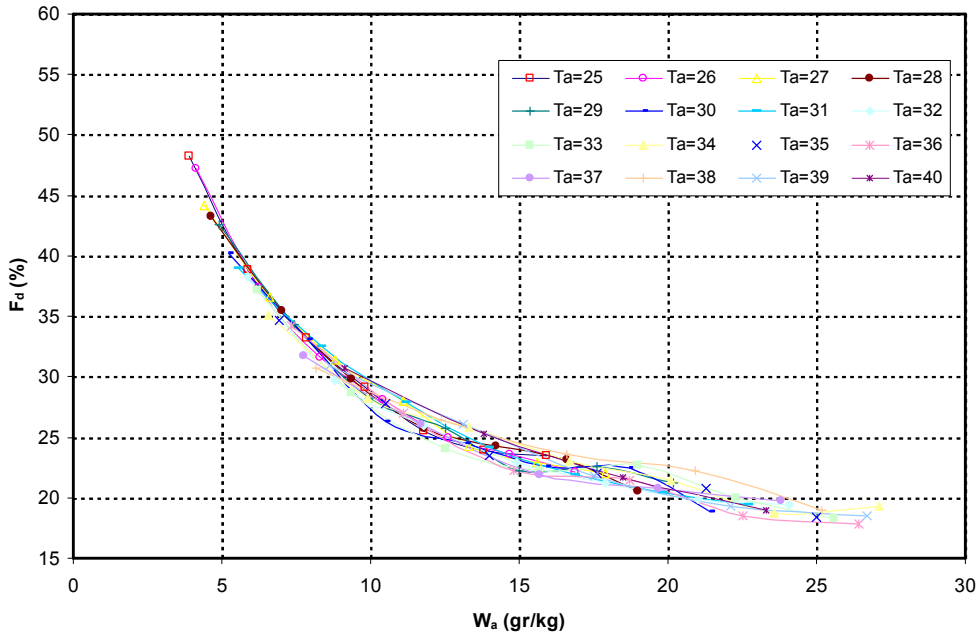

Figure 4.1. Variation of F_d at 70 ^oC regeneration temperature with ambient humidity ratio for different ambient dry bulb temperatures

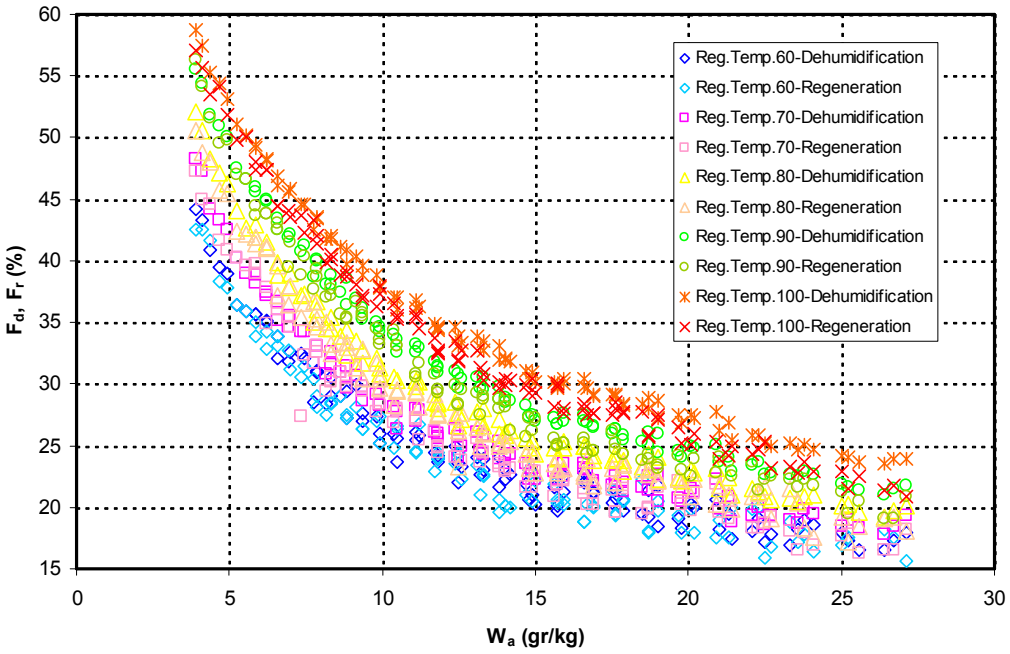

Figure 4.2. The values of F_d and F_r calculated at different regeneration temperatures for dehumidification and humidity removal processes

Figure 4.3 shows variation of F_d and F_r, which were obtained at different regeneration temperatures, with ambient humidity ratio. The curves which were fitted (using least square method) to the calculated data (F_d and F_r) for given regeneration temperature are also shown in the figure. The equations of the curves are listed below:

$$T_r = 60\ ^oC: \quad F_d = F_r = 82.136 \times W_a^{-0.4901} \quad (R^2=0.957) \quad (4.1)$$

$$T_r = 70\ ^oC: \quad F_d = F_r = 92.289 \times W_a^{-0.509} \quad (R^2=0.970) \quad (4.2)$$

$$T_r = 80\ ^oC: \quad F_d = F_r = 102.45 \times W_a^{-0.518} \quad (R^2=0.977) \quad (4.3)$$

$$T_r = 90\ ^oC: \quad F_d = F_r = 112.41 \times W_a^{-0.5188} \quad (R^2=0.983) \quad (4.4)$$

$$T_r = 100\ ^oC: \quad F_d = F_r = 116.80 \times W_a^{-0.4979} \quad (R^2=0.983) \quad (4.5)$$

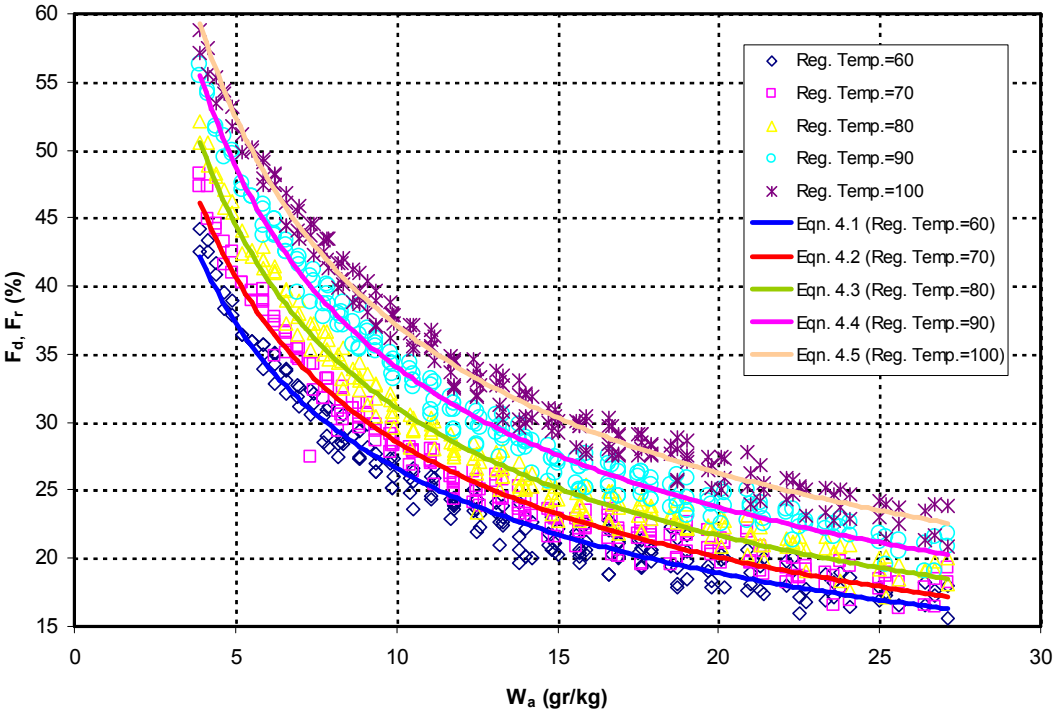

Figure 4.3. Variation of F_d and F_r, which were obtained at different regeneration temperatures, with the ambient humidity ratio (Equations 4.1-4.5)

Use of only one equation that is valid for all regeneration temperatures would be easier than use of separate equations for each regeneration temperature. In the next step of the study, possibility of representing all the data with only one equation was investigated. As a result, Equation 4.6 that includes influence of both ambient humidity ratio and regeneration temperature was obtained:

$$F_d = F_r = 5.18 \times W_a^{-0.507} \times T_r^{0.652} \qquad (R^2=0.96) \qquad (4.6)$$

Figure 4.4 shows the comparison of the calculated data with the ones obtained. As seen from the figure, Equation 4.6 follows the data successfully.

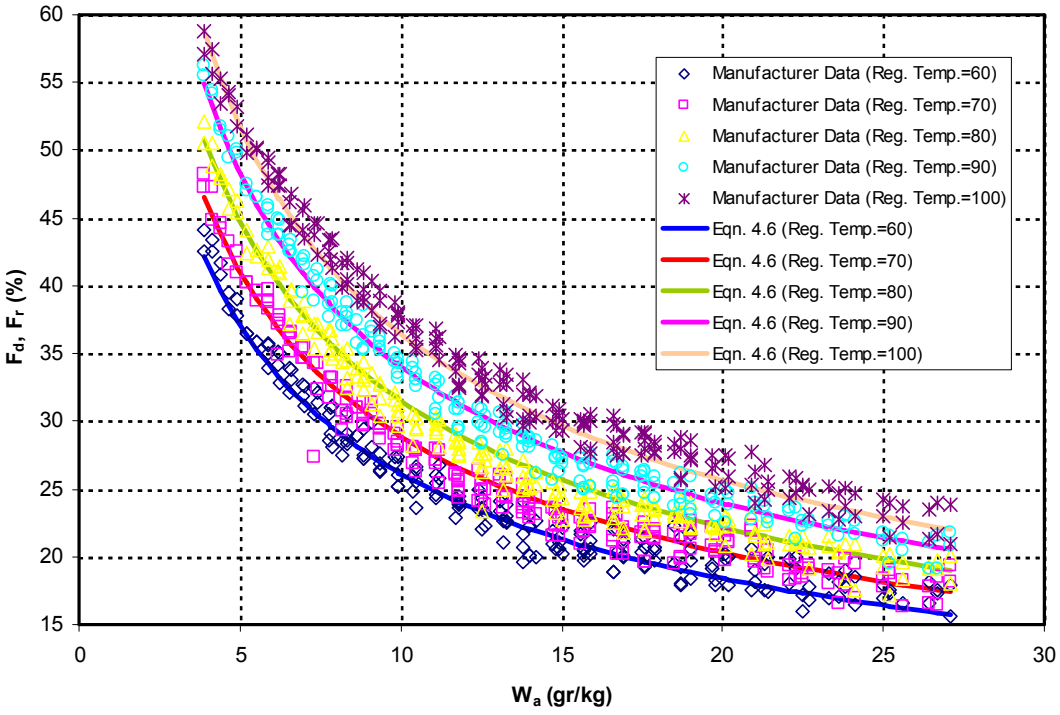

Figure 4.4. Variation of F_d and F_r, which were obtained at different regeneration temperatures, with the ambient humidity ratio (Equation 4.6)

4.2. Results Obtained from the Computer Program Written

Performance of the system studied was analyzed using the hourly climate data (dry bulb temperature and relative humidity) measured by The State Meteorological Affairs (DMİ) during 21 years (1986-2006) for Adana. In order to analyze the performance of the system under summer conditions, the climate data, which were measured between the months June and September for 07:00, 14:00 and 21:00 hours (relative humidity is measured terdiurnal by DMİ), were used in the calculations.

The input used in the program is dry bulb temperature and relative humidity of ambient air (state 1). The psychrometric properties of the each state of the system were calculated using the equations given in Section 3.8 and ASHRAE (ASHRAE Fundamentals Handbook, 2001) and the values given in Table 4.1. It should be noted that the humidity ratio changes only during the processes of dehumidification (1→2), humidity removal (15→16) and humidification (9→10). It is not changed during the other processes. In the analysis, the climate data were not taken into consideration, if the humidity ratio of the ambient is less than that of the air-conditioning room.

Tablo 4. 1. The values used in the calculations

Parameter	**Value**
Total cooling load of the air-conditioned room (kW)	10
Comfort conditions of air-conditioned room (dry bulb temperature (^{o}C) and relative humidity (%))	26 - 50
Flow rate of the fresh, waste and regeneration air (m^3/h)	4000
Effectiveness of the recuperators (%)	65
Effectiveness of the regenerator (%)	85
Effectiveness of the evaporative cooler (%)	90
Efficiency of the fans (%)	60
Powers of the fans (kW) (waste-fresh-regeneration)	1-3-4

The analyses firstly were made only for 21st July that is the design day for Adana. The dry bulb temperature and relative humidity measured at 07:00, 14:00 and 21:00 hours on 21st July during 21 years (1986-2006) were used to obtain average dry bulb temperature and relative humidity for 21st July. These average values were

used to calculate the psychrometric properties of the each state of the system and parameters given in Table 3.4 at 07:00, 14:00 and 21:00 hours on 21st July.

Table 4.2 shows results of the psychrometric analysis of the system at 07:00 h. Fresh ambient air (26.30 ^{o}C dry bulb temperature, 85.9 % relative humidity) is sucked into the desiccant wheel. After the dehumidification process, the dry bulb temperature of fresh air increases to 52.48 ^{o}C and relative humidity decreases to 11.81 %. The fresh air leaves heat exchanger 1 and 2 at 35.56 ^{o}C and 25.15 ^{o}C, respectively. The fresh air must be brought into heat exchanger 3 in order to obtain the desired blowing temperature (18.10 ^{o}C).

The air, which is sucked from the air-conditioned room, gets hotter (26.29 ^{o}C) while passing through the fan. The waste air is humidified (93.28 % relative humidity) in order to increase saving during heat exchanger 2. In the evaporative cooler the waste air cools down to 19.54 ^{o}C. The waste air leaving the heat exchanger 2 is rejected to the outdoors (29.93 ^{o}C dry bulb temperature and 50.13 % relative humidity).

In regeneration process, the dry bulb temperature of regeneration air is increased to 43.32 ^{o}C in heat exchanger 1 and to 56.18 ^{o}C in the rotary regenerator. In order to remove moisture in the desiccant wheel, the dry bulb temperature of the regeneration air is increased to 84.44 ^{o}C with the help of electric heaters. The regeneration air leaving the desiccant wheel comes to the rotary regenerator and cools down to 46.81 ^{o}C, before discharged to the outdoors.

Table 4.3 shows results of the psychrometric analysis of the system at 14:00 h. The ambient fresh air conditions at 07:00 h and 14:00 h are different. At 14:00 h, dry bulb temperature increases up to 32.91 ^{o}C and relative humidity decreases to 53.14 %. This difference affects the fresh air process and regeneration process of the system. The amount of the moisture removed by dehumidifier decreases. Therefore, the dry bulb temperature of regeneration air, which is used to remove moisture, decreases.

Table 4.4 shows that the results of the psychrometric analysis of the system at 07:00 h and 21:00 h are almost the same. This is because of the fact that ambient air conditions (dry bulb temperature and relative humidity) are very close to each other.

Psychrometric diagrams of the system for 07:00, 14:00 and 21:00 hours on 21st July are shown in Figures 4.5-4.7, respectively.

Table 4.2. Some psychrometric properties of the system at 07:00 h on 21st July (ambient air temperature is 26.3 °C and relative humidity is 85.9 %)

State	t_{db} (°C)	W (gr/kg)	t_{wb} (°C)	RH (%)	t_{dp} (°C)	h (kJ/kg)	d (kg/m^3)
1	26.30	18.59	24.42	85.90	23.75	73.83	1.17
2	52.48	10.29	26.00	11.81	14.50	79.50	1.08
3	35.56	10.29	21.48	28.39	14.50	62.17	1.14
4	25.15	10.29	18.25	51.55	14.50	51.49	1.18
5	18.10	10.29	15.81	79.37	14.50	44.27	1.20
6	18.99	10.29	16.14	75.07	14.50	45.18	1.20
7	26.00	10.50	18.70	50.00	14.81	52.90	1.17
8	26.29	10.50	18.79	49.14	14.81	53.20	1.17
9	19.54	13.29	18.79	93.28	18.45	53.38	1.20
10	29.93	13.29	21.96	50.13	18.45	64.08	1.16
11	26.30	18.59	24.42	85.90	23.75	73.83	1.17
12	43.32	18.59	28.52	33.44	23.75	91.53	1.10
13	56.18	18.59	31.20	17.64	23.75	104.90	1.06
14	84.44	18.59	36.20	5.19	23.75	134.28	0.98
15	58.45	26.89	35.19	22.63	29.79	128.90	1.05
16	45.63	26.89	32.93	42.38	29.79	115.38	1.09
17	46.81	26.89	33.15	39.91	29.79	116.62	1.09

Table 4.3. Some psychrometric properties of the system at 14:00 h on 21st July (ambient air temperature is 32.91 °C and relative humidity is 53.14 %)

State	t_{db}(°C)	W(gr/kg)	t_{wb}(°C)	RH(%)	t_{dp}(°C)	h(kJ/kg)	d(kg/m^3)
1	32.91	16.78	25.02	53.14	22.11	76.07	1.14
2	53.20	10.28	26.17	11.40	14.50	80.22	1.07
3	40.07	10.28	22.76	22.23	14.50	66.77	1.12
4	26.73	10.28	18.76	46.94	14.50	53.10	1.17
5	17.93	10.28	15.75	80.17	14.50	44.09	1.21
6	18.84	10.28	16.08	75.74	14.50	45.02	1.20
7	26.00	10.50	18.70	50.00	14.81	52.90	1.17
8	26.29	10.50	18.79	49.14	14.81	53.20	1.17
9	19.54	13.29	18.79	93.28	18.45	53.38	1.20
10	32.60	13.29	22.72	43.09	18.45	66.82	1.15
11	32.91	16.78	25.02	53.14	22.11	76.07	1.14
12	46.10	16.78	28.17	26.23	22.11	89.74	1.09
13	51.71	16.78	29.40	19.81	22.11	95.55	1.08
14	72.81	16.78	33.51	7.56	22.11	117.42	1.01
15	52.70	23.28	32.67	25.92	27.41	113.44	1.07
16	47.10	23.28	31.60	34.24	27.41	107.57	1.09
17	48.30	23.28	31.84	32.22	27.41	108.83	1.08

Table 4.4. Some psychrometric properties of the system at 21:00 h on 21st July (ambient air temperature is 27.17 °C and relative humidity is 83.1 %)

State	t_{db}(°C)	W(gr/kg)	t_{wb}(°C)	RH(%)	t_{dp}(°C)	h(kJ/kg)	d(kg/m^3)
1	27.17	18.94	24.86	83.10	24.05	75.63	1.16
2	54.52	10.29	26.49	10.70	14.50	81.59	1.07
3	36.85	10.29	21.86	26.45	14.50	63.48	1.13
4	25.60	10.29	18.40	50.19	14.50	51.95	1.17
5	18.07	10.29	15.81	79.49	14.50	44.24	1.20
6	18.96	10.29	16.13	75.17	14.50	45.15	1.20
7	26.00	10.50	18.70	50.00	14.81	52.90	1.17
8	26.29	10.50	18.79	49.14	14.81	53.20	1.17
9	19.54	13.29	18.79	93.28	18.45	53.38	1.20
10	30.74	13.29	22.19	47.87	18.45	64.91	1.15
11	27.17	18.94	24.86	83.10	24.05	75.63	1.16
12	44.95	18.94	29.05	31.30	24.05	94.12	1.10
13	57.38	18.94	31.60	16.97	24.05	107.05	1.06
14	86.73	18.94	36.70	4.84	24.05	137.58	0.97
15	59.57	27.59	35.65	22.02	30.22	131.91	1.04
16	47.18	27.59	33.51	40.14	30.22	118.83	1.08
17	48.36	27.59	33.73	37.82	30.22	120.08	1.08

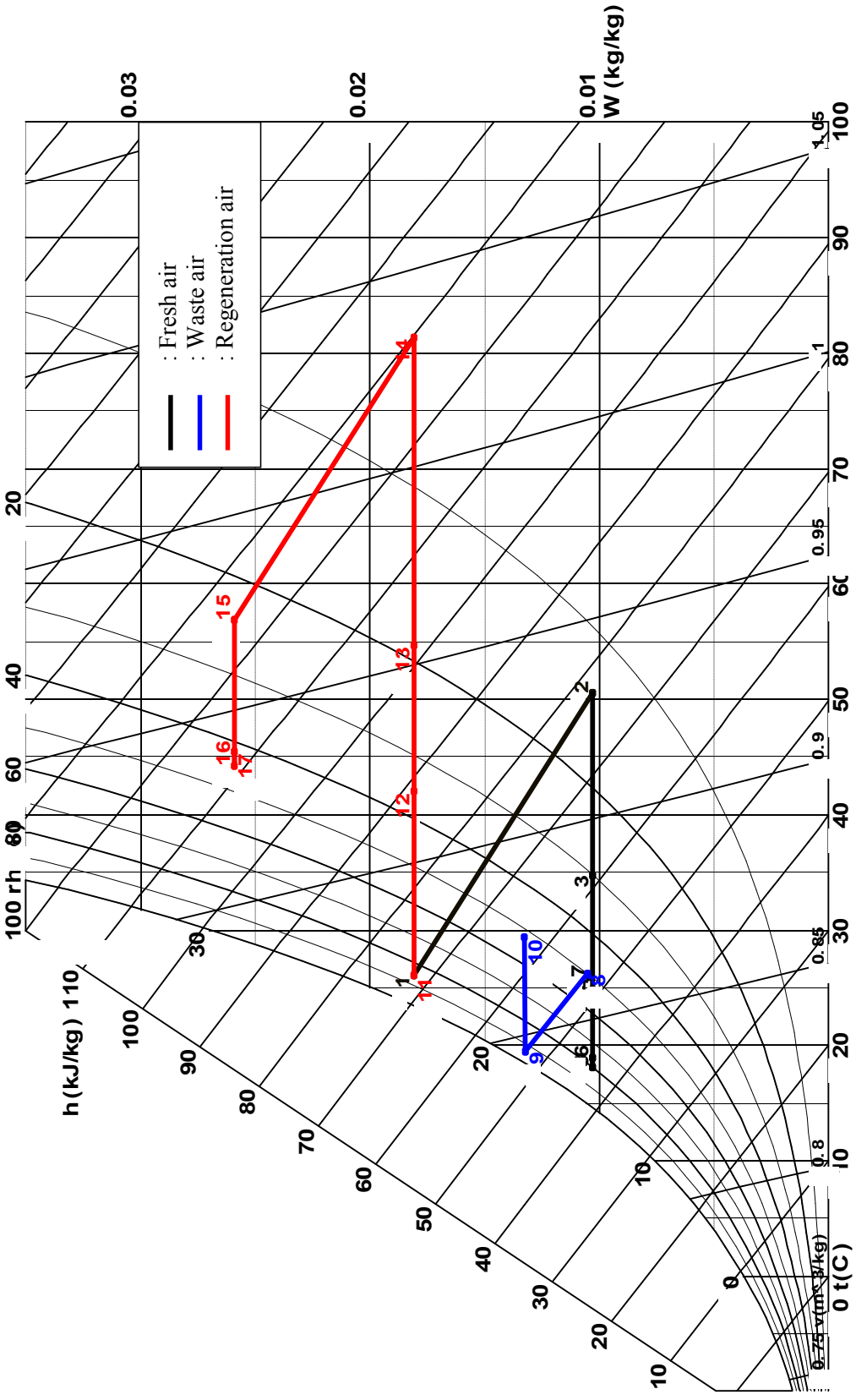

Figure 4.5. Psychrometric diagram of the system at 07:00 h on 21st July

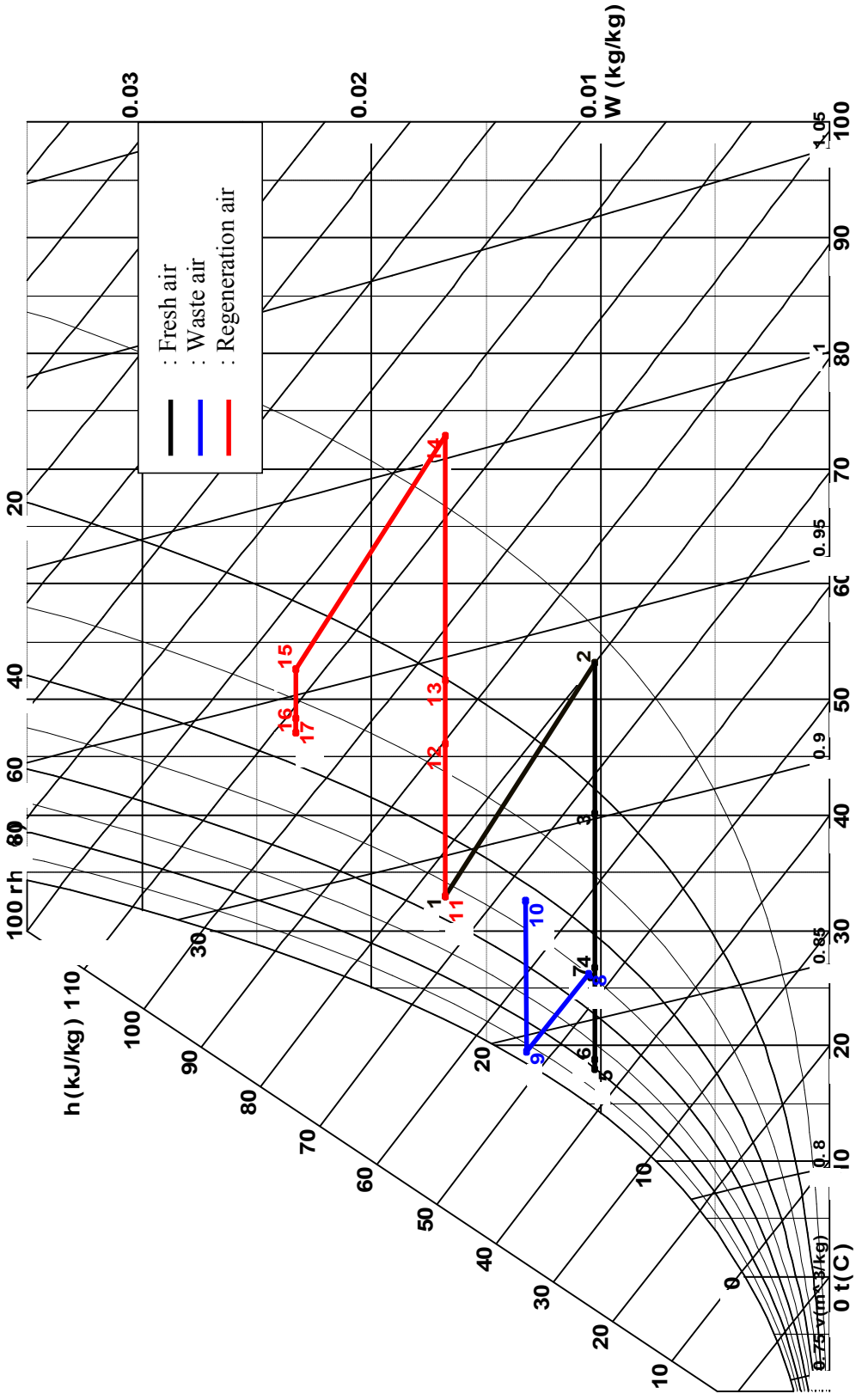

Figure 4.6. Psychrometric diagram of the system at 14:00 h on 21st July

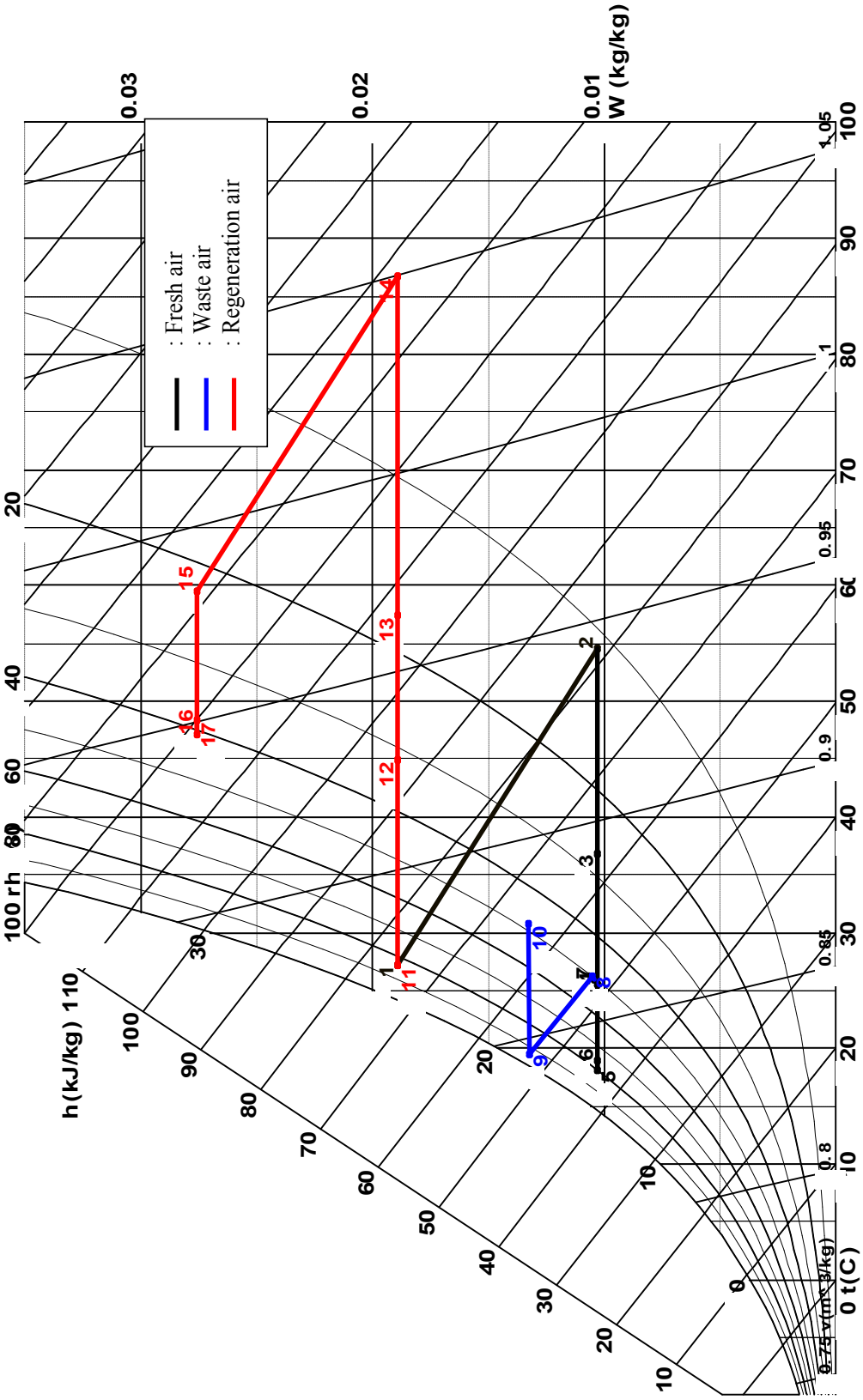

Figure 4.7. Psychrometric diagram of the system at 21:00 h on 21st July

Figure 4.8 shows the amount of heat transferred in the heat exchangers and electric heater unit at 07:00, 14:00 and 21:00 hours on 21st July. As can be seen from the figure, the amount of heat transferred in the heat exchanger 1, electric heater unit, rotary regenerator (heat exchanger 4) at 07:00 and 21:00 hours is greater than at 14:00 h. This is due to fact that the relative humidity of ambient air is higher and dry bulb temperature of ambient air is lower at 07:00 and 21:00 hours. Since the dry bulb temperature difference between regeneration air and fresh air in the heat exchanger 1 at 07:00 and 21:00 hours is greater than at 14:00 h, the amount of heat transferred in the heat exchangers 2 and 3 at 14:00 h is greater than at 07:00 and 21:00 hours. Therefore, the maximum heat transfer in the heat exchanger 1 is 24 kW at 21:00 h. The amount of heat transferred in the rotary regenerator is higher at 07:00 and 21:00 hours than at 14:00. This due to fact that, dry bulb temperature of the air leaving the desiccant wheel at 07:00 and 21:00 hours are higher than 14:00 h. Average heat transfer in the rotary regenerator is 17 kW at 07:00 and 21:00 hours.

Desiccant wheel absorbs more moisture from the fresh air at 07:00 and 21:00 hours than at 14:00 h. In order to remove moisture from the desiccant wheel, more heat must be given to regeneration air by the electric heaters. The amount of heat given by the electric heaters is approximately 38 kW at 07:00 and 21:00 hours. The reason of the maximum heat transfer in the heat exchanger 2 and 3 at 14:00 h is that the dry bulb temperature of the fresh air at the exit of heat exchanger 1 is higher at 14:00 h than at 07:00 h and 21:00 h.

Figures 4.9-4.11 show the amount of heat transferred in the heat exchangers and electric heater unit during summer season (from June to September) at 07:00, 14:00 and 21:00 hours, respectively. Heat load required for removing moisture (state 13-14) on desiccant wheel is between 8 to 42 kW at 07:00 h, between 3 to 30 kW at 14:00 h, and between 13 to 43 kW at 21:00 h. It can also be seen from these figures that the amount of heat transferred in the heat exchangers starts to increase in June, reaches to the maximum level in July and August and decreases in September. If the daily period is considered, the amount of heat transfers in each heat exchanger at 07:00 h and 21:00 h are greater than at 14:00 h.

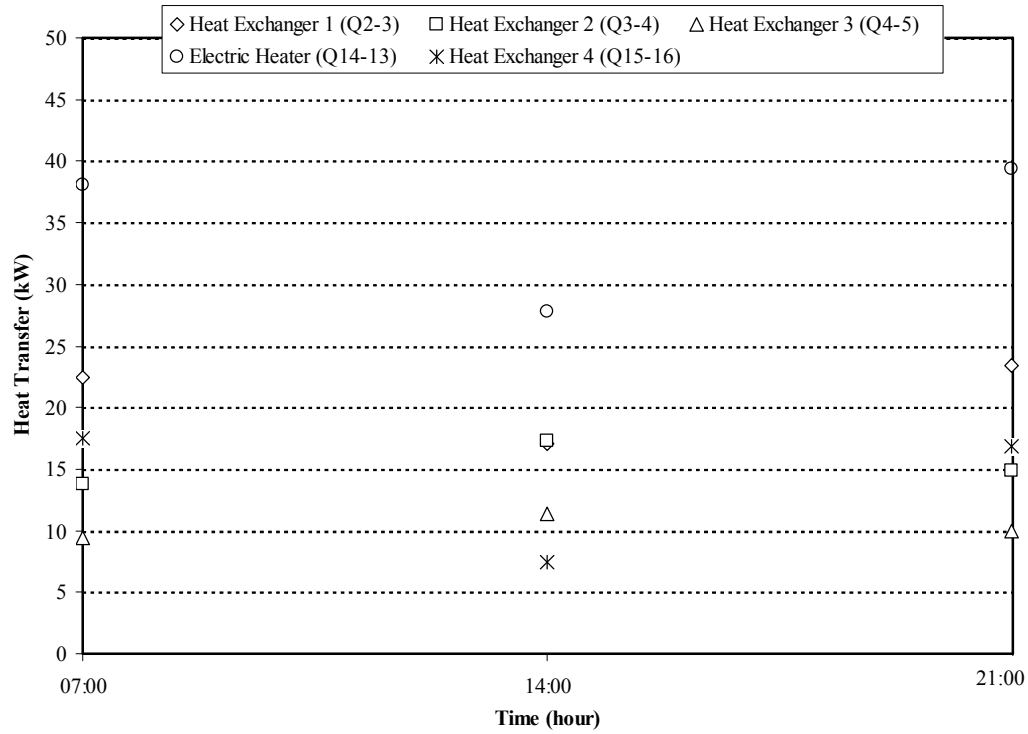

Figure 4.8. Amount of heat transferred in the heat exchangers at 07:00, 14:00 and 21:00 hours on 21st July

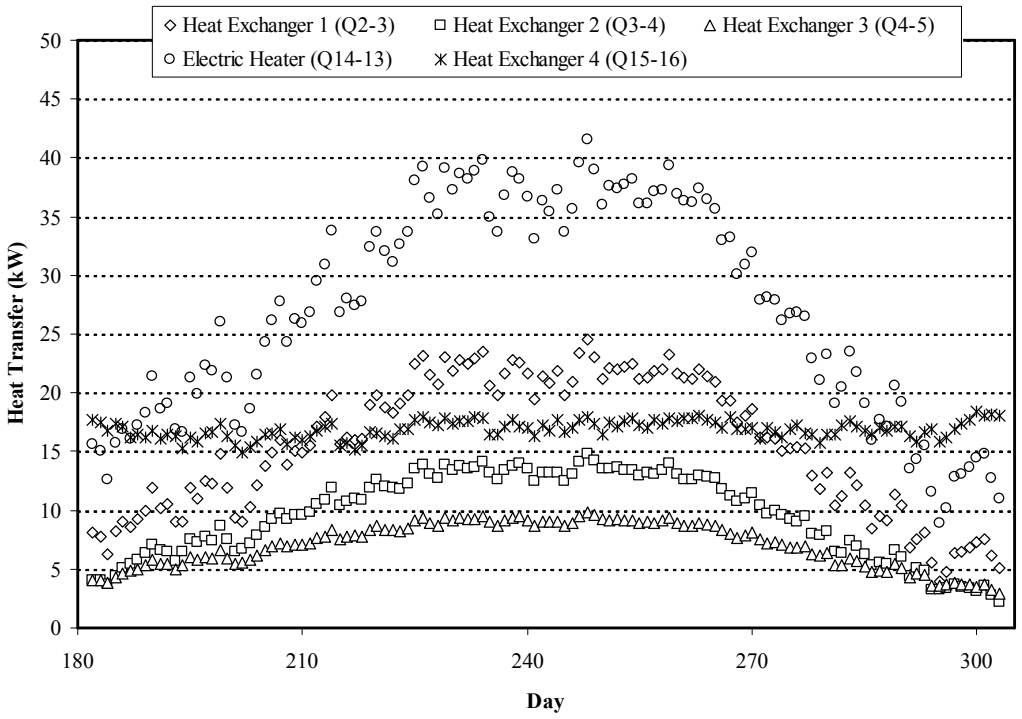

Figure 4.9. Amount of heat transferred in the heat exchangers and electric heater unit at 07:00 h during summer season

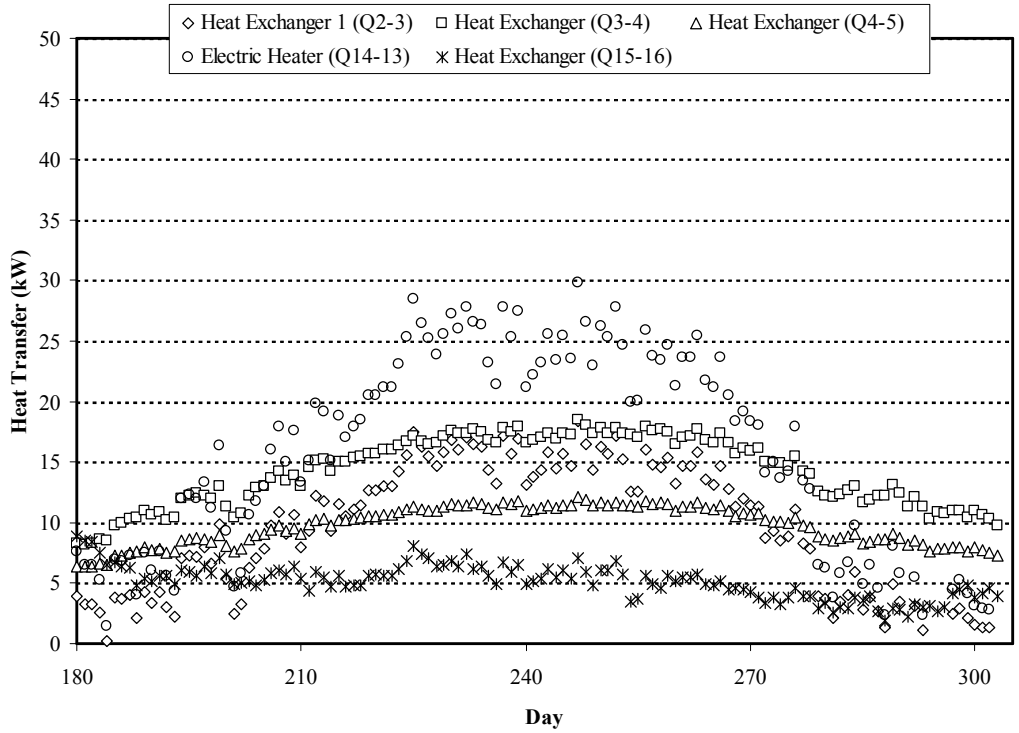

Figure 4.10. Amount of heat transferred in the heat exchangers and electric heater unit at 14:00 h during summer season

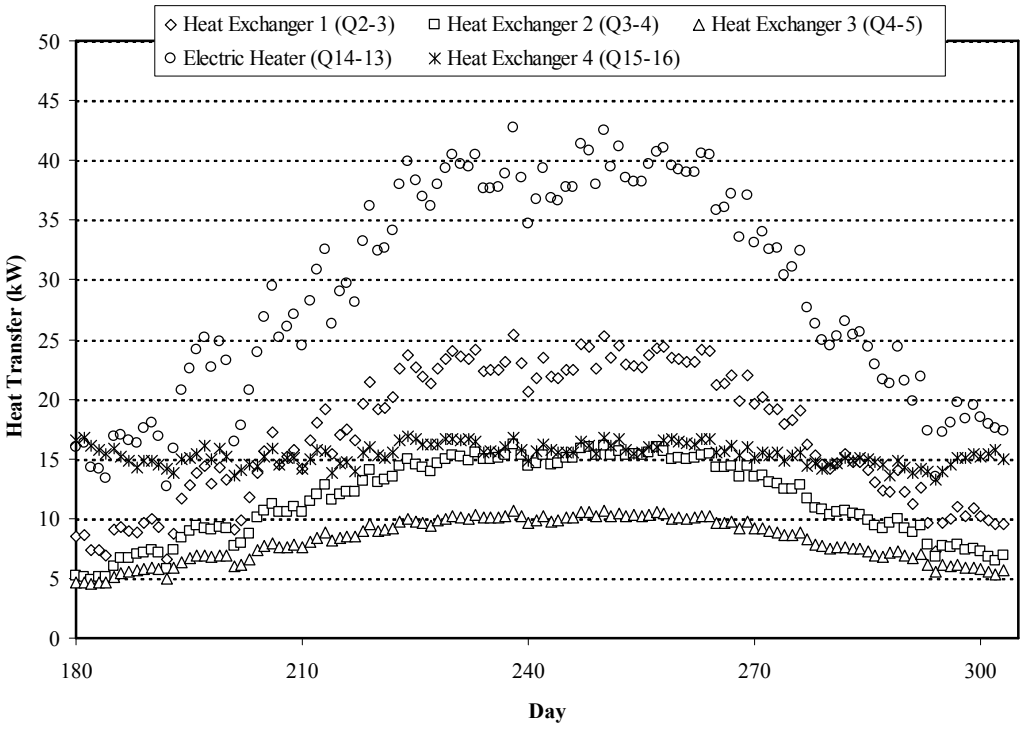

Figure 4.11. Amount of heat transferred in the heat exchangers and electric heater unit at 21:00 h during summer season

4.3. Results Obtained from the Experiments

The results obtained from the experiments during the cooling season of 2008, were evaluated to determine the performance characteristics of the system investigated. Two series of experiments were carried out in the system. In the first series, flow rate of the air streams (fresh, waste and regeneration) were kept constant with a value of 4000 m^3/h (the R/P ratio (regeneration air/process air) is 1). In the second series, flow rate of the fresh and waste air streams were adjusted to a constant value of 4000 m^3/h, but flow rate of the regeneration air stream was kept constant with a value of 3000 m^3/h (the R/P ratio is 3/4). These very high flow rate values were selected to simulate very high-standard hygienic air-conditioning (ASHRAE, Applications Handbook, 2003), which in turn leads to very high cooling loads. Temperature and relative humidity of the air-conditioned room were adjusted 26 ^oC and 50%, respectively, according to ASHRAE comfort zone (ASHRAE Fundamentals Handbook, 2001).

4.3.1. Results of the Experiments Carried out with Equal Process and Regeneration Air Flow Rates

Table 4.5 shows the test conditions of the experiments that were carried out with equal process and regeneration air flow rates. Figures 4.12-4.16 present dry bulb temperatures and relative humidities of air measured at the states shown in Figure 3.1 during a typical experiment (Test ID-290708). At the beginning of the test, regeneration temperature is set to 120 ^oC. Figures 4.12-4.15 show variation of dry bulb temperature during the day at different states for fresh, waste and regeneration air streams, respectively. As can be seen from the figures, all the air temperatures except the ambient (T_1 and T_{11}) and the air-conditioned room (T_7) fluctuate with time. The fluctuations originate from the start-up and shut-down of the electric heaters, which is needed for the control of humidity in the air-conditioned room.

Table 4.5. Experiments that were carried out at equal process and regeneration air flow rates

Test ID	Regeneration Temperature Set Value (°C)	Air Conditioned Room Temperature Set Value (°C)	Air Conditioned Room Relative Humidity Set Value (%)	Tank Water Temperature Set Value (°C)	Daily Average Ambient Temperature (°C)	Daily Average Ambient Relative Humidity (%)	Daily Average Ambient Humidity Ratio (kg/kg)
300708	80	26	50	7	32.41	56.09	0.0171
310708	80	26	50	7	32.54	45.47	0.0139
010808	80	26	50	7	32.20	50.91	0.0152
040808	80	26	50	7	31.94	57.00	0.0164
070808	80	26	50	7	31.88	53.50	0.0158
080808	80	26	50	7	31.93	57.00	0.0169
130808	80	26	50	7	30.72	60.65	0.0169
020708	100	26	50	7	30.58	50.76	0.0139
030708	100	26	50	7	30.99	51.50	0.0145
040708	100	26	50	7	31.17	45.30	0.0127
070708	100	26	50	7	31.50	47.88	0.0138
090708	100	26	50	7	31.23	46.99	0.0133
100708	100	26	50	7	31.70	52.20	0.0153
140808	100	26	50	7	31.83	55.36	0.0164
150708	120	26	50	7	31.90	51.30	0.0152
160708	120	26	50	7	32.24	52.03	0.0157
170708	120	26	50	7	31.71	56.15	0.0165
210708	120	26	50	7	32.15	56.10	0.0169
290708	120	26	50	7	31.54	55.07	0.0161
150808	120	26	50	7	31.48	57.61	0.0167

As can be seen from Figure 4.12, dry bulb temperature of fresh ambient air that enters the fresh air channel at 28 °C (T_1), increases to 55–60 °C (T_2) after the dehumidification process and then its temperature decreases down to blowing temperature (approximately 22 °C) by passing through the heat exchangers ($T_2 \rightarrow T_6$).

Figure 4.13 shows dry bulb temperature of waste air stream at different states. It can be seen that after a short time (30 min), dry bulb temperature of the air-conditioned room (T_7) decreases down to set value 26 ^oC and remains constant rest of the day. It can also be seen from the figure that temperature of the air sucked from the room (T_7) is decreased down to 20 ^oC (T_9) with the help of the evaporative cooler before entering into heat exchanger 2.

Variation of regeneration temperature (T_{14}) during the day is shown in Figure 4.14. Although the regeneration temperature is set to 120 ^oC in this test, maximum temperature remains around 100 ^oC. This is because, when the relative humidity at the air-conditioned room reaches to the set value of 50%, the electric heaters shut-down. Therefore, without the need of regeneration temperature to reach 120 ^oC, the desired humidity value is obtained in the room.

Figure 4.15 shows the relative humidities measured during the day at different states. As can be seen from the figure, relative humidity of the air-conditioned room changes around the set value of 50% within a band of ±3%. Similar fluctuations with different amplitudes are also evident in the humidities at states 3, 6, 9 and 16. In this study, control of the humidity inside the air-conditioned room is achieved with the control of the temperature of the regeneration air. Due to the thermal inertia of the electric heaters, the dehumidifier and the air mass inside the channels, it is not possible to keep the humidity inside the air-conditioned room steady. However, amplitude of the fluctuations can be minimized by feeding the influence of the parameters above into the PLC. It can also be seen from the figure that humidity of the waste air is increased from 50% to approximately 95% by the evaporative cooler.

Figure 4.16 shows all the processes on a psychrometric diagram at 10:30 am.

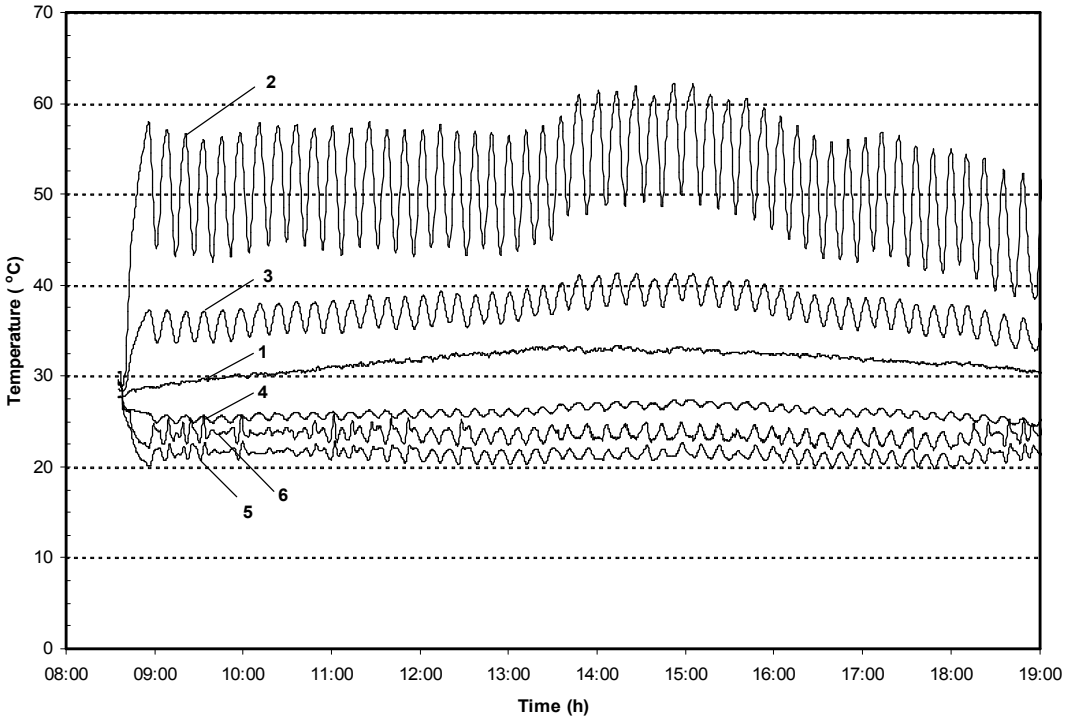

Figure 4.12. Variation of dry bulb temperature during the day at different states for fresh air stream (Test ID-290708)

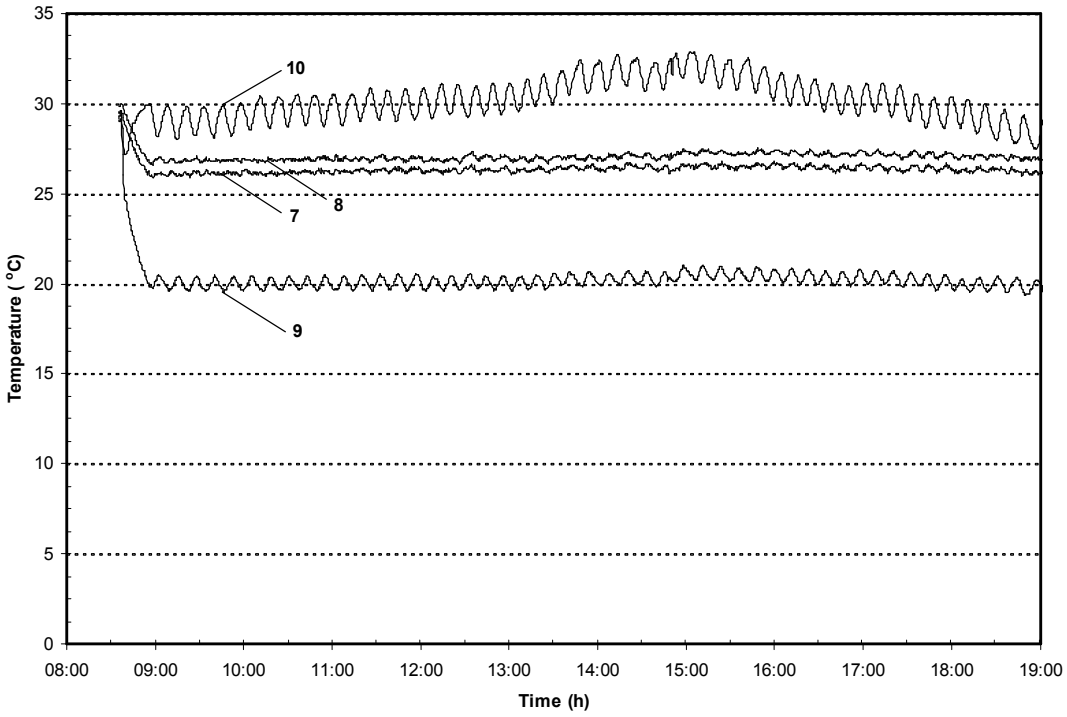

Figure 4.13. Variation of dry bulb temperature during the day at different states for waste air stream (Test ID-290708)

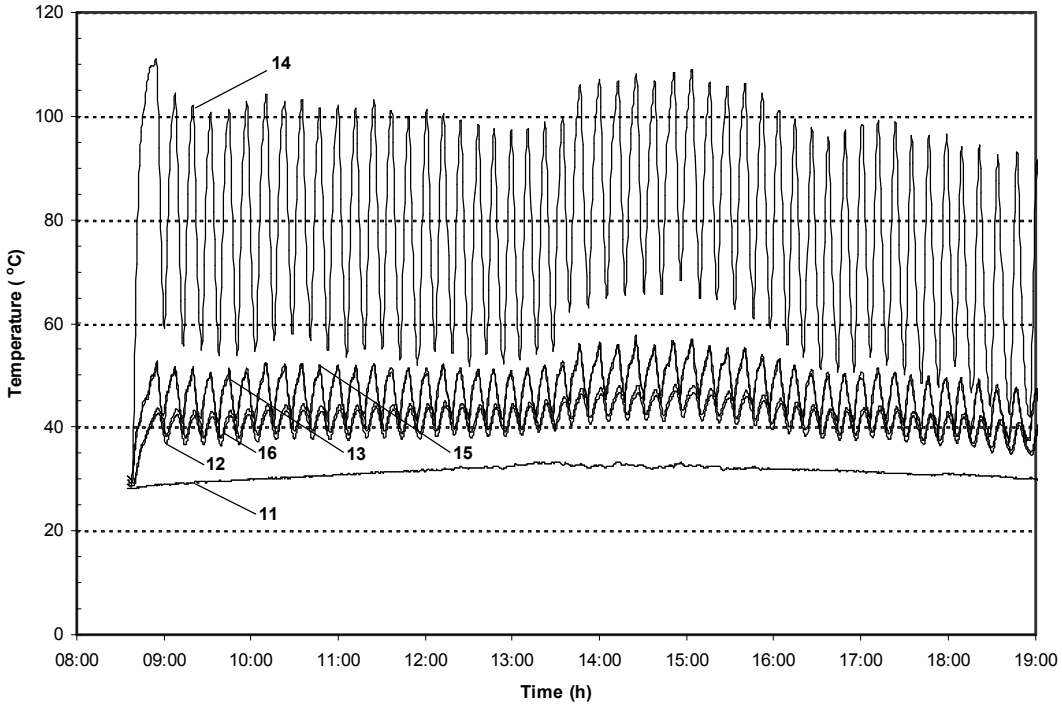

Figure 4.14. Variation of dry bulb temperature during the day at different states for regeneration air stream (Test ID-290708)

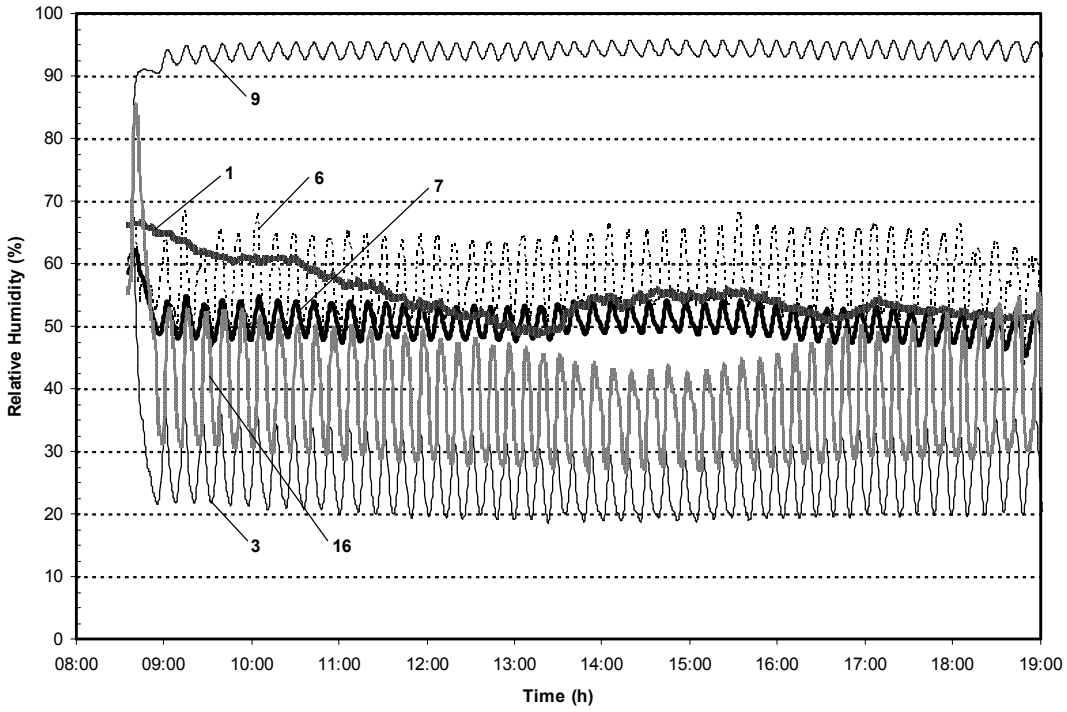

Figure 4.15. Variation of relative humidity during the day at different states (Test ID-290708)

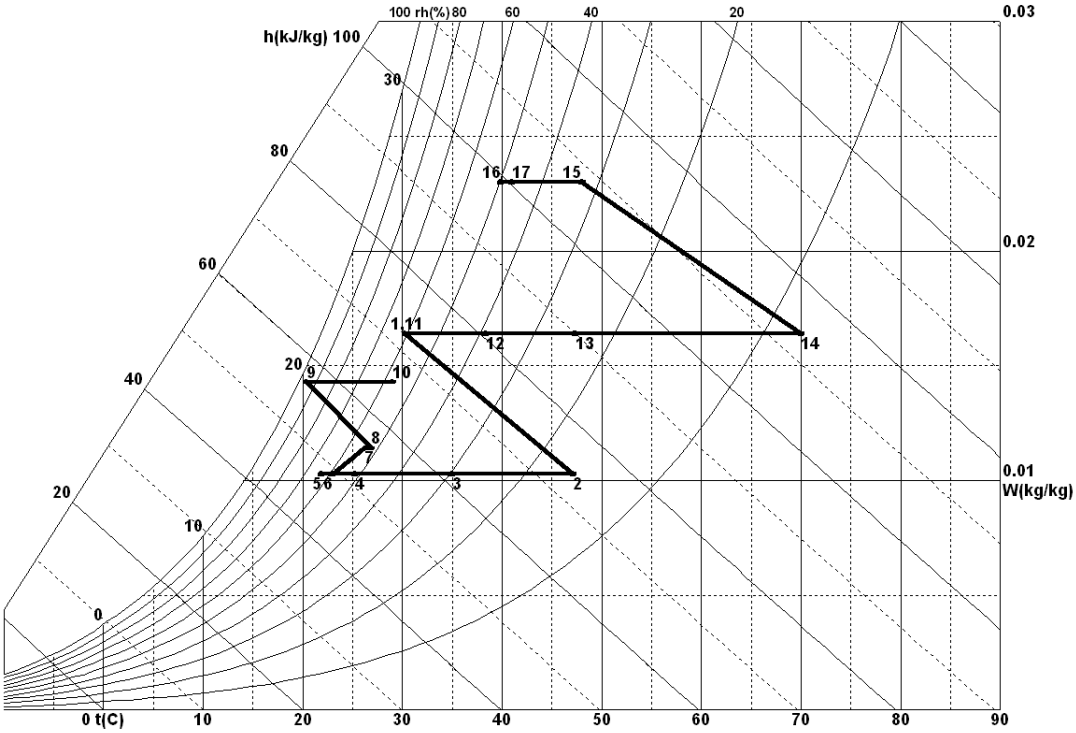

Figure 4.16. Psychrometric diagram showing all processes at 10:30 am. (Test ID-290708)

Variation of effectiveness of the evaporative cooler and the heat exchangers during the day is shown in Figure 4.17. Effectiveness is approximately 65-75% for heat exchangers 1 and 2, 60% for heat exchanger 3, and 90% for heat exchanger 4 and the evaporative cooler. It can be seen from the figure that fluctuations are evident in the effectiveness values, again due to start-up and shut-down of the electric heaters to control the humidity in the air-conditioned room.

Temperature of the fresh ambient air increases significantly during the dehumidification process. It is precooled in heat exchangers 1 and 2 before brought to the desired blowing temperature in heat exchanger 3. Figure 4.18 presents the contribution of each heat exchanger to the total cooling requirement after dehumidification process (state 2 to 5) in percentage. As can be seen from the figure, approximately 45% of cooling requirement is met by heat exchanger 1, 40% by heat exchanger 2 and the remaining 15% by heat exchanger 3 (cooling coil). It is clear that use of heat exchangers 1 and 2 reduces significantly the cooling requirement. Approximately 85% of cooling is met without any external energy consumption.

Temperature of the regeneration air is a very important parameter for the moisture removal from the supply air. Regeneration air is preheated with the help of heat exchangers 1 and 4 before brought to the final regeneration temperature by the external regeneration heat source. Contribution of heat exchangers 1 and 4, and the regeneration heat to the total heating in percentage is given in Figure 4.19. Approximately 65% of the heating requirement is met by the regeneration heat, 25% by heat exchanger 1 and 10% by heat exchanger 4. Use of heat exchangers 1 and 4 reduces the heating requirement approximately 35%.

Daily total contribution of heat exchangers 1 to 4 and the regeneration heat to the heating and cooling requirement is presented in Figure 4.20. The contribution of heat exchangers 1 and 2 can clearly be seen from the figure.

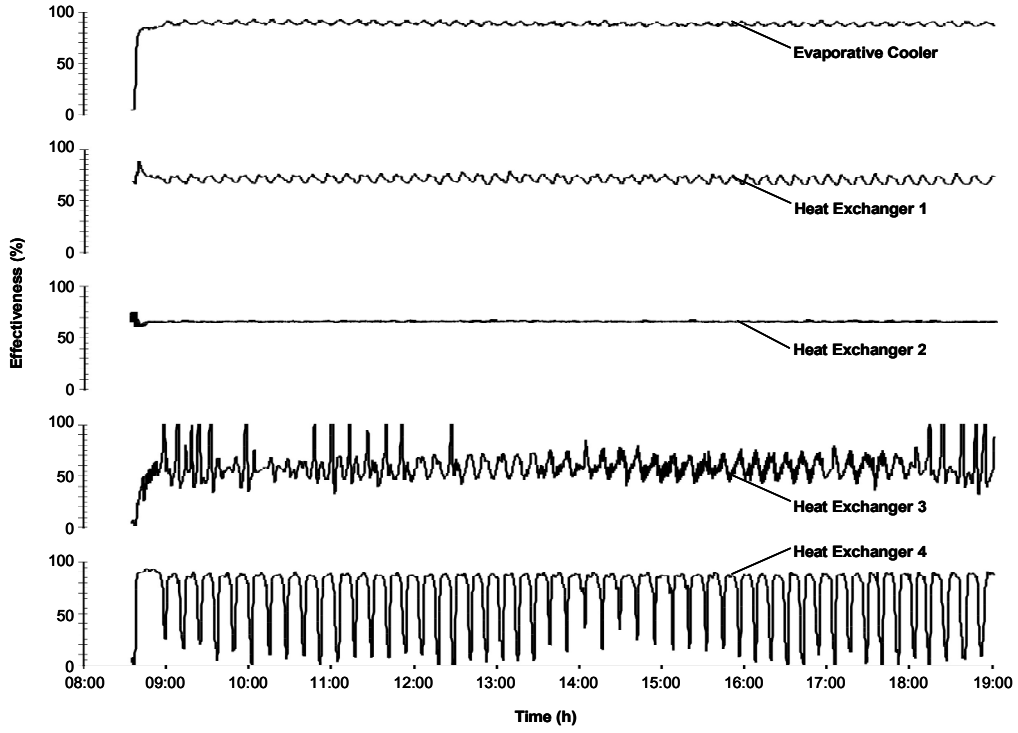

Figure 4.17. Variation of effectiveness of evaporative cooler and heat exchangers during the day (Test ID-290708)

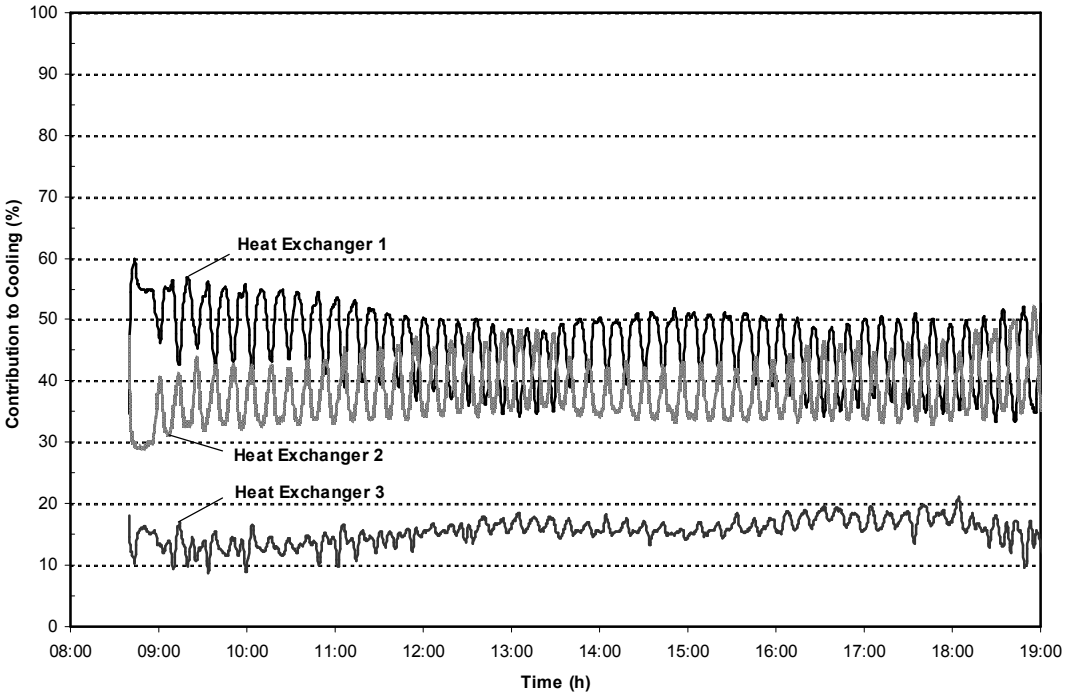

Figure 4.18. Contribution of heat exchangers 1-3 to total cooling (Test ID-290708)

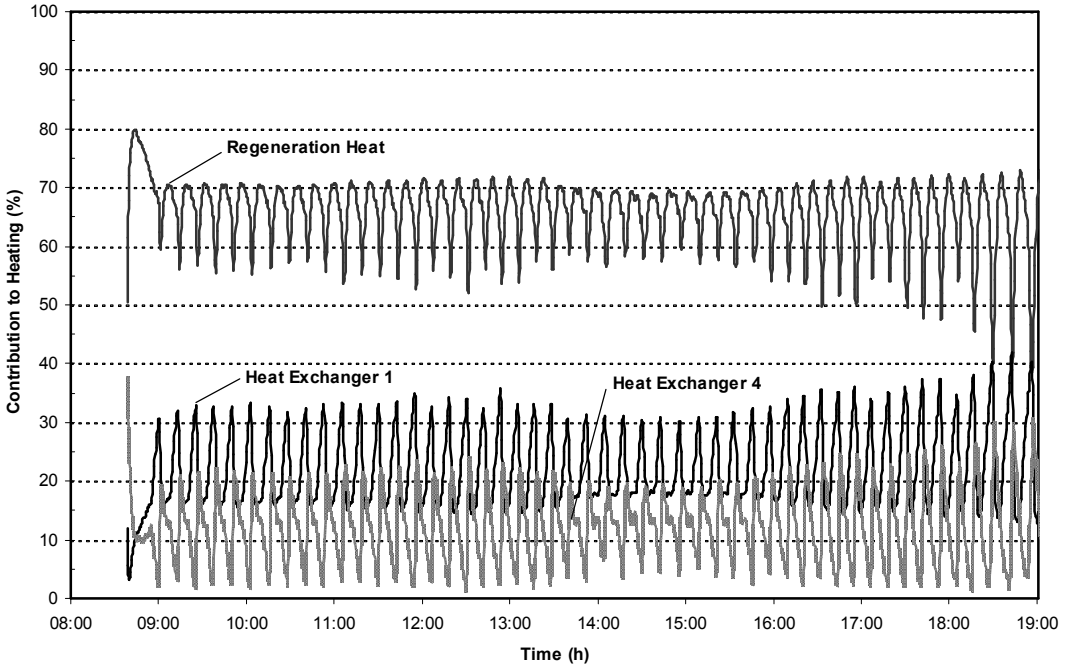

Figure 4.19. Contribution of heat exchangers 1 and 4, and regeneration heat to the total heating (Test ID-290708)

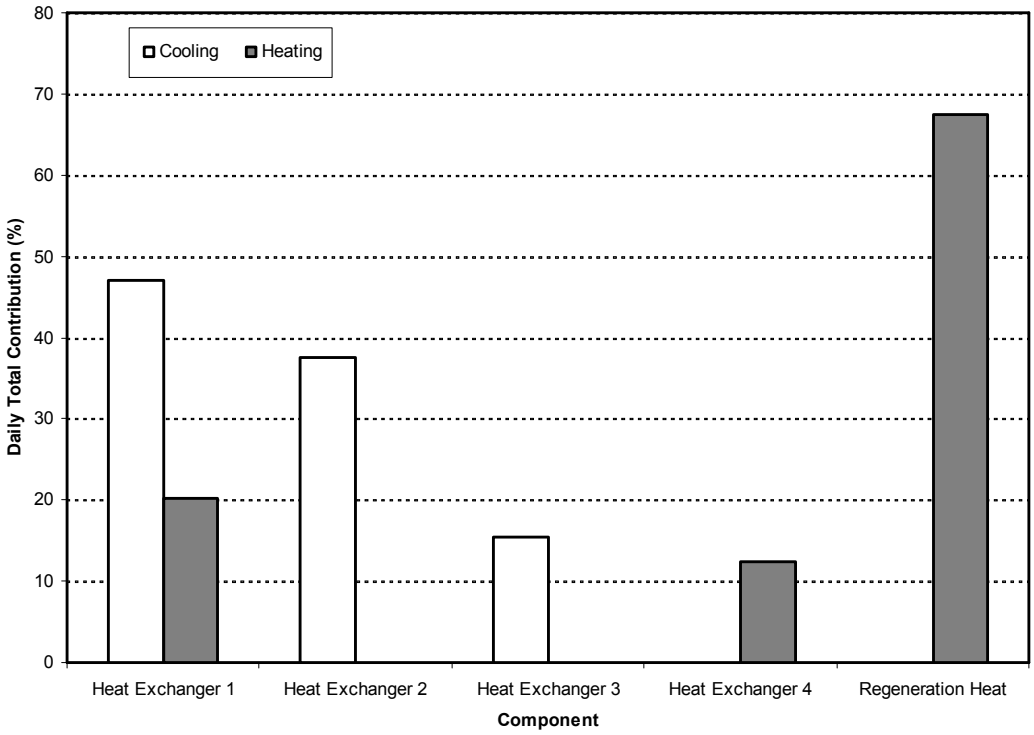

Figure 4.20. Daily total contribution of heat exchangers 1-4 and regeneration heat to the heating and cooling requirement (Test ID-290708)

To provide comfort conditions in the air-conditioned room, in addition to the regeneration heat, which is produced by the electric heaters in this study, the fans, the refrigeration unit and other auxiliary electrical components (motors of the dehumidifier, the regenerator and the water pumps) consume energy. Sum of all these constitute total energy consumption ($\dot{E}_{tot}$). Figure 4.21 shows the energy consumption of these units. Although power consumption of the fans and the auxiliary electrical components is constant during the day, variations in the regeneration heat and the refrigeration unit are significant.

The maximum energy consumption occurs in regeneration heat (Figure 4.22). It is followed by the fans, compressor of the refrigeration unit and other electrical components. The figure shows the importance of using cheap heat source in desiccant cooling systems.

Figure 4.23 shows variation of cooling capacity during the day. Cooling capacity exhibits fluctuations with a magnitude of approximately ±5 kW. An average

30 kW of cooling effect is produced by the system to provide comfort conditions in the air-conditioned room.

Variation of moisture removal during the day is shown in Figure 4.24. As can be seen from the figure on average 0.007 kg/s moisture is removed from the ambient air in the desiccant wheel during the experiment.

Coefficient of performance (COP) of the system is shown in Figure 4.25. Although COP changes between 0.4 and 4 according to the electric heaters switching on or off, the daily mean value is 1.35. This value is in the range of the COP values reported in the literature for these kinds of systems.

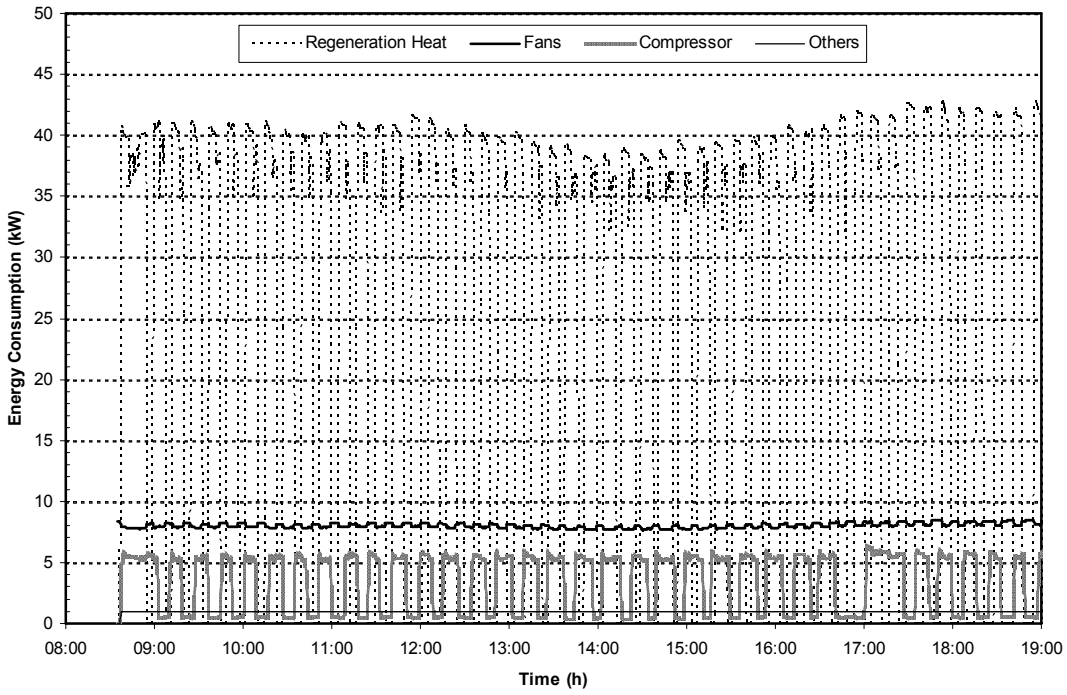

Figure 4.21. Variation of energy consumption of regeneration heat and each electrical component during the day (Test ID-290708)

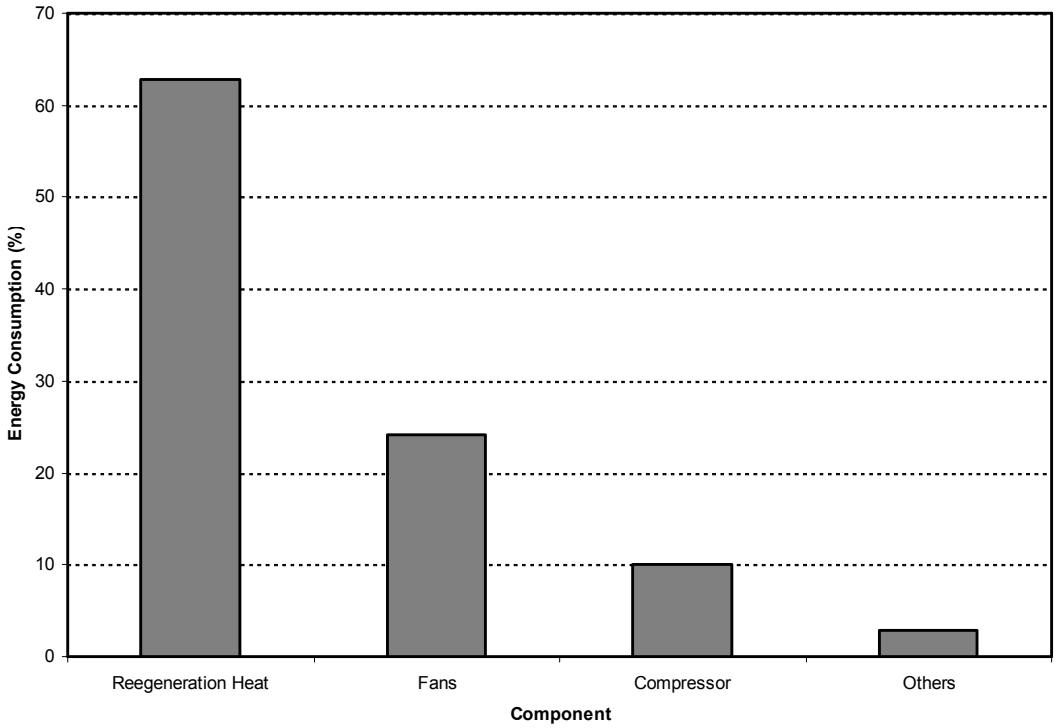

Figure 4.22. Daily total energy consumption of regeneration heat and each electrical component (Test ID-290708)

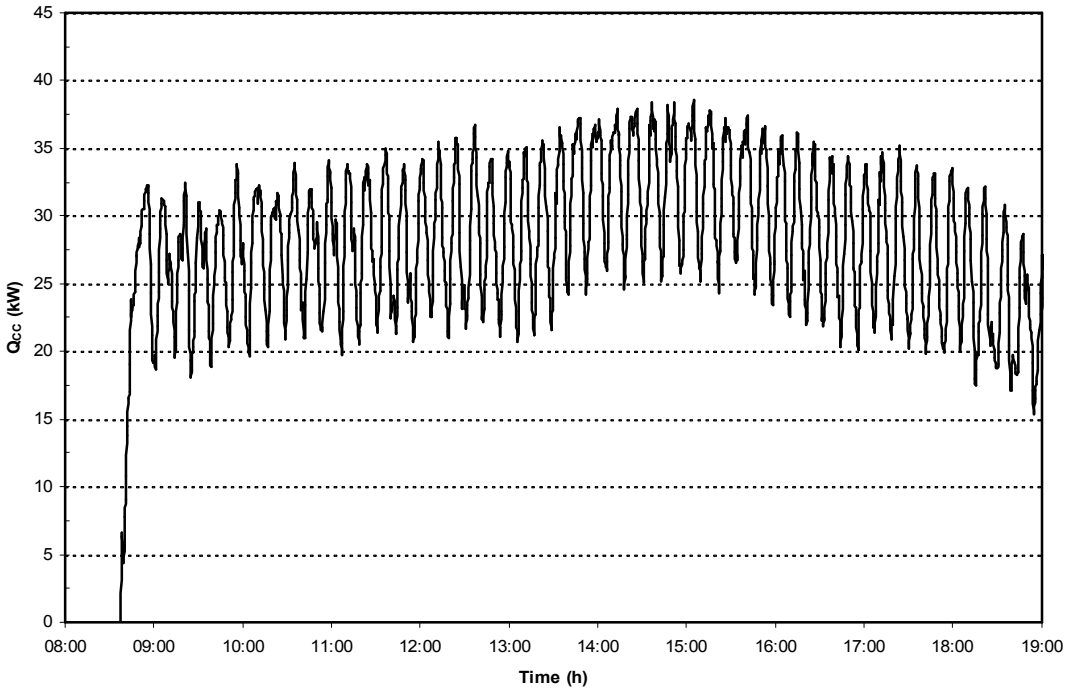

Figure 4.23. Variation of cooling capacity during the day (Test ID-290708)

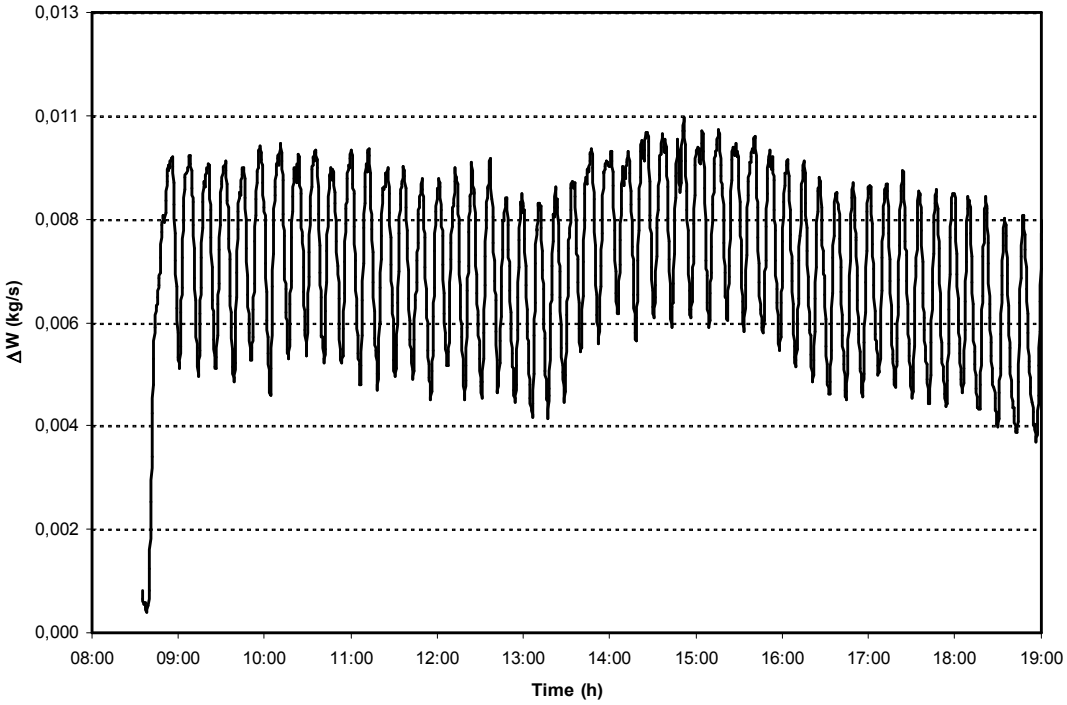

Figure 4.24. Variation of moisture removal during the day (Test ID-290708)

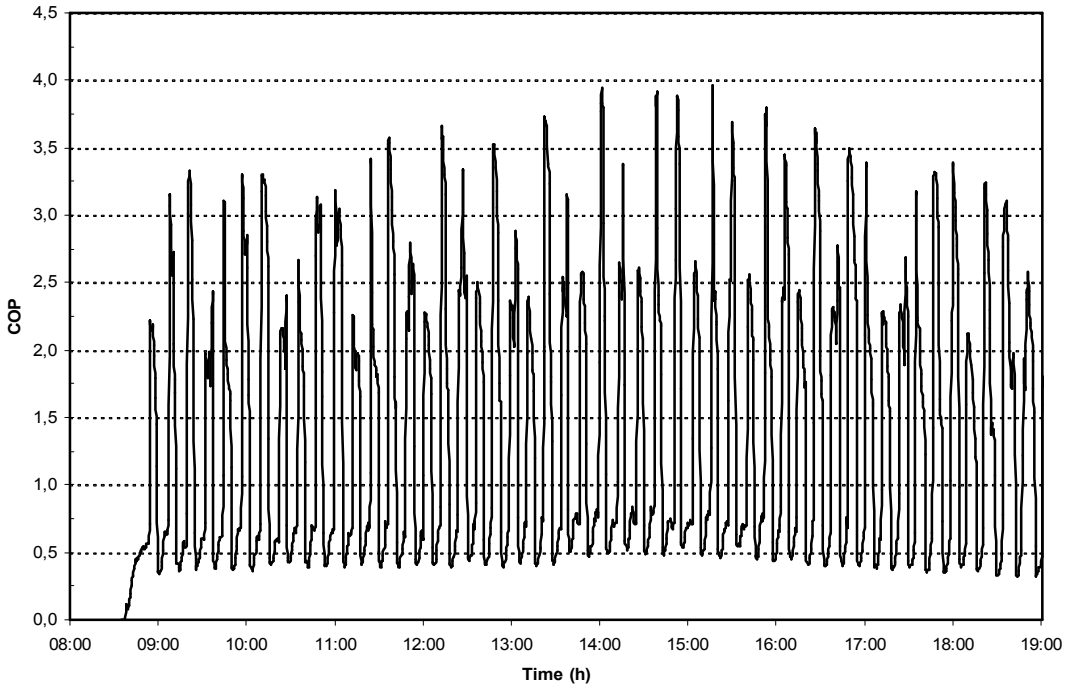

Figure 4.25. Variation of coefficient of performance during the day (Test ID-290708)

Similar results are obtained from the other experiments given in Table 4.5. As can be seen from the figures (Figures 4.12-4.25), the measured and the calculated parameters fluctuate with time because of the automatic control strategy of the system as explained in Section 3.6.8. This makes analyzing the effect of parameters on the system complicated. Therefore, it was decided to carry out the analysis in terms of daily average or daily total values of the parameters (moisture removal, energy consumptions, cooling effect, COP). Daily average values of ambient air conditions and regeneration temperature set value are given in Table 4.5 for the experiments performed.

Figures 4.26-4.27 show effect of daily average ambient temperature ($T_{a,da}$) and regeneration temperature (T_r) on daily total moisture removal (ΔW_{dt}, kg) for different regeneration temperature set values (80, 100 and 120). It is clear from the figures that there is no correlation between the ambient or regeneration temperatures and daily total moisture removal for the experiments carried out with equal process and regeneration air flow rates (R/P=1).

Effect of daily average ambient relative humidity ($\varphi_{a,da}$) and humidity ratio ($W_{a,da}$) on daily total moisture removal for different regeneration temperature set values is shown in Figures 4.28-4.29. As can be seen from the figures, the amount of daily total moisture removal increases with the increase of relative humidity and humidity ratio for all regeneration temperature set values. However, regeneration temperature has no considerable effect on daily total moisture removal.

From the results of experiments carried out with equal process and regeneration air flow rates (R/P=1), it was found that there is no correlation between the ambient or regeneration temperature and daily average or daily total parameters (energy consumptions, cooling effect, COP). Effect of ambient relative humidity and humidity ratio on the daily average or daily total parameters is almost same as seen from the Figures 4.28-4.29. Therefore, only the relations between daily average humidity ratio and other parameters (energy consumptions, cooling effect and COP) are given below.

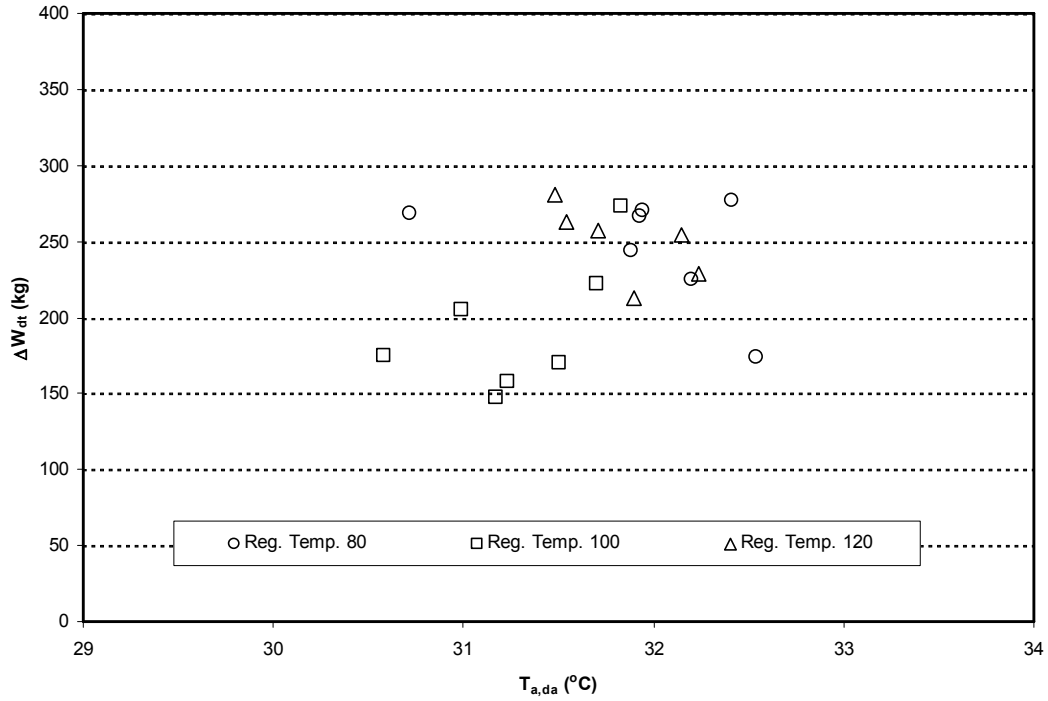

Figure 4.26. Effect of daily average ambient temperature on daily total moisture removal for different regeneration temperature set values (R/P=1)

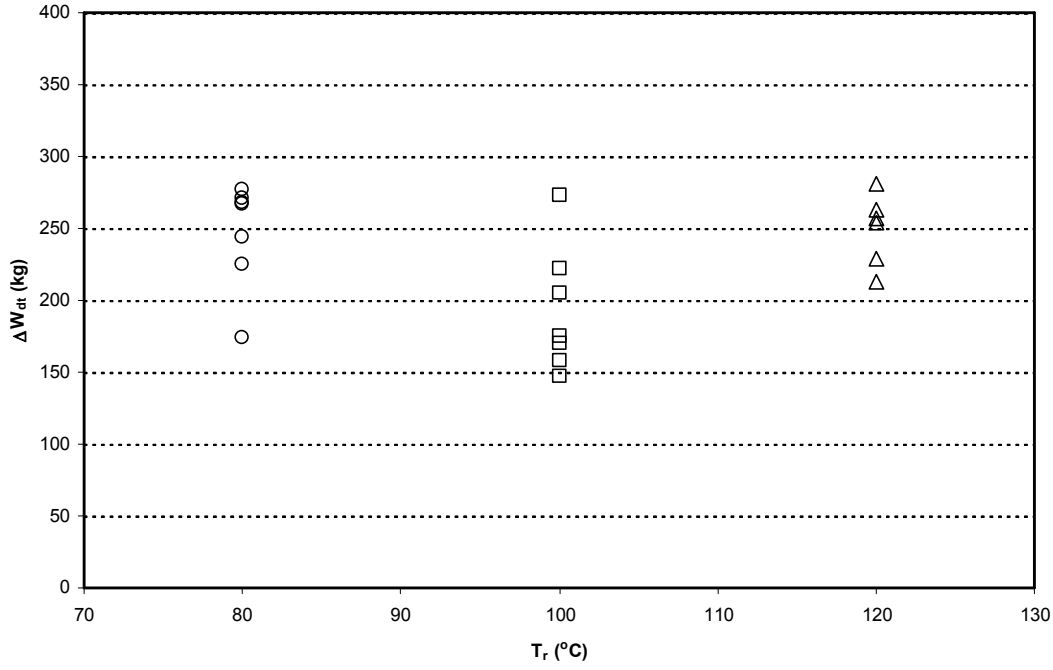

Figure 4.27. Effect of regeneration temperature on daily total moisture removal for different regeneration temperature set values (R/P=1)

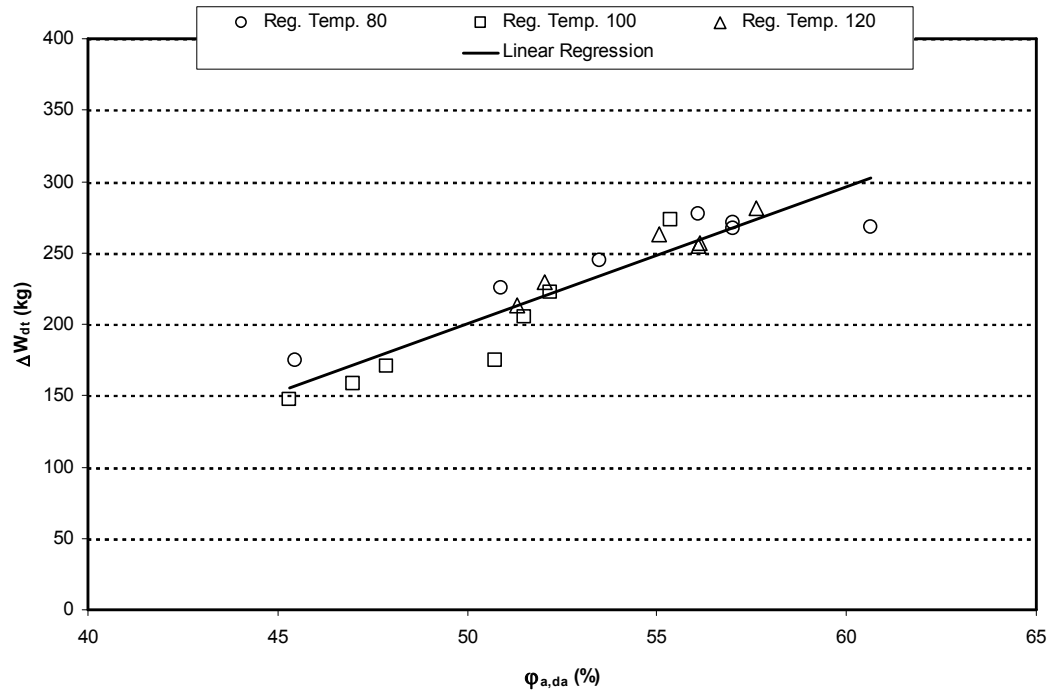

Figure 4.28. Effect of daily average ambient relative humidity on daily total moisture removal for different regeneration temperature set values (R/P=1)

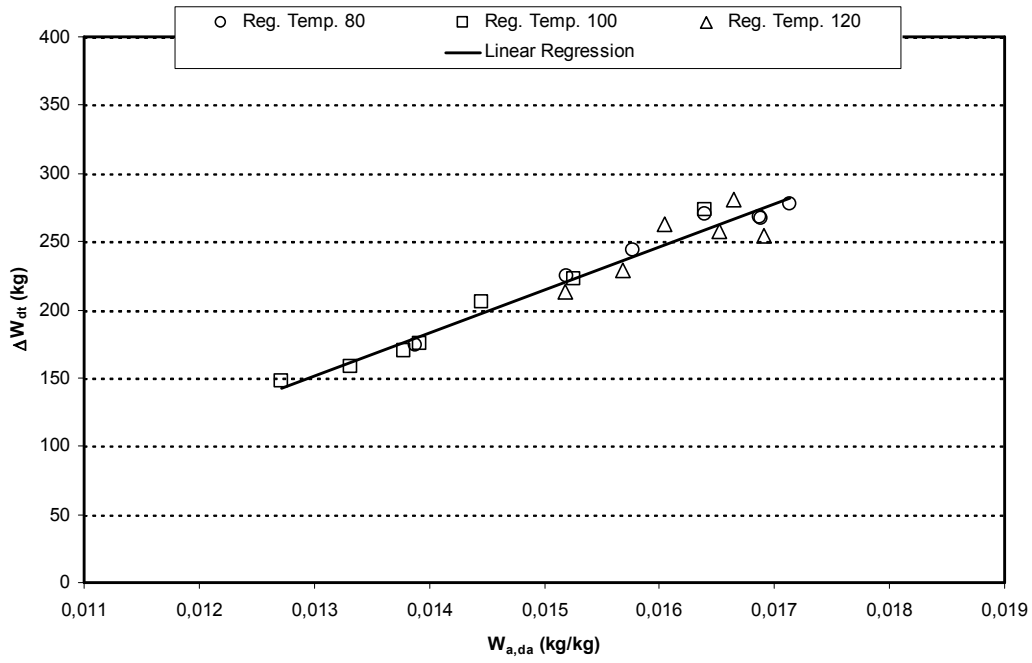

Figure 4.29. Effect of daily average ambient humidity ratio on daily total moisture removal for different regeneration temperature set values (R/P=1)

Figure 4.30 shows the effect of daily average ambient humidity ratio on daily total regeneration heat ($Q_{reg,dt}$, kJ) for different regeneration temperature set values. As can be seen from the figure, for all regeneration temperature set values, the amount of daily total regeneration heat increases with the increase of ambient humidity ratio. However, regeneration temperature has no considerable effect on daily total regeneration heat. Similar results are obtained for daily total energy consumption of the system ($E_{tot,dt}$, kJ) and daily total cooling capacity ($Q_{CC,dt}$, kJ) (Figures 4.31-4.32).

Effect of daily average ambient humidity ratio on daily average coefficient of performance of the system (COP_{da}) for different regeneration temperature set values is shown in Figures 4.33. It is clear from the figure that COP_{da} decreases with the increase of ambient humidity ratio for all regeneration temperature set values. However, regeneration temperature has no considerable effect on COP_{da}. Least-square method was applied to the data obtained from the experiments and the equation given below is obtained.

$$COP_{da} = 1.52\text{-}35.80^{*} W_{a,da} \quad (R/P=1) \tag{4.7}$$

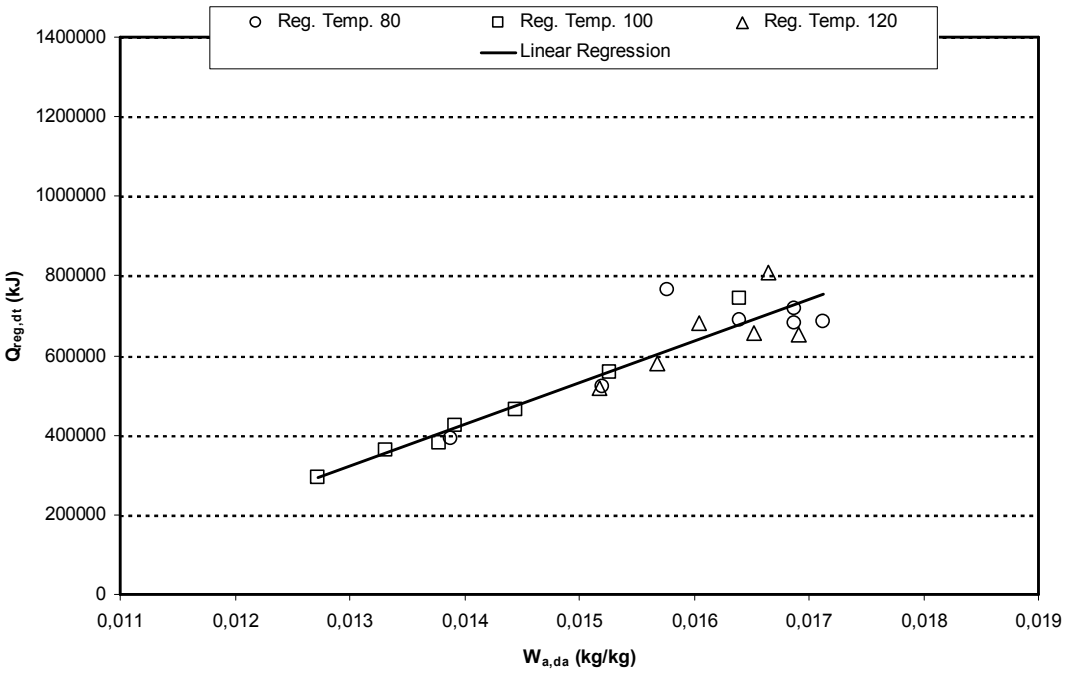

Figure 4.30. Effect of daily average ambient humidity ratio on daily total regeneration heat for different regeneration temperature set values (R/P=1)

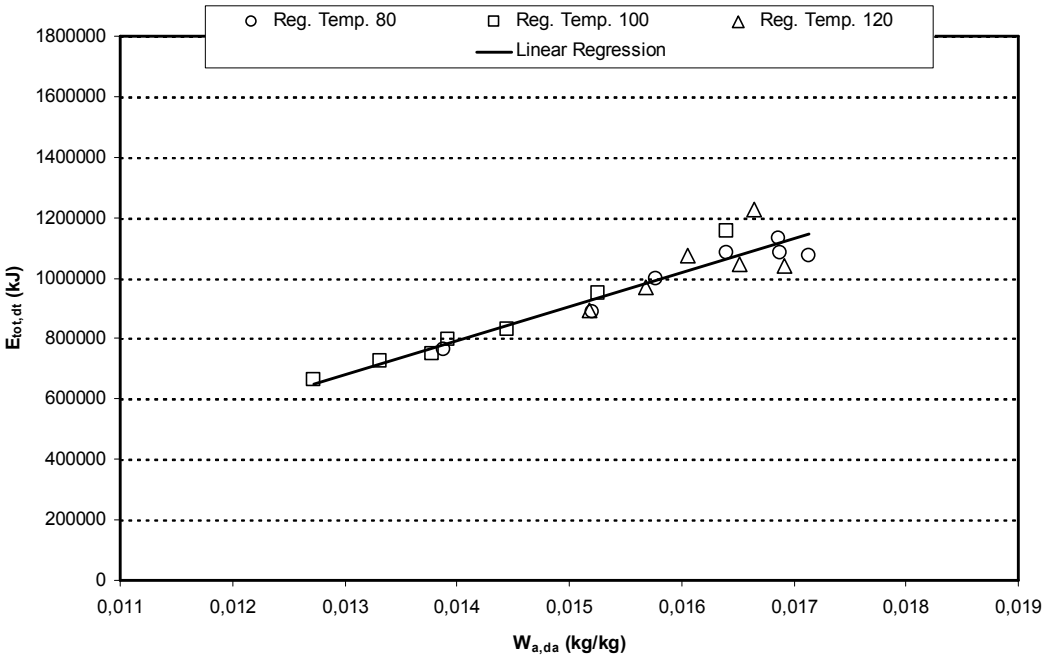

Figure 4.31. Effect of daily average ambient humidity ratio on daily total energy consumption of the system for different regeneration temperature set values (R/P=1)

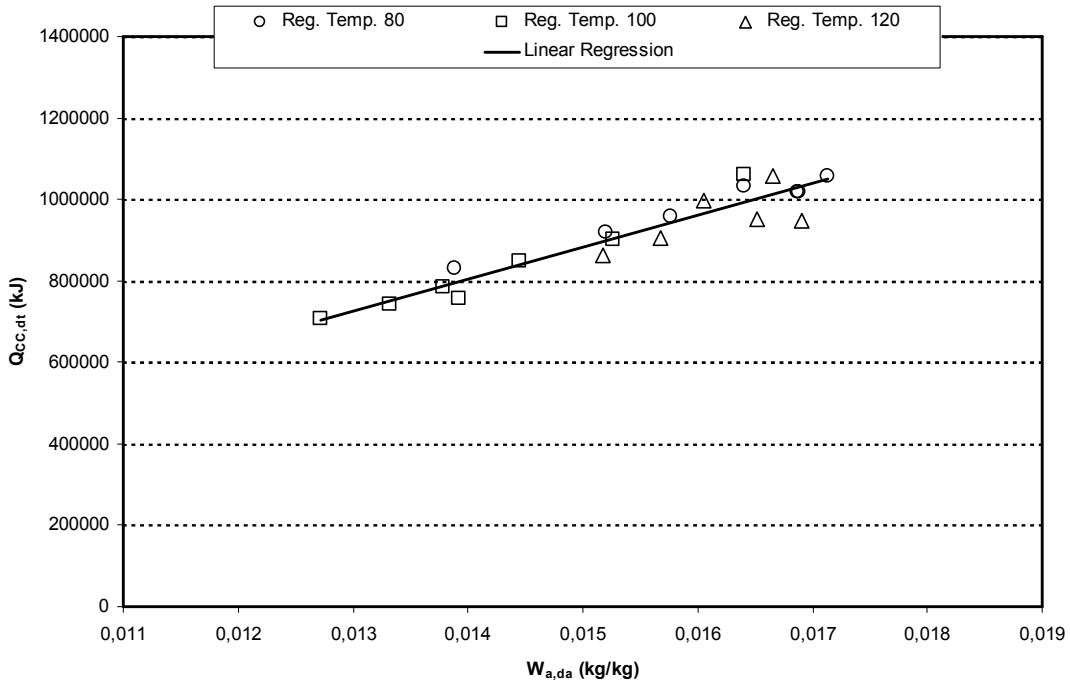

Figure 4.32. Effect of daily average ambient humidity ratio on daily total cooling capacity for different regeneration temperature set values (R/P=1)

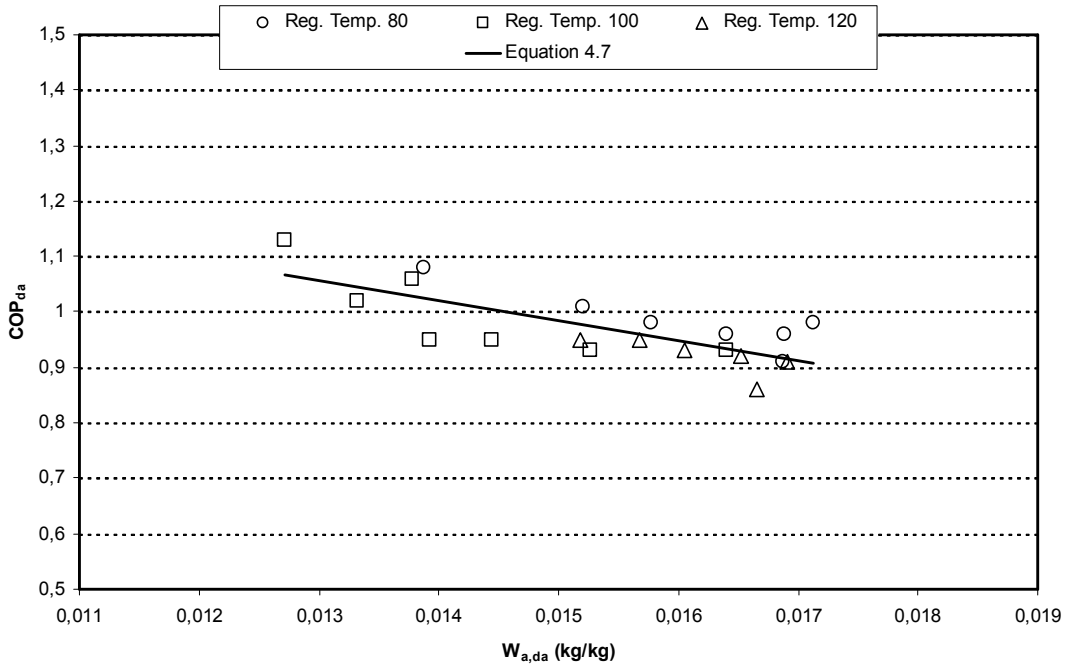

Figure 4.33. Effect of daily average ambient humidity ratio on daily average COP for different regeneration temperature set values (R/P=1)

4.3.2. Results of the Experiments Carried out with Different Process and Regeneration Air Flow Rates

Table 4.6 shows the test conditions of the experiments that are carried out with different process and regeneration air flow rates (R/P=3/4). Figures 4.34-4.37 present dry bulb temperatures and relative humidities of air measured at the states shown in Figure 3.1 during a typical experiment (Test ID-050908). At the beginning of the test, regeneration temperature is set to 100 ^{o}C. Figures 4.34-4.36 show variation of dry bulb temperature during the day at different states for fresh, waste and regeneration air streams, respectively. As can be seen from the figures, all the air temperatures except the ambient (T_1 and T_{11}) and the air-conditioned room (T_7) fluctuate with time. The fluctuations originate from the start-up and shut-down of the electric heaters, which is needed for the control of humidity in the air-conditioned room.

As can be seen from Figure 4.34, the dry bulb temperature of fresh ambient air that enters the fresh air channel at 27 ^{o}C (T_1), increases into 45–55 ^{o}C (T_2) after the dehumidification process and then its temperature decreases down to blowing temperature (approximately 22 ^{o}C) by passing through the heat exchangers ($T_2 \rightarrow T_6$).

Figure 4.35 shows dry bulb temperature of waste air stream at different states. It can be seen that after a short time (15 min), dry bulb temperature of the air-conditioned room (T_7) decreases down to set value 26 ^{o}C and remains constant rest of the day. It can also be seen from the figure that temperature of the air sucked from the room (T_7) is decreased down to 20 ^{o}C (T_9) with the help of the evaporative cooler before entering into heat exchanger 2.

Variation of regeneration temperature (T_{14}) during the day is shown in Figure 4.36. As can be seen from the figure, the regeneration temperature remains around set value 100 ^{o}C.

Figure 4.37 shows the relative humidities measured during the day at different states. Relative humidity of the air-conditioned room changes around the set value of 50% within a band of ±2%. Similar fluctuations with different amplitudes are also evident in the humidities at states 3, 6, 9 and 16. It can also be seen from the

figure that humidity of the waste air is increased from 50% to approximately 92% by the evaporative cooler.

Figure 4.38 shows all the processes on a psychrometric diagram at 11:45 am.

Table 4.6. Experiments that were carried out at different process and regeneration air flow rates

Test ID	Regeneration Temperature Set Value (°C)	Air Conditioned Room Temperature Set Value (°C)	Air Conditioned Room Relative Humidity Set Value (%)	Tank Water Temperature Set Value (°C)	Daily Average Ambient Temperature (°C)	Daily Average Ambient Relative Humidity (%)	Daily Average Ambient Humidity Ratio (kg/kg)
010908	100	26	50	7	31.07	57.44	0.0163
020908	100	26	50	7	30.71	56.39	0.0156
030908	100	26	50	7	30.47	52.69	0.0143
040908	100	26	50	7	30.40	53.17	0.0144
050908	100	26	50	7	31.17	53.18	0.0151
250808	120	26	50	7	29.64	54.76	0.0143
260808	120	26	50	7	32.01	52.45	0.0156
270808	120	26	50	7	33.35	40.32	0.0125
280808	120	26	50	7	32.88	58.58	0.0184
290808	120	26	50	7	32.36	57.49	0.0175
090908	130	26	50	7	30.68	57.30	0.0158
100908	130	26	50	7	30.73	55.66	0.0154
110908	130	26	50	7	30.27	52.44	0.0141
120908	130	26	50	7	30.11	53.63	0.0143
150908	130	26	50	7	30.77	54.44	0.0151
160908	130	26	50	7	30.38	59.32	0.0161
170908	130	26	50	7	30.12	57.09	0.0152
180908	130	26	50	7	29.48	51.68	0.0133

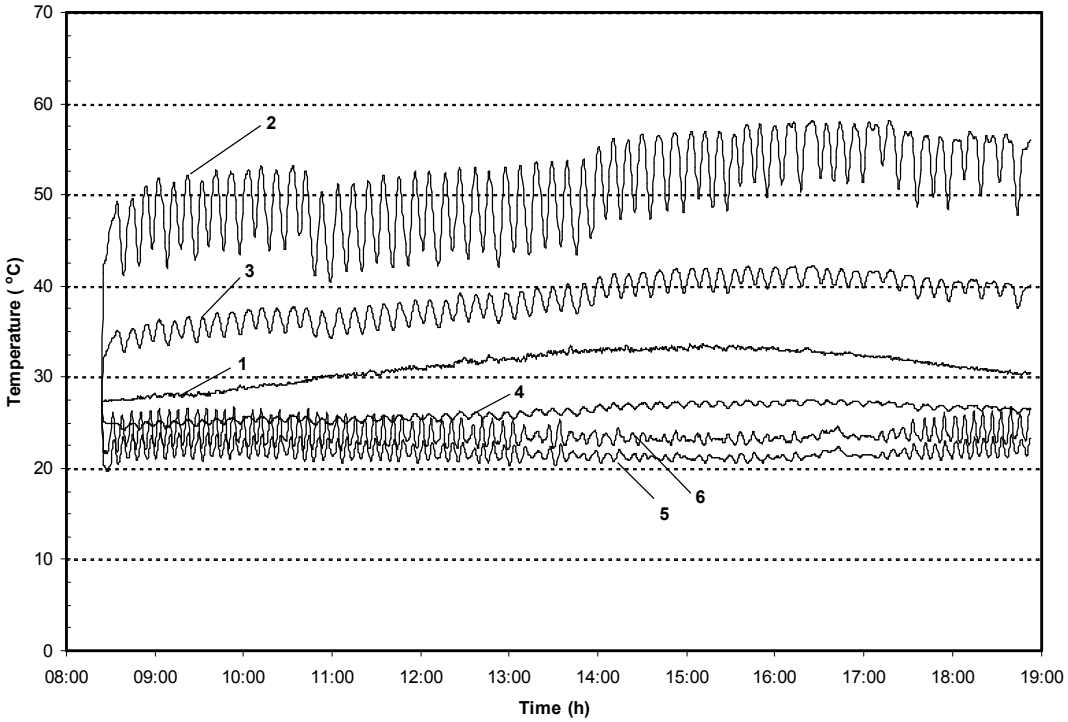

Figure 4.34. Variation of dry bulb temperature during the day at different states for fresh air stream (Test ID-050908)

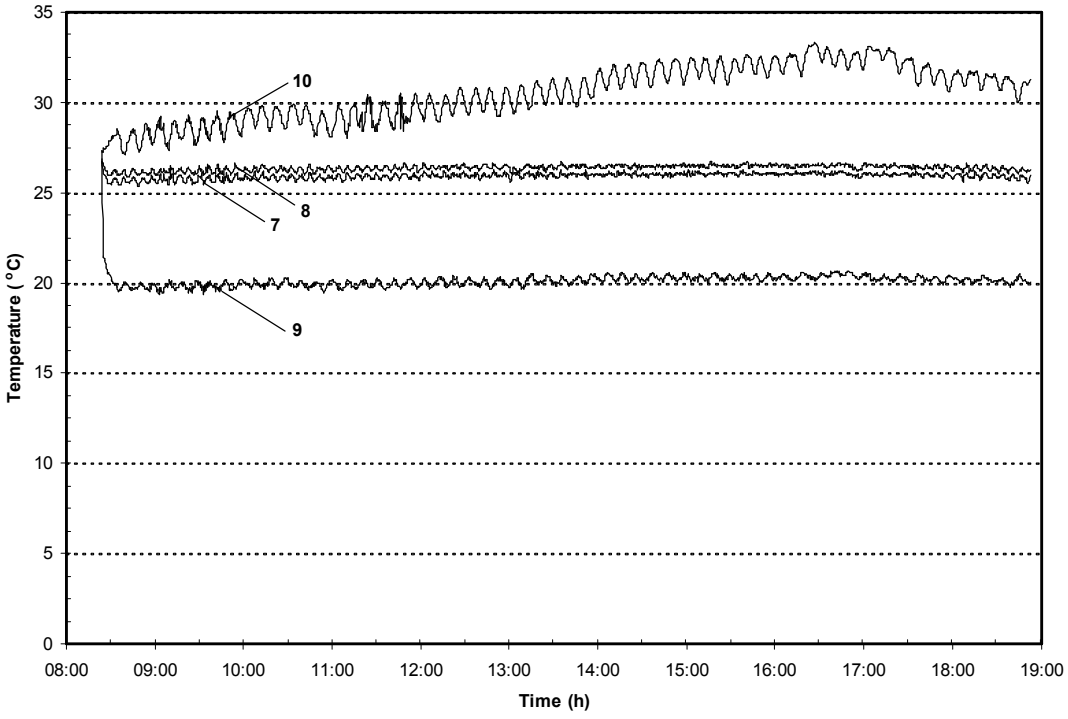

Figure 4.35. Variation of dry bulb temperature during the day at different states for waste air stream (Test ID-050908)

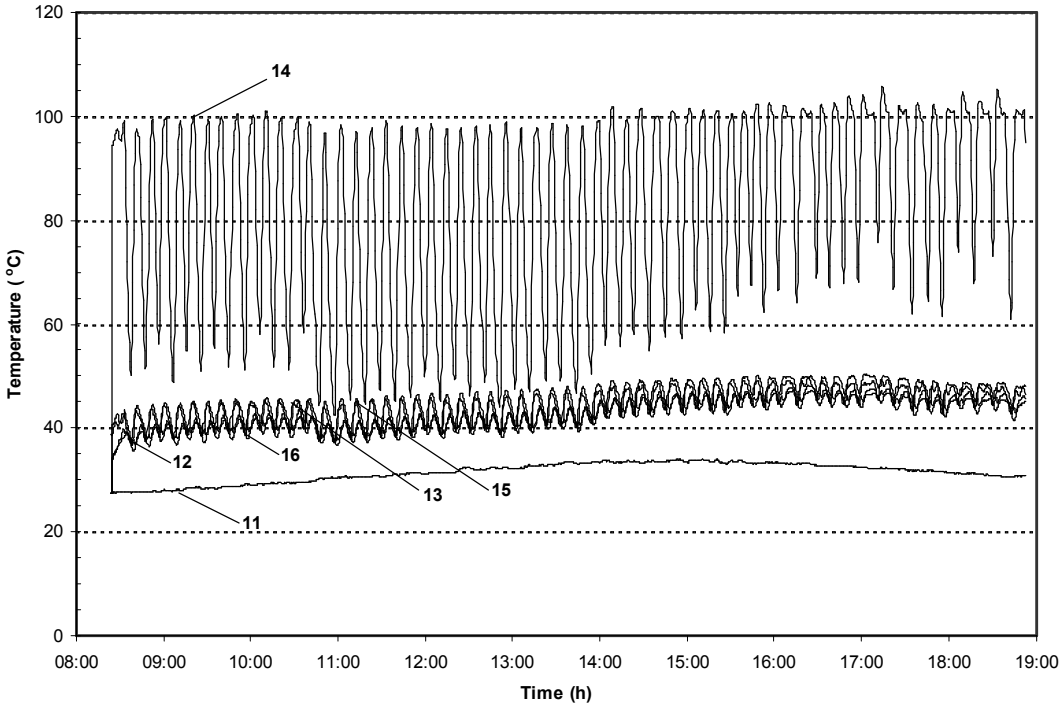

Figure 4.36. Variation of dry bulb temperature during the day at different states for regeneration air stream (Test ID-050908)

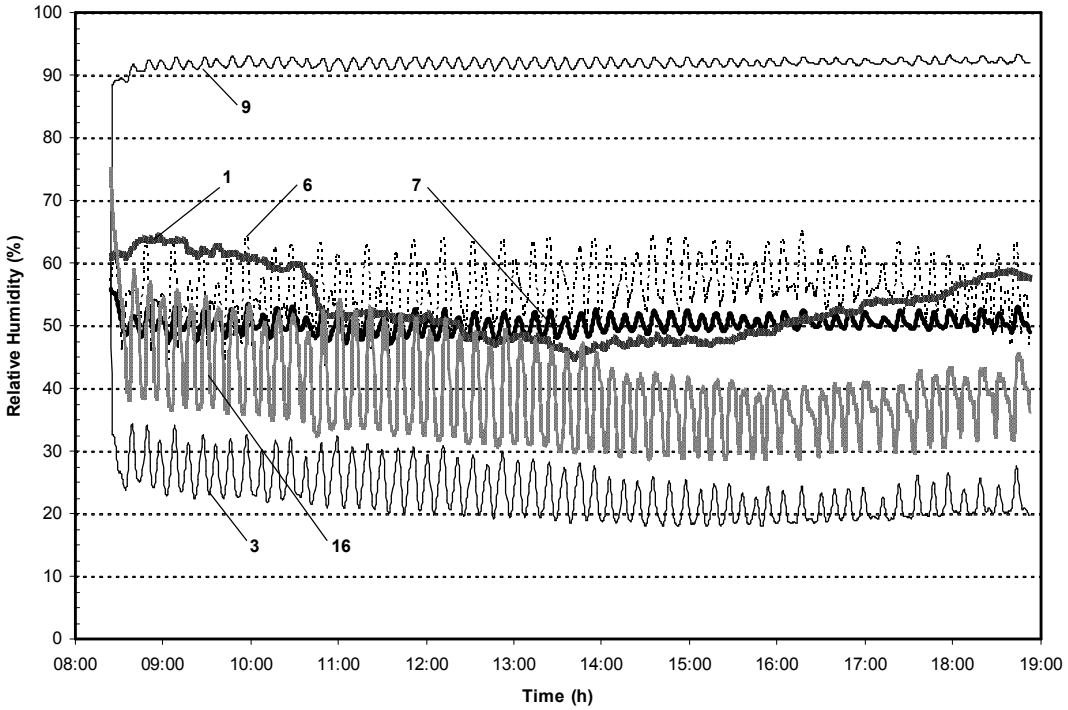

Figure 4.37. Variation of relative humidity during the day at different states (Test ID-050908)

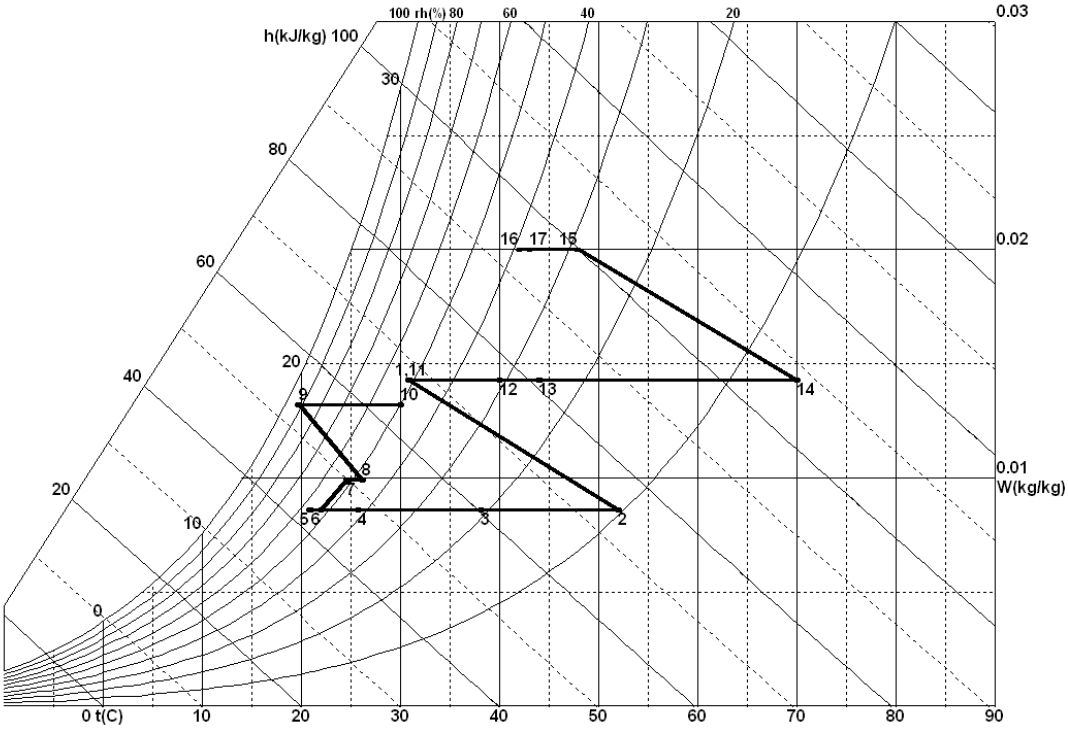

Figure 4.38. Psychrometric diagram showing all processes at 11:45 am. (Test ID-050908)

Variation of effectiveness of the evaporative cooler and the heat exchangers during the day is shown in Figure 4.39. Effectiveness is approximately 85% for heat exchangers 1and 4, 65% for heat exchanger 2, 60% for heat exchanger 3, and 90% for the evaporative cooler. It can be seen from the figure that fluctuations are evident in the effectiveness values, again due to start-up and shut-down of the electric heaters to control the humidity in the air-conditioned room.

Figure 4.40 presents the contribution of each heat exchanger to the total cooling requirement after dehumidification process (state 2 to 5) in percentage. As can be seen from the figure, approximately 40% of cooling requirement is met by heat exchanger 1, 45% by heat exchanger 2 and the remaining 15% by heat exchanger 3 (cooling coil). It is clear that use of heat exchangers 1 and 2 reduces significantly the cooling requirement. Approximately 85% of cooling is met without any external energy consumption.

Contribution of heat exchangers 1 and 4, and the regeneration heat to the total heating in percentage is given in Figure 4.41. Approximately 68% of the heating

requirement is met by the regeneration heat, 25% by heat exchanger 1 and 7% by heat exchanger 4. Use of heat exchangers 1 and 4 reduces the heating requirement approximately 32%.

Daily total contribution of heat exchangers 1 to 4 and the regeneration heat to the heating and cooling requirement is presented in Figure 4.42. The contribution of heat exchangers 1 and 2 can clearly be seen from the figure.

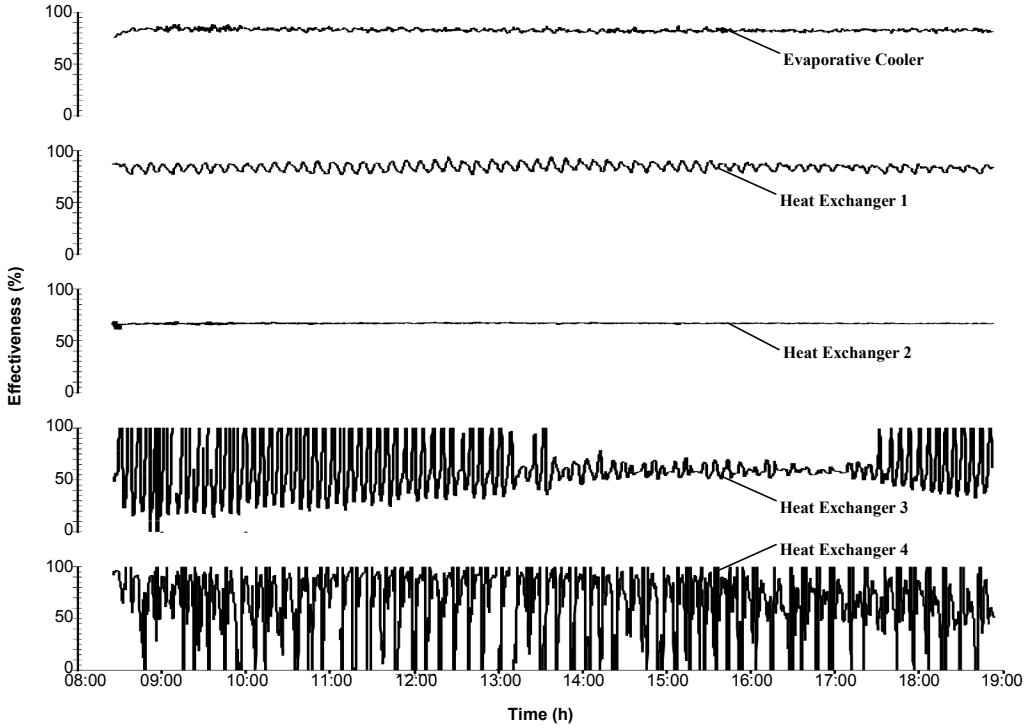

Figure 4.39. Variation of effectiveness of evaporative cooler and heat exchangers during the day (Test ID-050908)

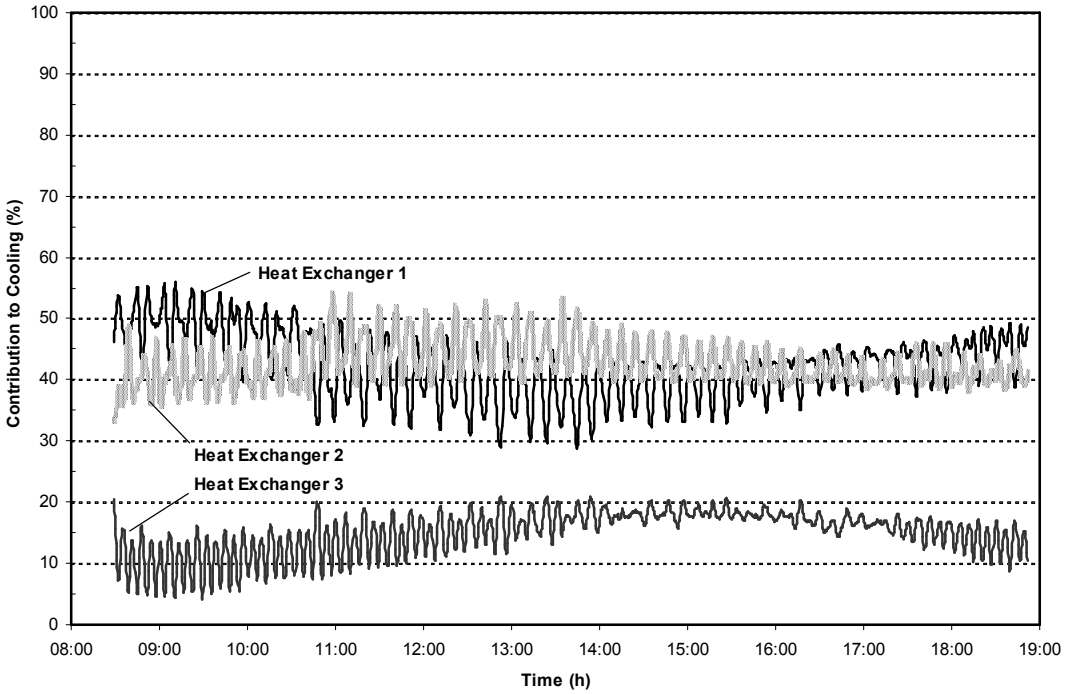

Figure 4.40. Contribution of heat exchangers 1-3 to total cooling (Test ID-050908)

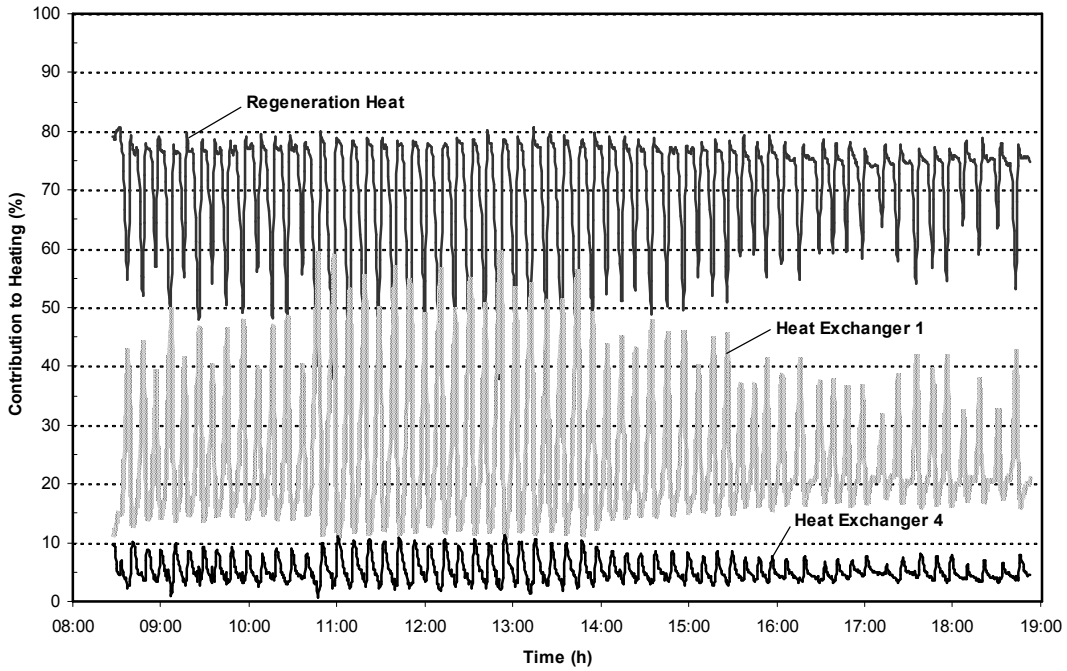

Figure 4.41. Contribution of heat exchangers 1 and 4, and regeneration heat to the total heating (Test ID-050908)

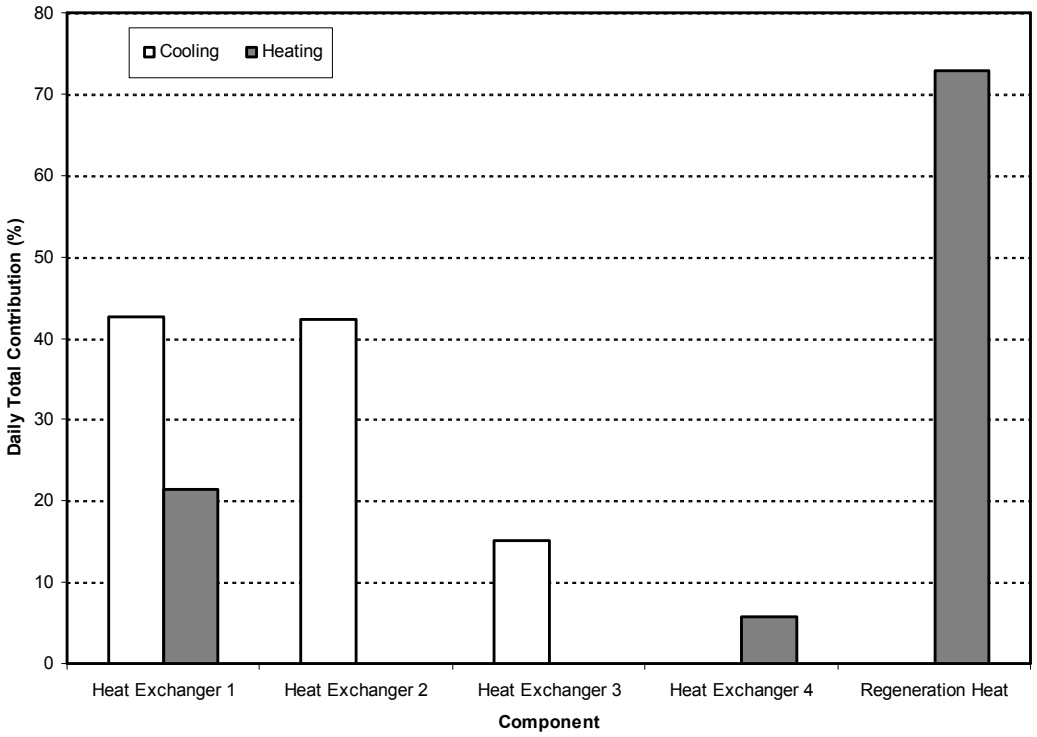

Figure 4.42. Daily total contribution of heat exchangers 1-4 and regeneration heat to the heating and cooling requirement (Test ID-050908)

Figure 4.43 shows the energy consumption of the units that consume energy (regeneration heat, fans, compressor and others). Although power consumption of the fans and the auxiliary electrical components is constant during the day, variations in the regeneration heat and the refrigeration unit are significant.

The maximum energy consumption occurs in regeneration heat (Figure 4.44). It is followed by the fans, compressor of the refrigeration unit and other electrical components. The figure shows the importance of using cheap heat source in desiccant cooling systems.

Figure 4.45 shows variation of cooling capacity during the day. Cooling capacity exhibits fluctuations with a magnitude of approximately ±5 kW. An average 22 kW of cooling effect is produced by the system to provide comfort conditions in the air-conditioned room.

Variation of moisture removal during the day is shown in Figure 4.46. As can be seen from the figure on average 0.006 kg/s moisture is removed from the ambient air in the desiccant wheel during the experiment.

Coefficient of performance (COP) of the system is shown in Figure 4.47. Although COP changes between 0.3 and 3.5 according to the electric heaters switching on or off, the daily mean value is 1.25. This value is in the range of the COP values reported in the literature for these kinds of systems.

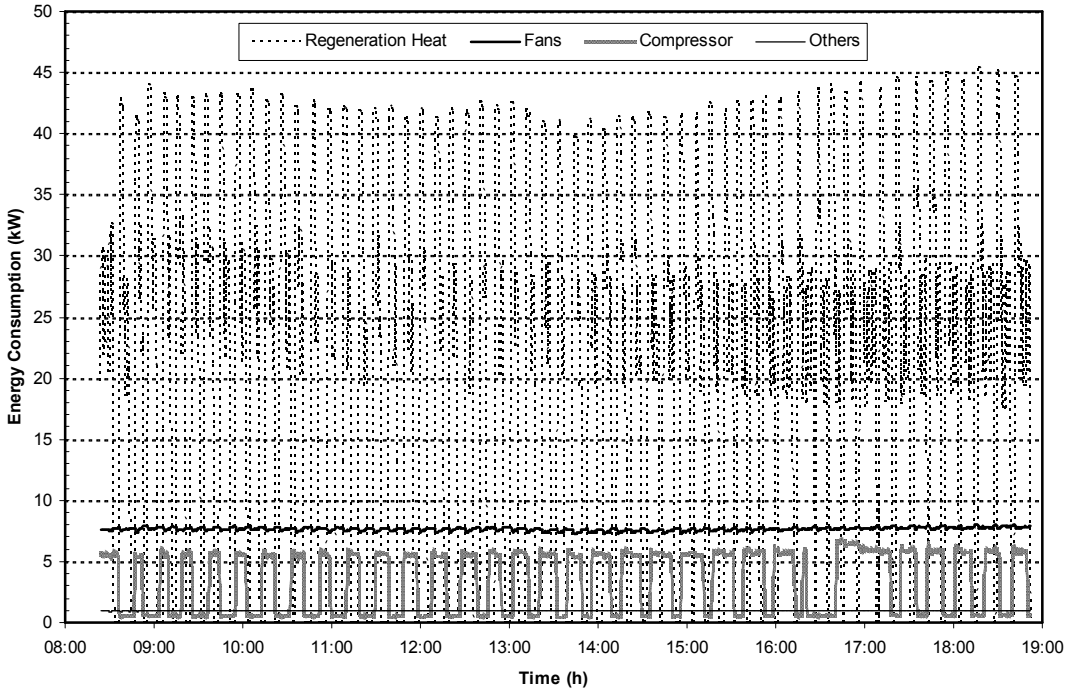

Figure 4.43. Variation of energy consumption of regeneration heat and each electrical component during the day (Test ID-050908)

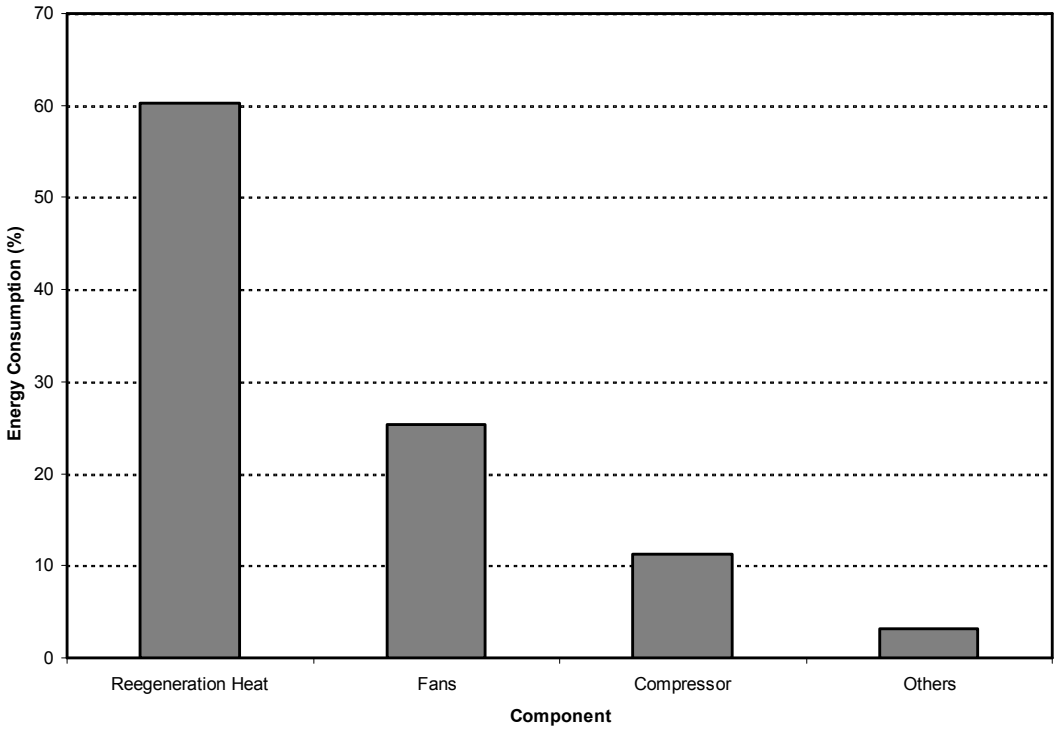

Figure 4.44. Daily total energy consumption of regeneration heat and each electrical component (Test ID-050908)

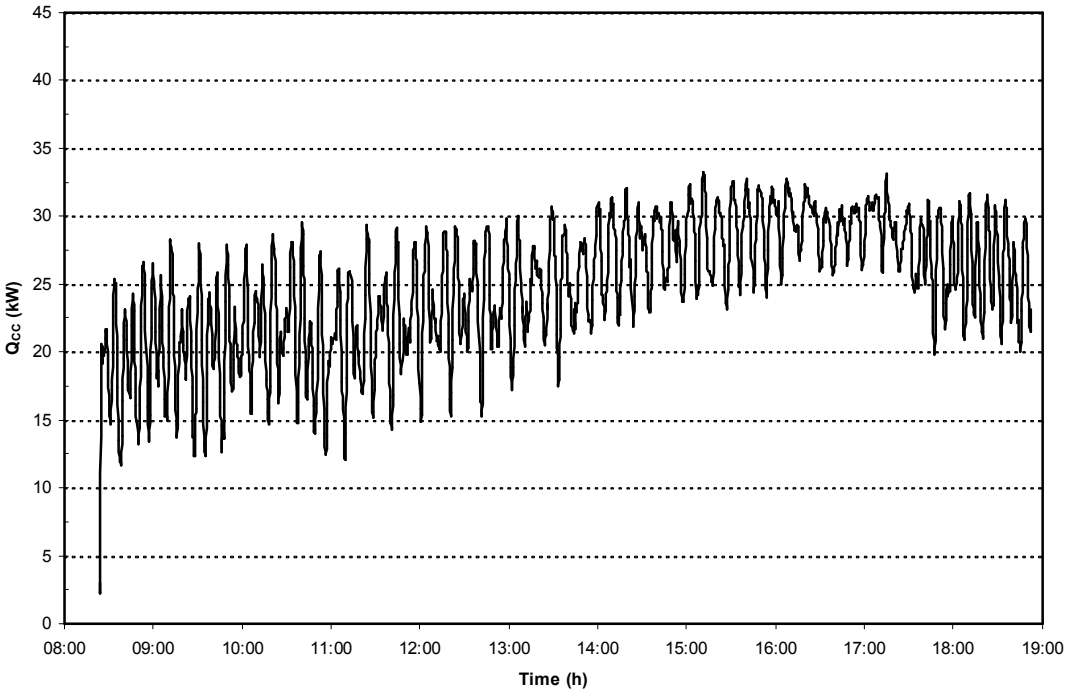

Figure 4.45. Variation of cooling capacity during the day (Test ID-050908)

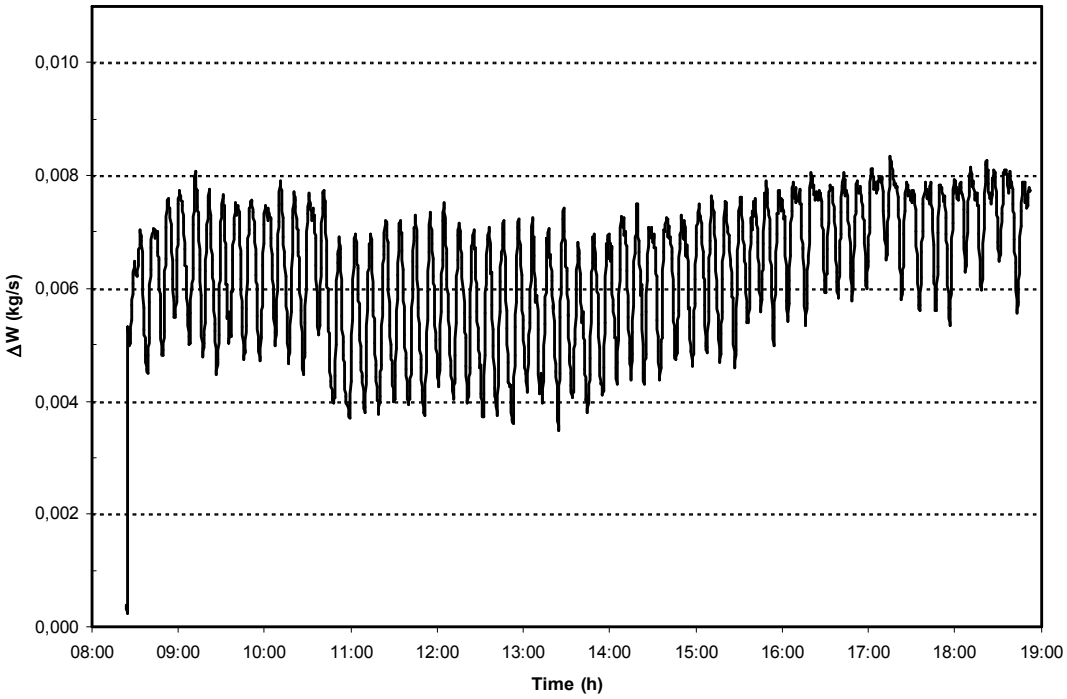

Figure 4.46. Variation of moisture removal during the day (Test ID-050908)

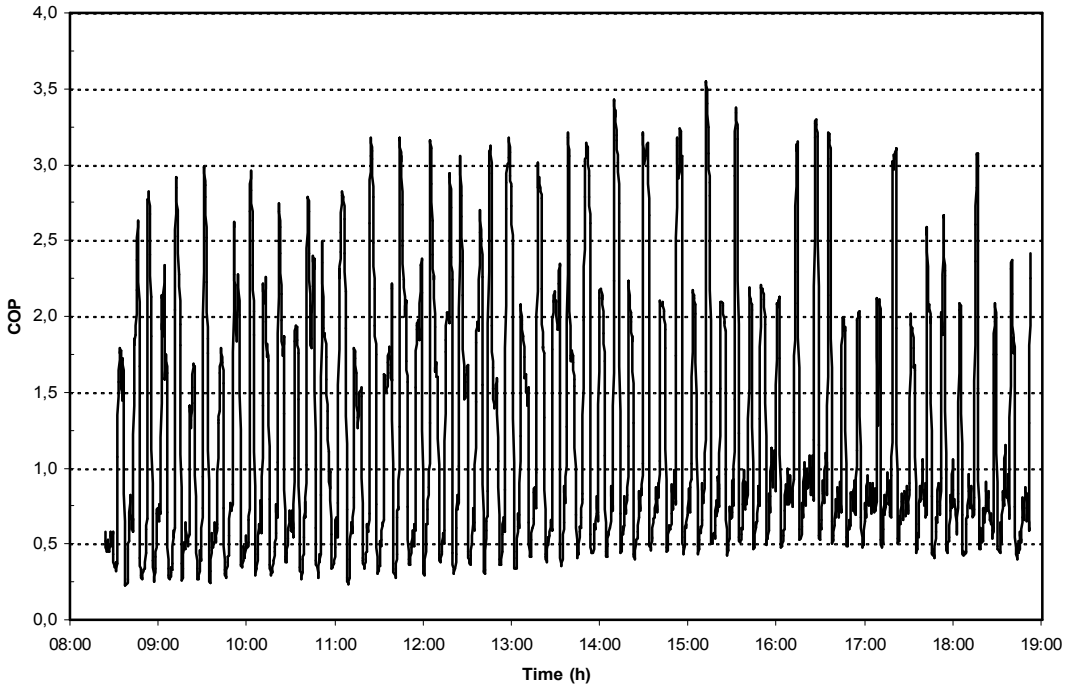

Figure 4.47. Variation of coefficient of performance during the day (Test ID-050908)

Figures 4.48-4.49 show the effect of daily average ambient temperature and regeneration temperature on daily total moisture removal for different regeneration temperature set values (100, 120 and 130). It is clear from the figures that there is no correlation between the ambient or regeneration temperatures and daily total moisture removal for the experiment carried out with different process and regeneration air flow rates (R/P=3/4).

Effect of daily average ambient relative humidity and humidity ratio on daily total moisture removal for different regeneration temperature set values is shown in Figures 4.50-4.51. As can be seen from the figures, the amount of daily total moisture removal increases with the increase of relative humidity and humidity ratio for all regeneration temperature set values. However, regeneration temperature has no considerable effect on daily total moisture removal.

From the results of experiments carried out with different process and regeneration air flow rates (R/P=3/4), it is found that there is no correlation between the ambient or regeneration temperatures and daily average or daily total parameters (energy consumptions, cooling effect, COP) obtained from each experiment. Effect of ambient relative humidity and humidity ratio on the daily average or daily total parameters is almost same as seen from the Figures 4.50-4.51. Therefore, only the relations between daily average humidity ratio and other parameters (energy consumptions, cooling effect and COP) are given below.

Figure 4.52 shows the effect of daily average ambient humidity ratio on daily total regeneration heat for different regeneration temperature set values. As can be seen from the figure, for all regeneration temperature set values, the amount of daily total regeneration heat increases with the increase of ambient humidity ratio. However, regeneration temperature has no considerable effect on daily total regeneration heat. Similar results are obtained for daily total energy consumption of the system and daily total cooling capacity (Figures 4.53-4.54).

Effect of daily average ambient humidity ratio on daily average coefficient of performance of the system for different regeneration temperature set values is shown in Figures 4.55. It is clear to see from the figure that COP_{da} decreases with the increase of ambient humidity ratio for all regeneration temperature set values.

However, regeneration temperature has no considerable effect on COP_{da}. Least-square method was applied to the data obtained from the experiments and the equation given below is obtained.

$$COP_{da} = 1.16\text{-}17.38^{*} W_{a,da} \text{ (R/P=3/4)} \quad (4.8)$$

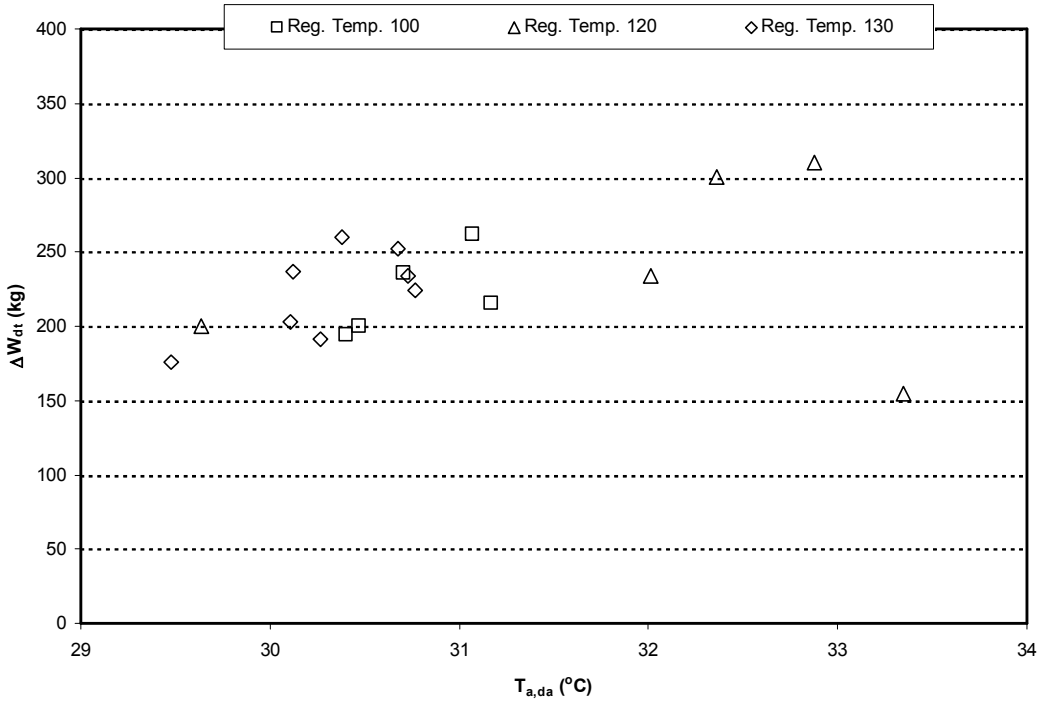

Figure 4.48. Effect of daily average ambient temperature on daily total moisture removal for different regeneration temperature set values (R/P=3/4)

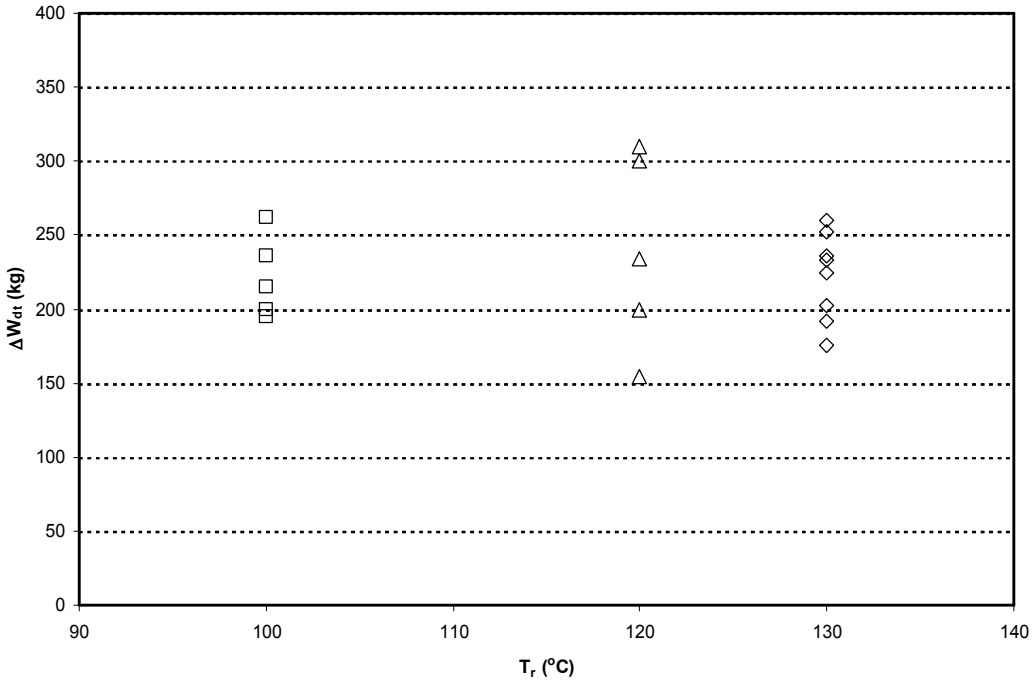

Figure 4.49. Effect of regeneration temperature on daily total moisture removal for different regeneration temperature set values (R/P=3/4)

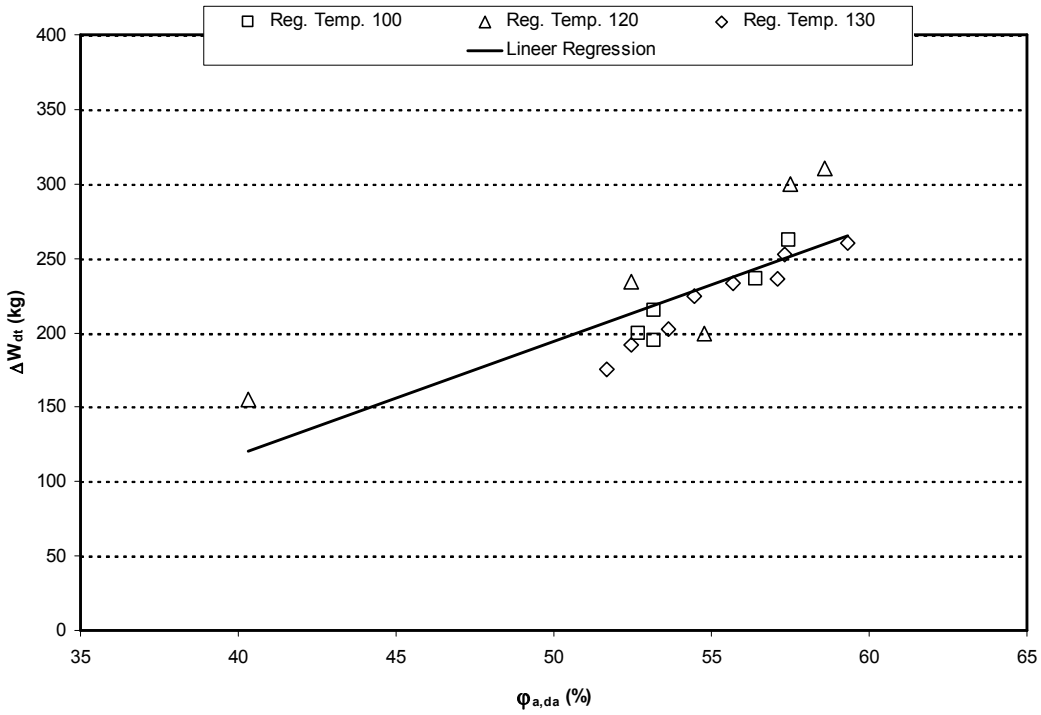

Figure 4.50. Effect of daily average ambient relative humidity on daily total moisture removal for different regeneration temperature set values (R/P=3/4)

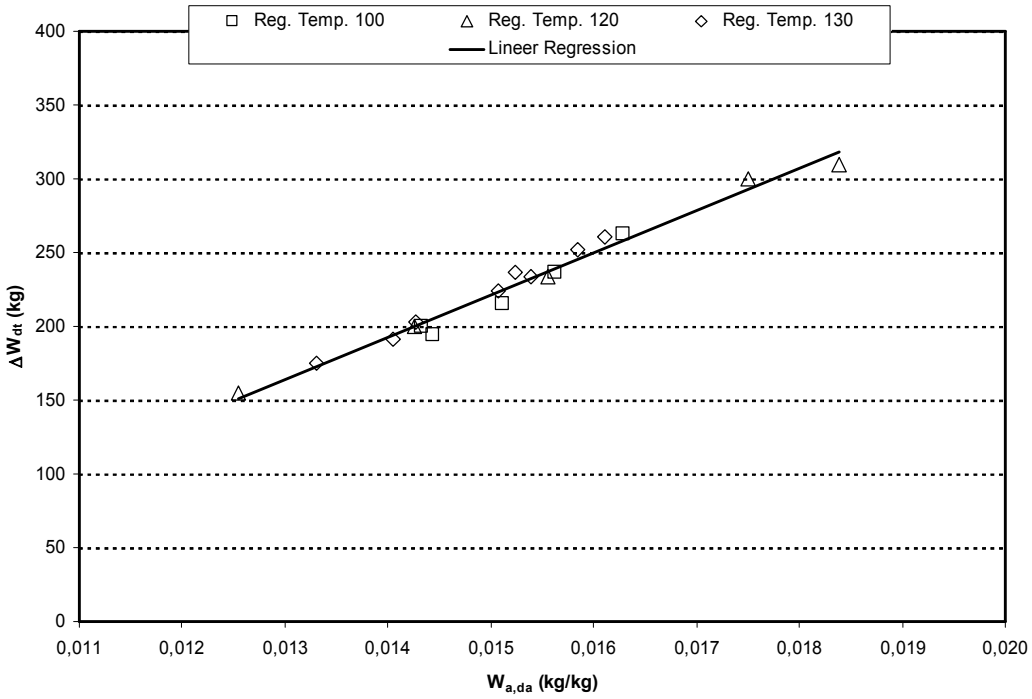

Figure 4.51. Effect of daily average ambient humidity ratio on daily total moisture removal for different regeneration temperature set values (R/P=3/4)

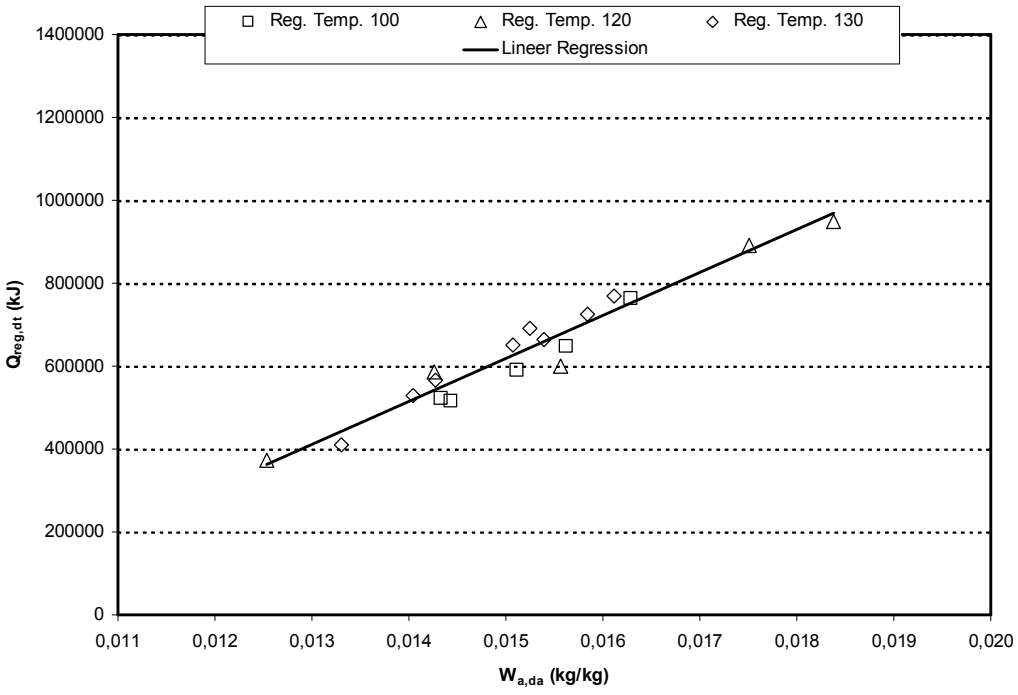

Figure 4.52. Effect of daily average ambient humidity ratio on daily total regeneration heat for different regeneration temperature set values (R/P=3/4)

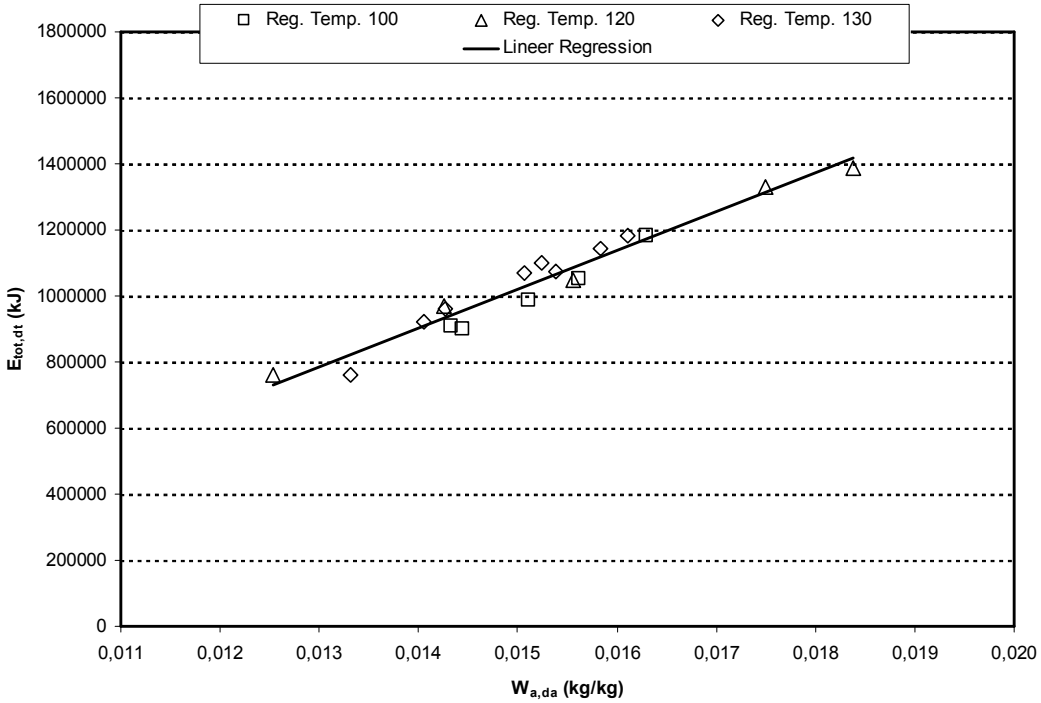

Figure 4.53. Effect of daily average ambient humidity ratio on daily total energy consumption of the system for different regeneration temperature set values (R/P=3/4)

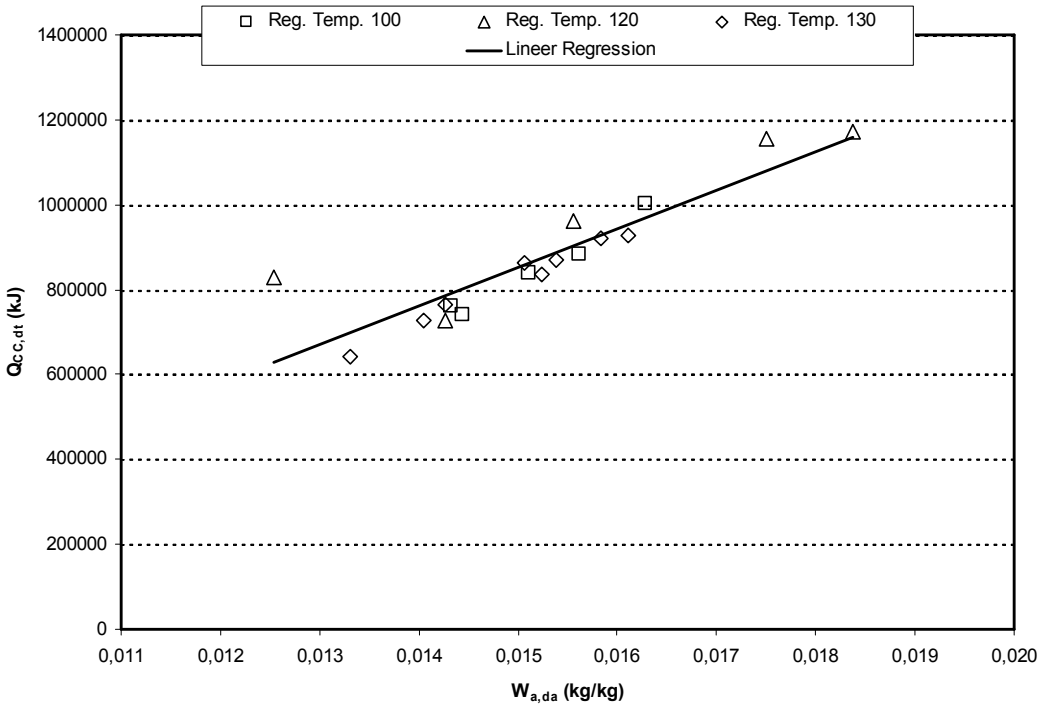

Figure 4.54. Effect of daily average ambient humidity ratio on daily total cooling capacity for different regeneration temperature set values (R/P=3/4)

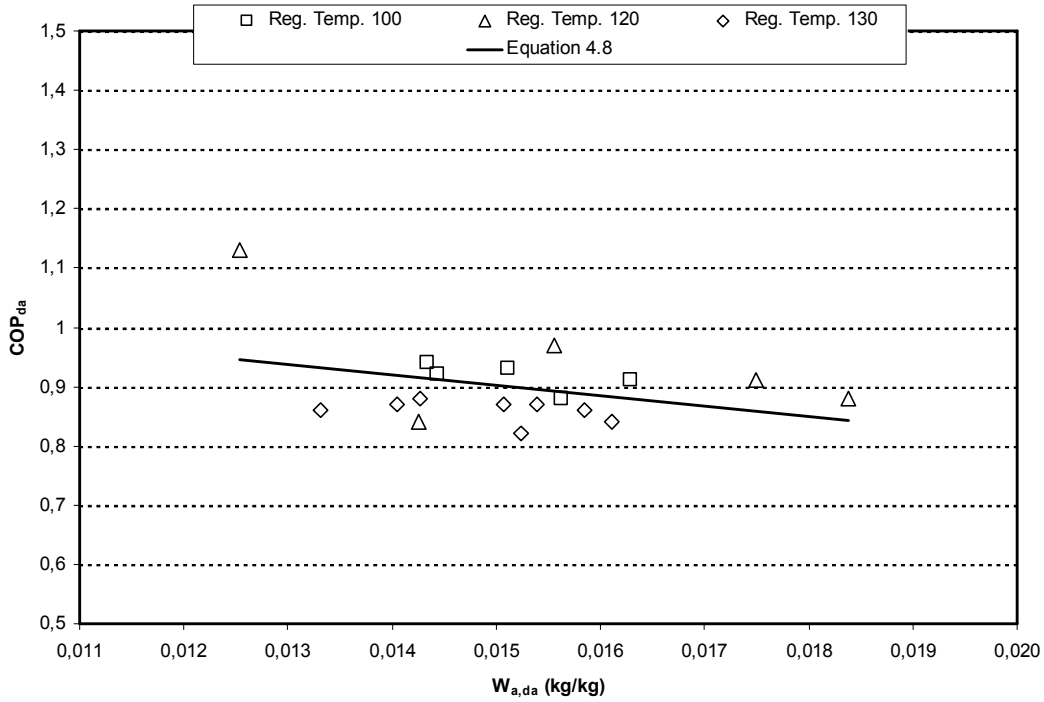

Figure 4.55. Effect of daily average ambient humidity ratio on daily average COP for different regeneration temperature set values (R/P=3/4)

4.3.3. Comparison of the Results of the Experiments Carried out with Equal and Different Process and Regeneration Air Flow Rates

The results obtained from the experiments that were carried out with equal and different process and regeneration air flow rates were evaluated in the Section 4.3.1 and 4.3.2, respectively. It is seen that regeneration temperature set value has no considerable effect on daily average or daily total parameters (moisture removal, energy consumptions, cooling effect, COP). In this section, the results obtained from the experiments that were carried out with equal and different process and regeneration air flow rates were compared.

Figures 4.56-4.58 show the results of the experiments carried out at 100^{o}C regeneration temperature set value. The effect of daily average ambient humidity ratio on daily total energy input to the system for the experiments carried out with equal (R/P=1) and different (R/P=3/4) process and regeneration air flow rates is shown in Figure 4.56. As can be seen from the figure, daily total energy input to the

system for the experiments in which R/P=3/4 is slightly higher than the experiments with R/P=1. Figure 4.57 shows effect of daily average ambient humidity ratio on daily total cooling capacity for the experiments carried out with equal and different process and regeneration air flow rates. Daily total cooling capacity for the experiments with R/P=1 is higher than the experiments in which R/P=3/4. The effect of daily average ambient humidity ratio on daily average COP for the experiments carried out with equal and different process and regeneration air flow rates is shown in Figure 4.58. Daily average COP for the experiments with R/P=1 is higher than the experiments with R/P=3/4.

Figures 4.59-4.61 show the results of the experiments carried out at 120^{o}C regeneration temperature set value. These figures indicate effect of daily average ambient humidity ratio on daily total energy consumption of the system, daily total cooling capacity, daily average COP for the experiments carried out with equal and different process and regeneration air flow rates. As can be seen from the figures, daily total energy consumption of the system, daily total cooling capacity and daily average COP for the experiments with R/P=3/4 is higher than the experiments with R/P=1. However, it is not possible to make a comparison for the experiments carried out at 100^{o}C or 120^{o}C regeneration temperature set values. This is because; it was not possible to carry out experiments under the same ambient air conditions.

When all regeneration temperature set values (80^{o}C, 100^{o}C, 120^{o}C, 130^{o}C) are taken into consideration, daily total energy input to the system for the experiments with R/P=3/4 is higher, however daily total cooling capacity and daily average COP is lower than the experiments with R/P=1 (Figures 4.62-4.64).

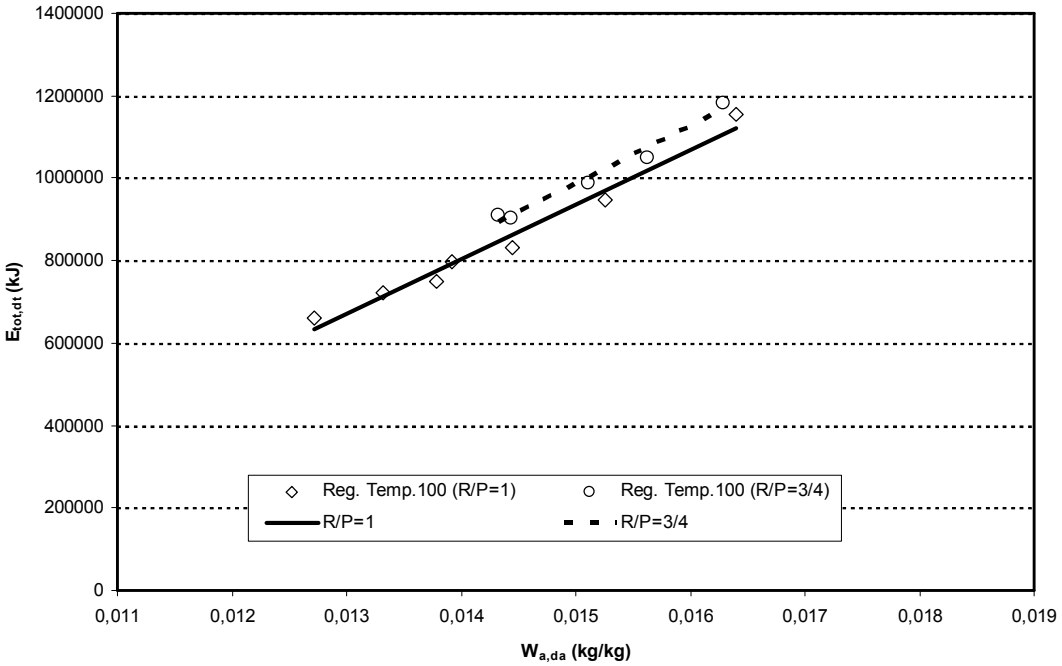

Figure 4.56. Effect of daily average ambient humidity ratio on daily total energy consumption of the system for the experiments carried out at 100°C regeneration temperature set value

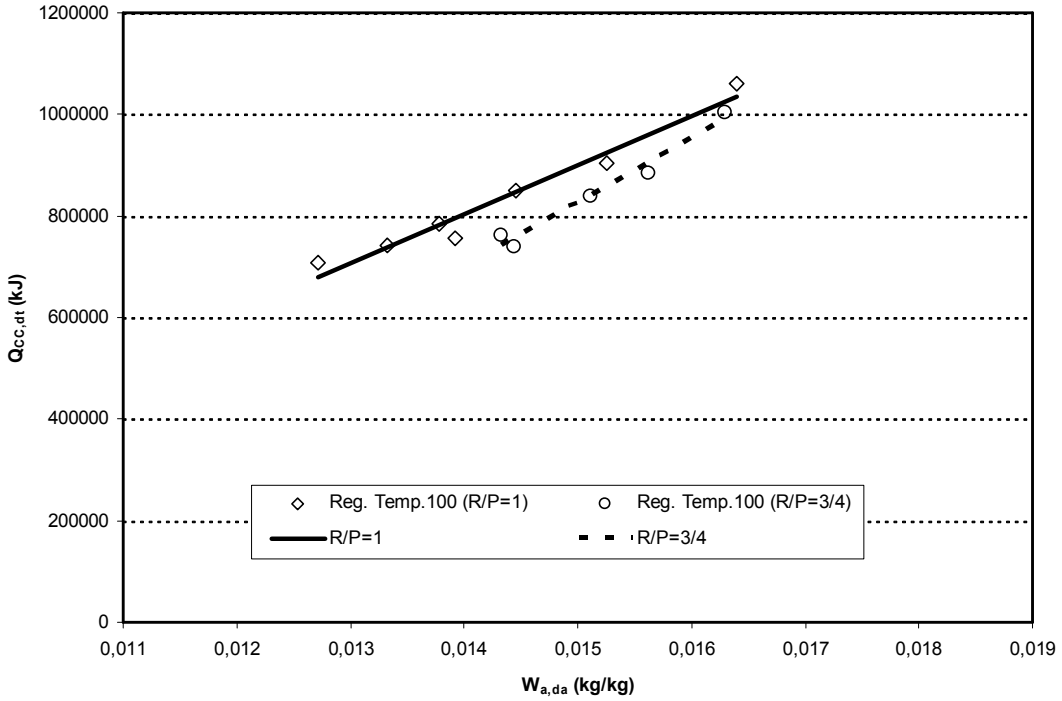

Figure 4.57. Effect of daily average ambient humidity ratio on daily total cooling capacity for the experiments carried out at 100°C regeneration temperature set value

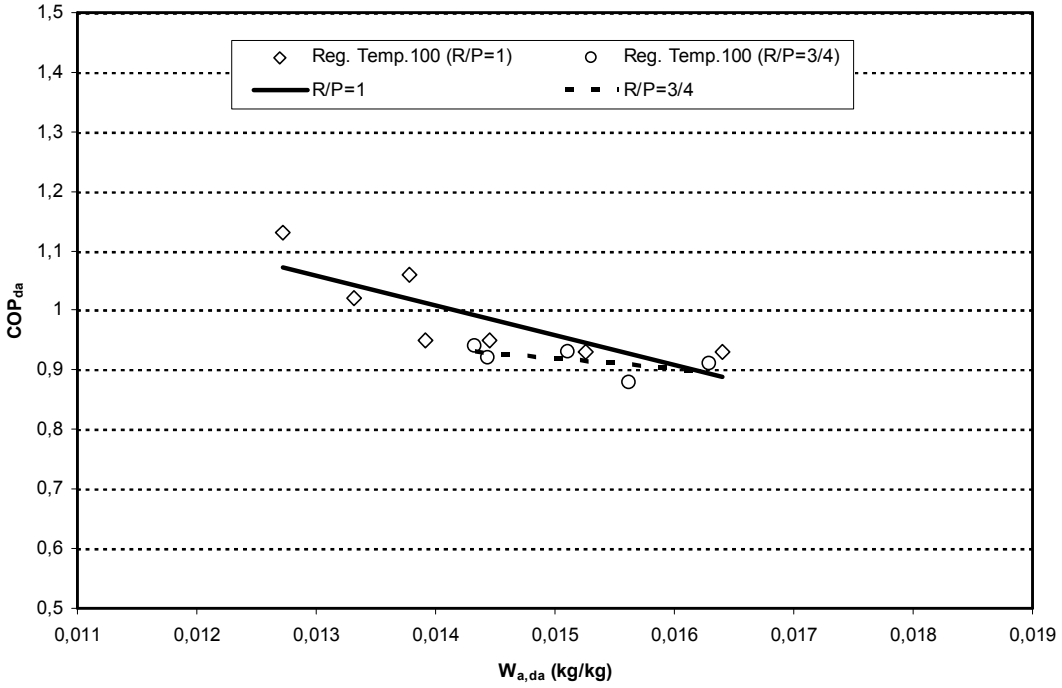

Figure 4.58. Effect of daily average ambient humidity ratio on daily average COP for the experiments carried out at 100°C regeneration temperature set value

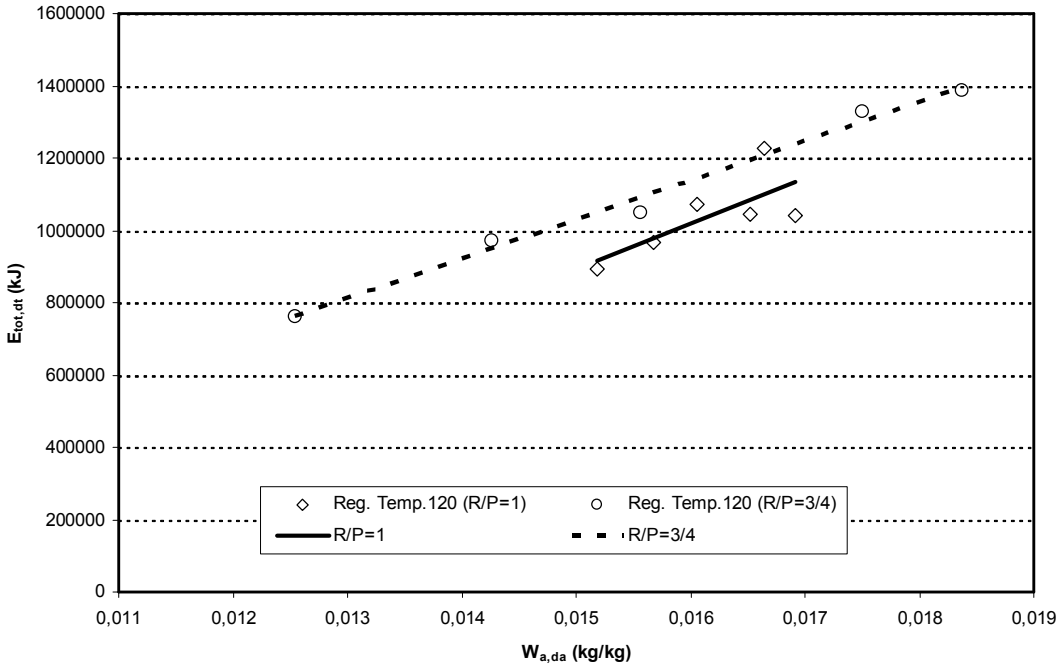

Figure 4.59. Effect of daily average ambient humidity ratio on daily total energy consumption of the system for the experiments carried out at 120°C regeneration temperature set value

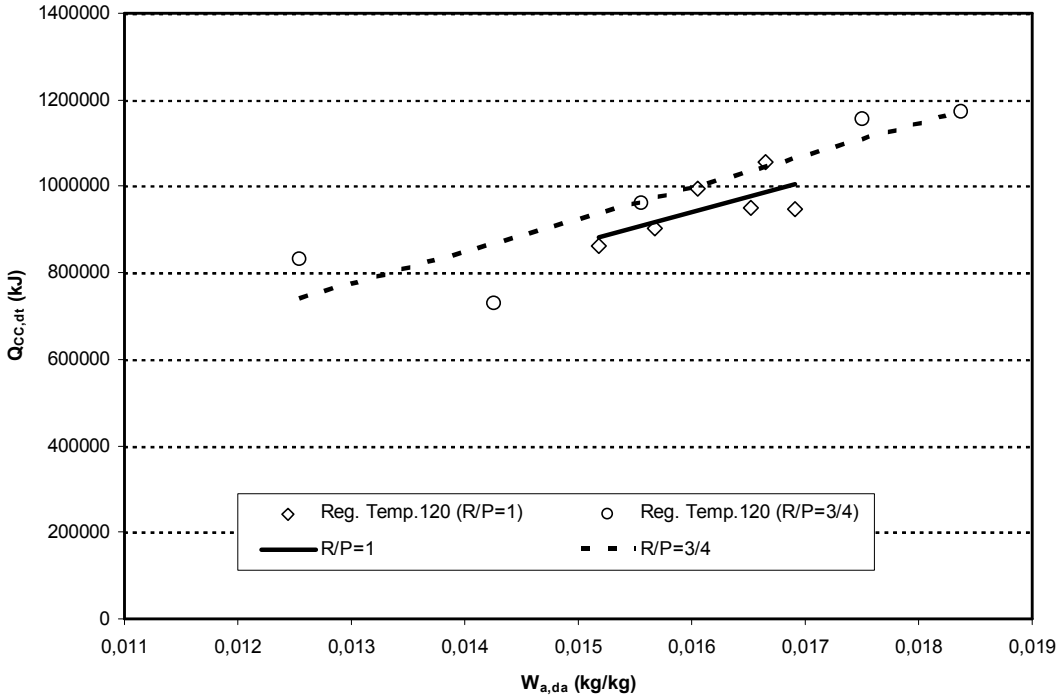

Figure 4.60. Effect of daily average ambient humidity ratio on daily total cooling capacity for the experiments carried out at 120°C regeneration temperature set value

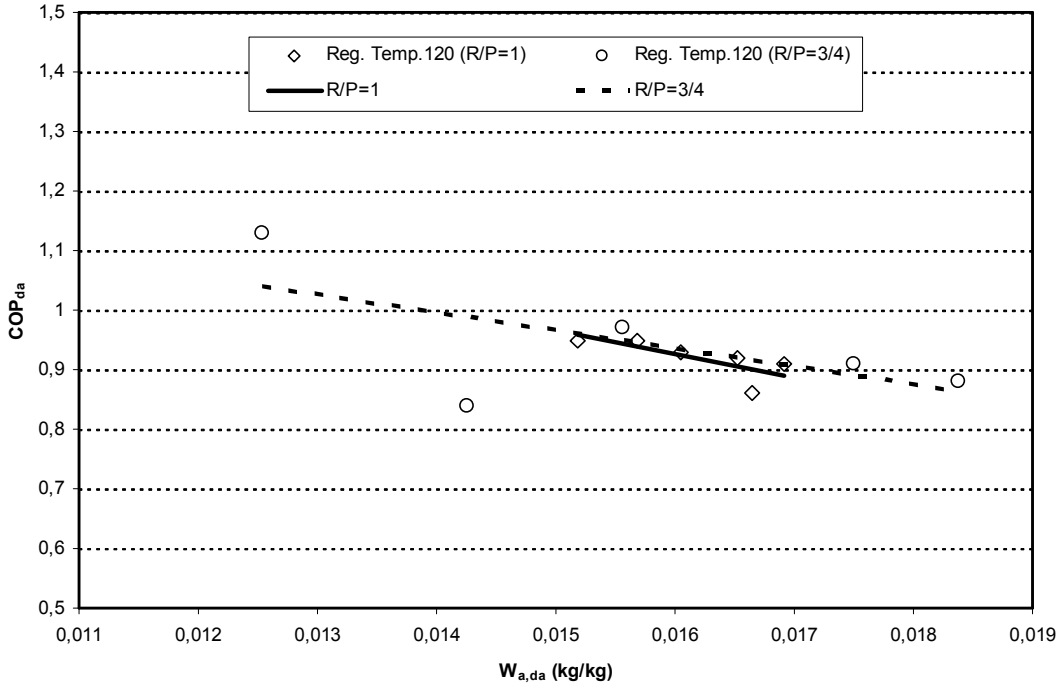

Figure 4.61. Effect of daily average ambient humidity ratio on daily average COP for the experiments carried out at 120°C regeneration temperature set value

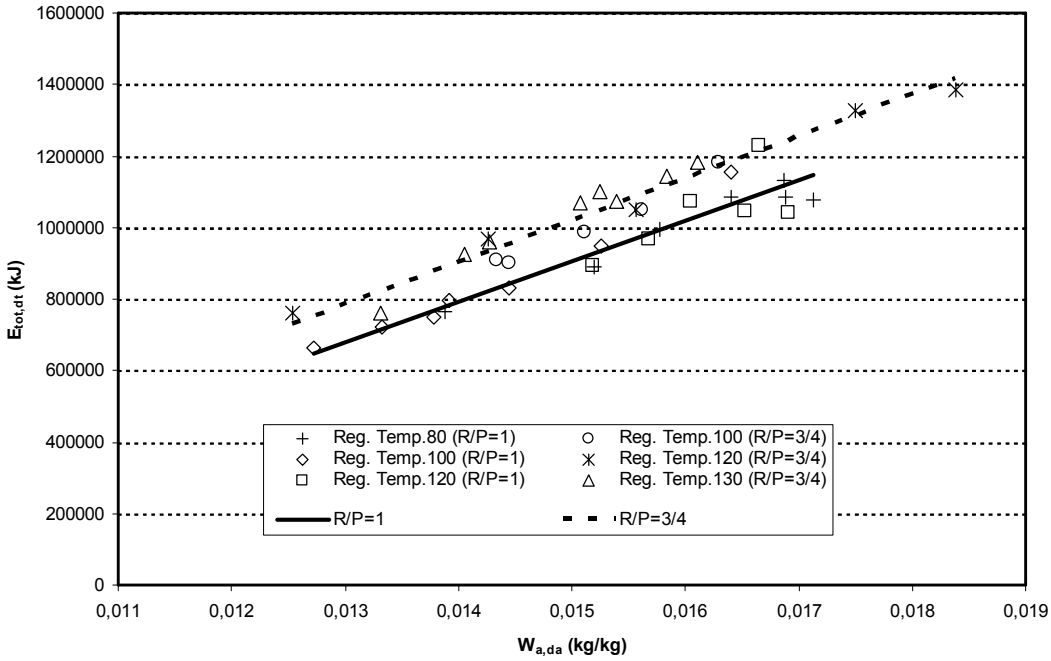

Figure 4.62. Effect of daily average ambient humidity ratio on daily total energy consumption of the system for the experiments carried out at all regeneration temperature set values (80°C, 100°C, 120°C, 130°C)

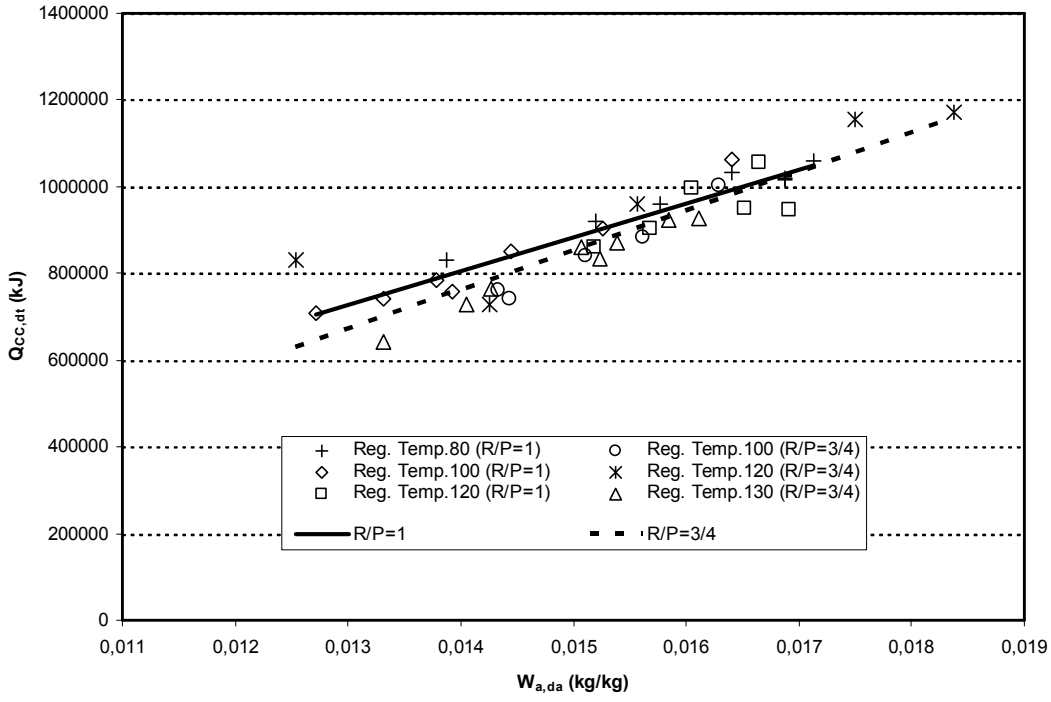

Figure 4.63. Effect of daily average ambient humidity ratio on daily total cooling capacity for the experiments carried out at all regeneration temperature set values (80°C, 100°C, 120°C, 130°C)

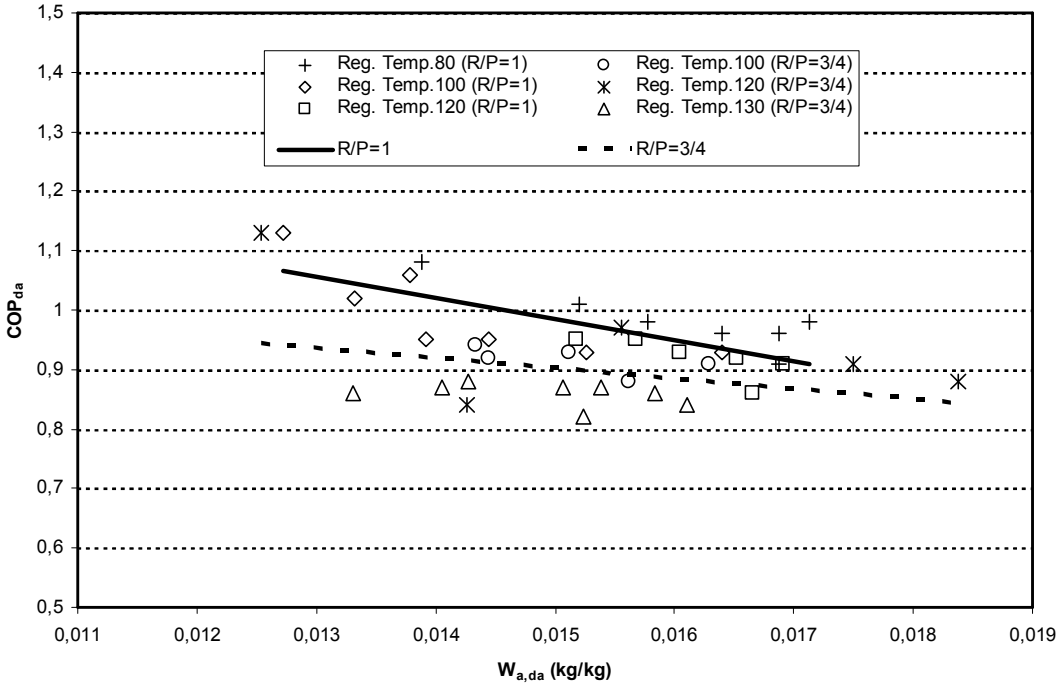

Figure 4.64. Effect of daily average ambient humidity ratio on daily average COP for the experiments carried out at all regeneration temperature set values (80^oC, 100^oC, 120^oC, 130^oC)

4.4. Results Obtained from the Solar Energy Studies

Dry bulb temperature (T_a) and total solar radiation ($\dot{q}$) are measured hourly by The State Meteorological Affairs (DMİ). However relative humidity (φ) is measured terdiurnal by DMİ. Since the meteorological data measured between 06:00-19:00 hours were used in the analysis, relative humidity at the hours that measurement is not carried out, should be determined.

Ambient humidity ratio does not fluctuate and it can be assumed to be constant during the day (YILMAZ, 1995; YILMAZ, 1996; AL-RABGHI, 2001). It was calculated at 07:00, 14:00 and 21:00 hours using the measured relative humidity and dry bulb temperatures at these hours. Daily mean humidity ratio was calculated using the humidity ratio calculated at 07:00, 14:00 and 21:00 hours. Relative humidity at hours between 06:00-19:00 was calculated using the daily mean humidity ratio and dry bulb temperatures at these hours.

The results given in this study were obtained using 21 years daily mean values of T_a, $\dot{q}$ and φ for Adana. Daily mean values were calculated using the data measured during 21 years by DMİ. Figures 4.65-4.67 show variation of T_a, $\dot{q}$ and φ between 06:00-19:00 hours during summer season, respectively.

The increase in the regeneration air temperature due to solar energy assistance is calculated using the model described in Section 3.11. The results obtained at various hours are given in Figures 4.68-4.72. In the figures, variation of ambient dry bulb temperature (T_a), air temperature at the entrance ($T_{a,en}$) and exit ($T_{a,ex}$) of the heat exchanger and the temperature of the water at the entrance of the heat exchanger ($T_{w,\ en}$) during summer season are shown. As can be seen from the figures, the increase in the regeneration air temperature ($T_{a,ex}$-$T_{a,en}$) is approximately 13-16^oC at noon depending on ambient dry bulb temperature and solar radiation, and it is approximately 9-10^oC for the remaining part.

Figure 4.73 shows variation of thermal energy transferred in one hour to the regeneration air from solar energy during the summer season. Although the amount of energy is a strong function of the time of the day, it does not change considerably from day to day during the cooling season except after 260. day. It is over 50000 kJ for the hours between 10:00-15:00.

Figure 4.74 shows variation of daily (06:00-19:00) total transferred thermal energy in a day from the solar energy during the summer season. The amount of daily total transferred thermal energy fluctuates within a band of $4*10^5$ -$5.5*10^5$ kJ and it decreases after 260. day.

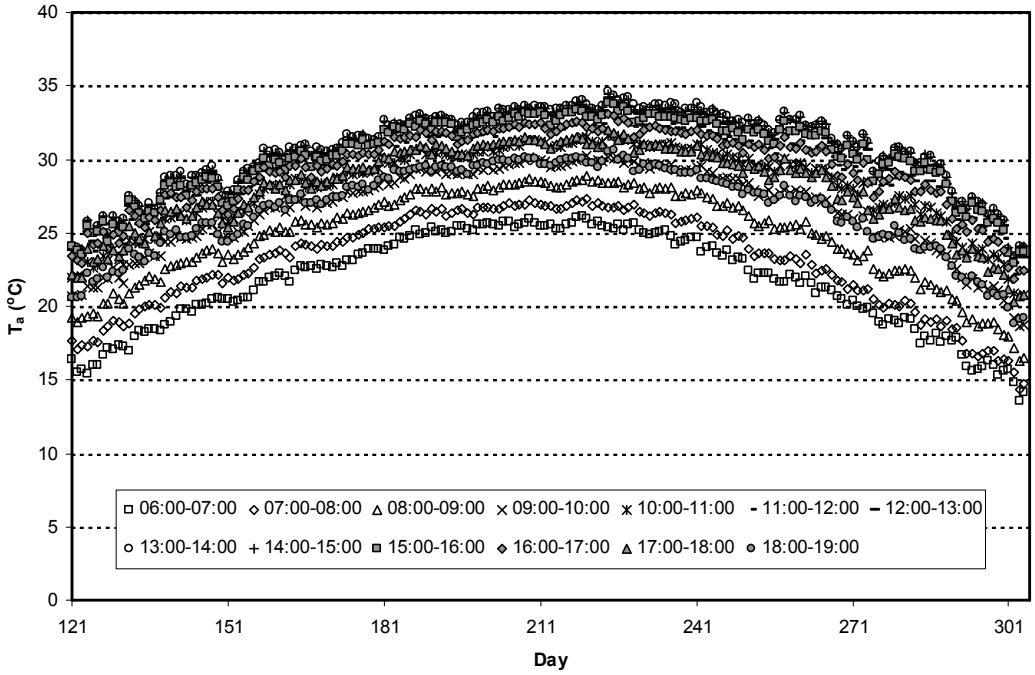

Figure 4.65. Variation of daily mean ambient dry bulb temperature between 06:00-19:00 hours during summer season

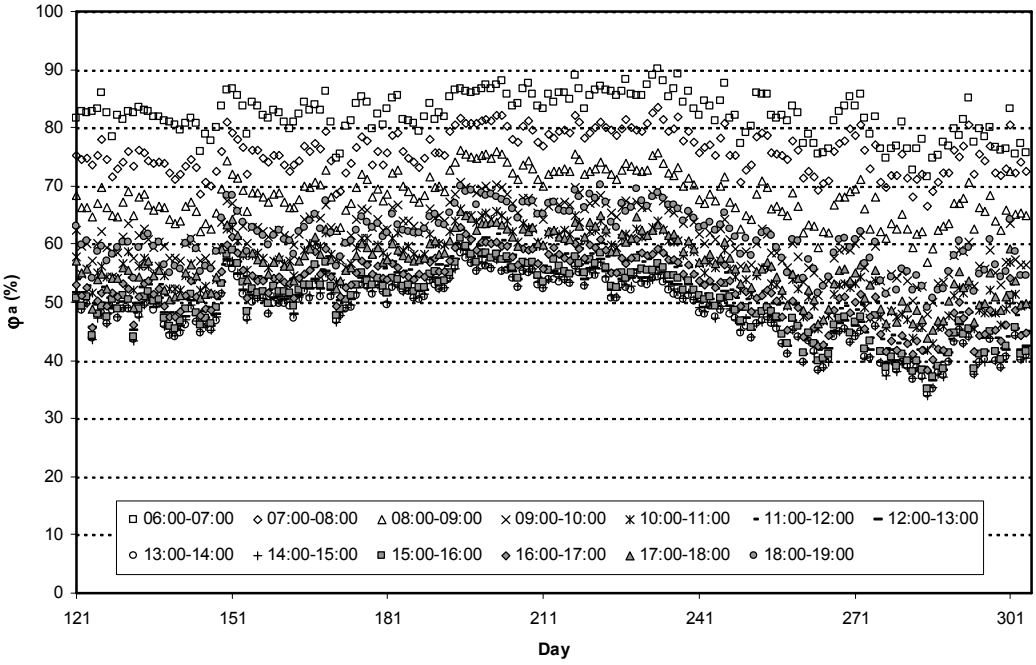

Figure 4.66. Variation of daily mean ambient relative humidity between 06:00-19:00 hours during summer season

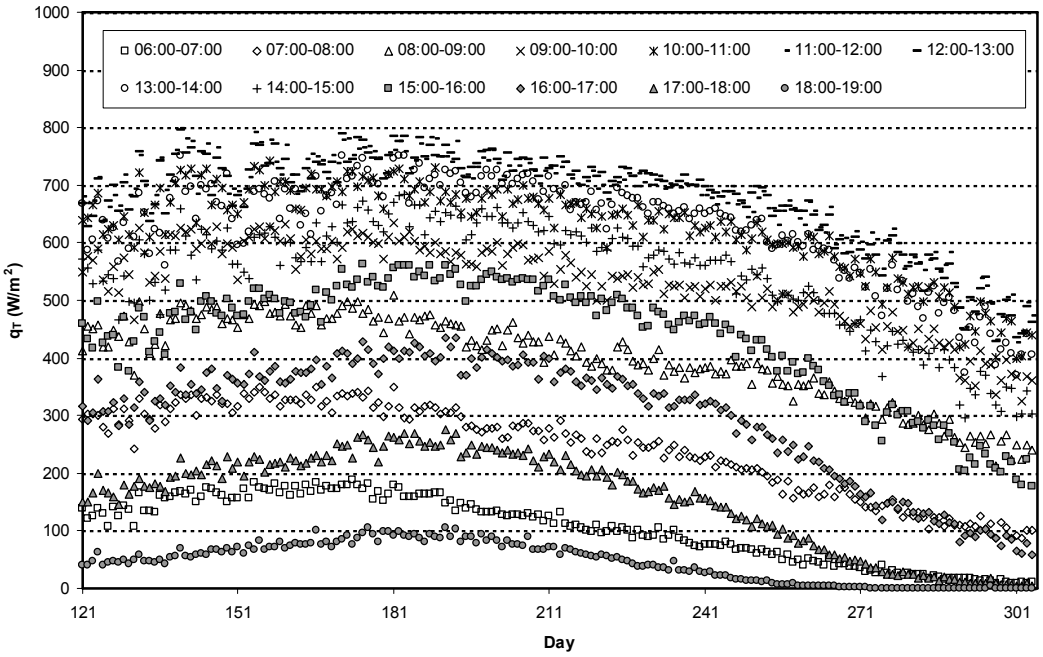

Figure 4.67. Variation of daily mean ambient total solar radiation between 06:00-19:00 hours during summer season

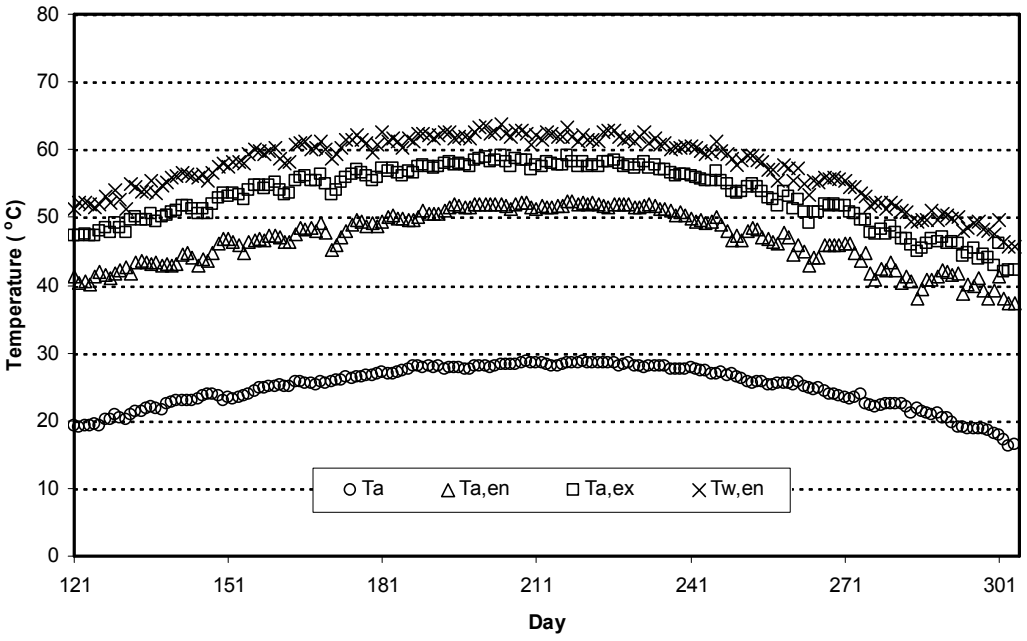

Figure 4.68. Variation of T_a, $T_{a,en}$, $T_{a,ex}$ and $T_{w,\,en}$ between 08:00-09:00 hours during summer season

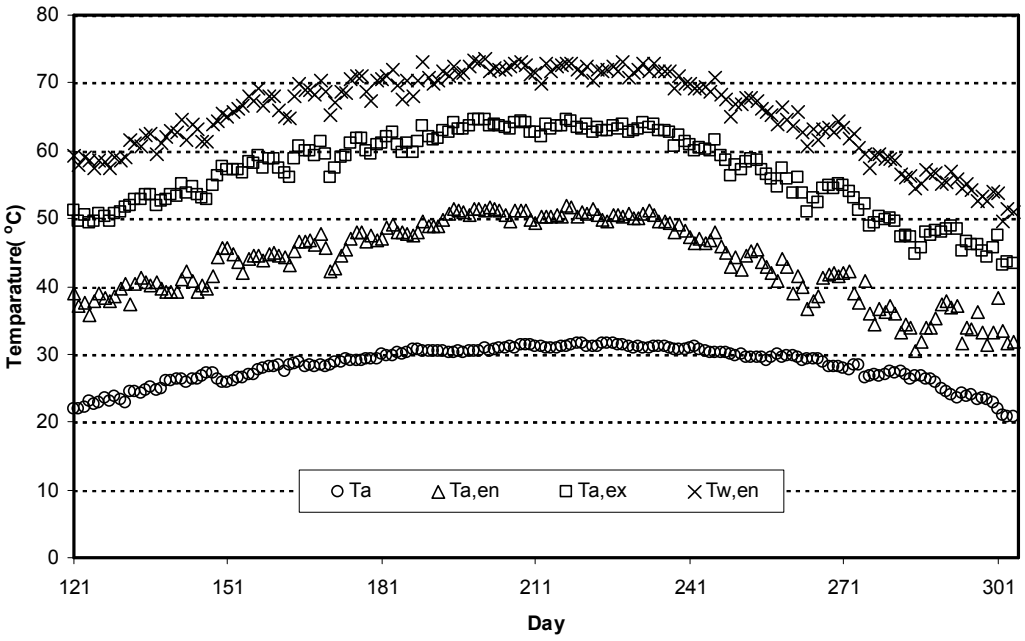

Figure 4.69. Variation of T_a, $T_{a,en}$, $T_{a,ex}$ and $T_{w,\,en}$ between 10:00-11:00 hours during summer season

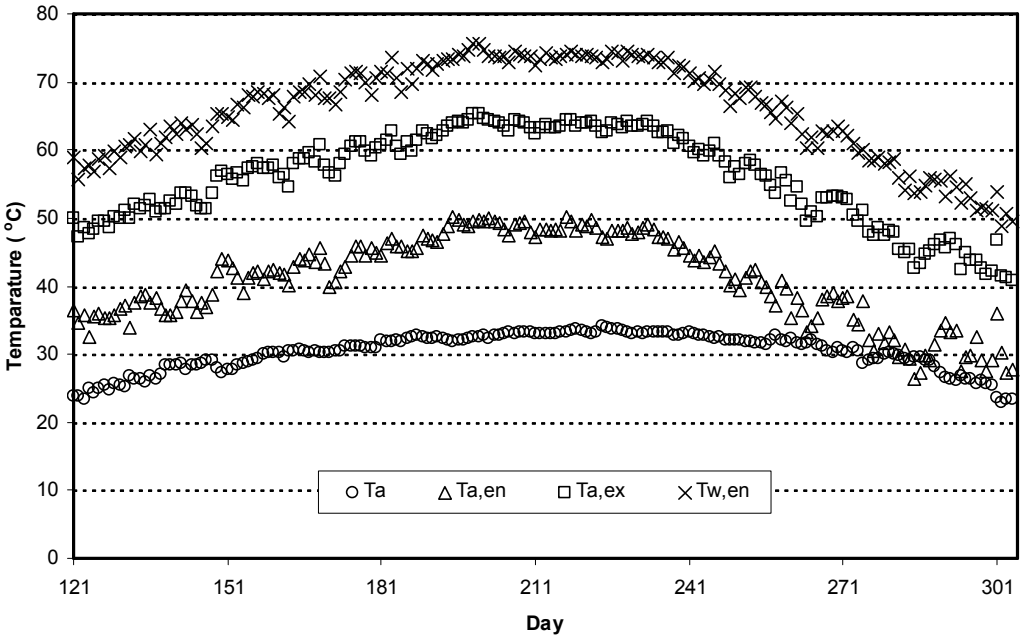

Figure 4.70. Variation of T_a, $T_{a,en}$, $T_{a,ex}$ and $T_{w,\,en}$ between 12:00-13:00 hours during summer season

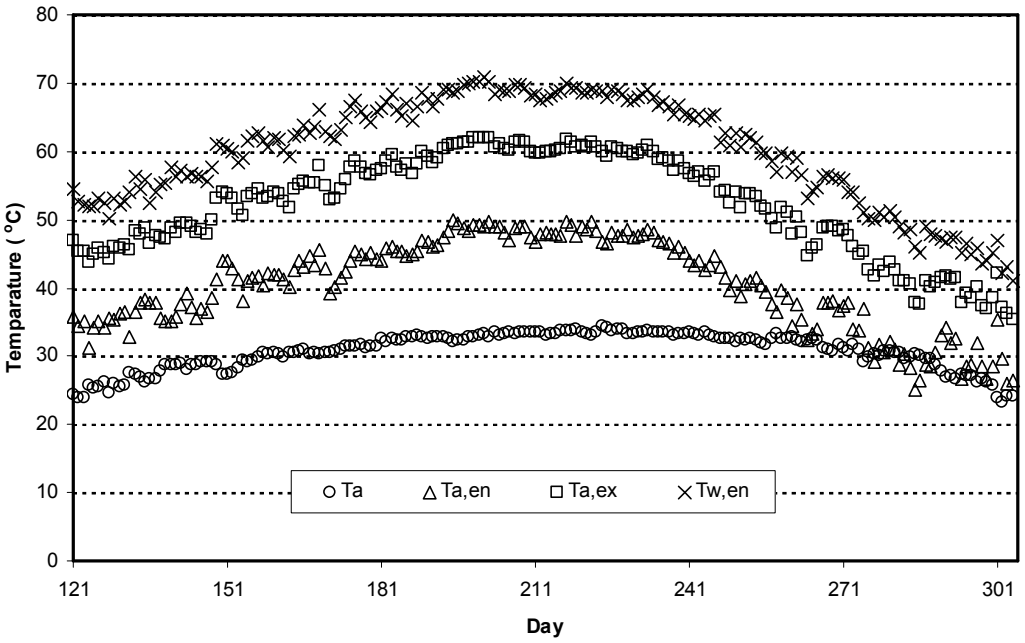

Figure 4.71. Variation of T_a, $T_{a,en}$, $T_{a,ex}$ and $T_{w,\,en}$ between 14:00-15:00 hours during summer season

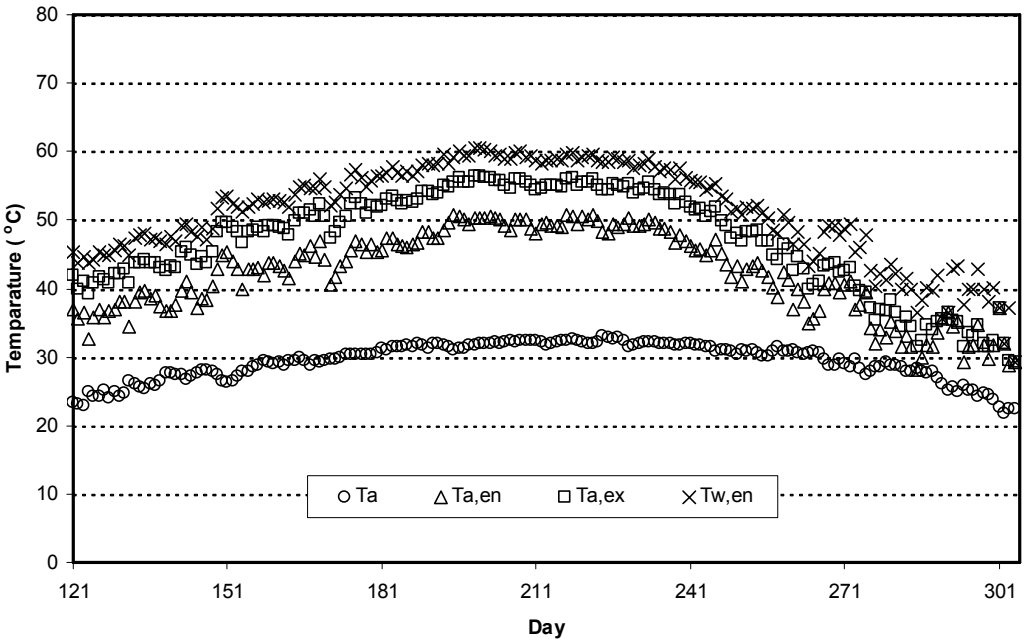

Figure 4.72. Variation of T_a, $T_{a,en}$, $T_{a,ex}$ and $T_{w,\,en}$ between 16:00-17:00 hours during summer season

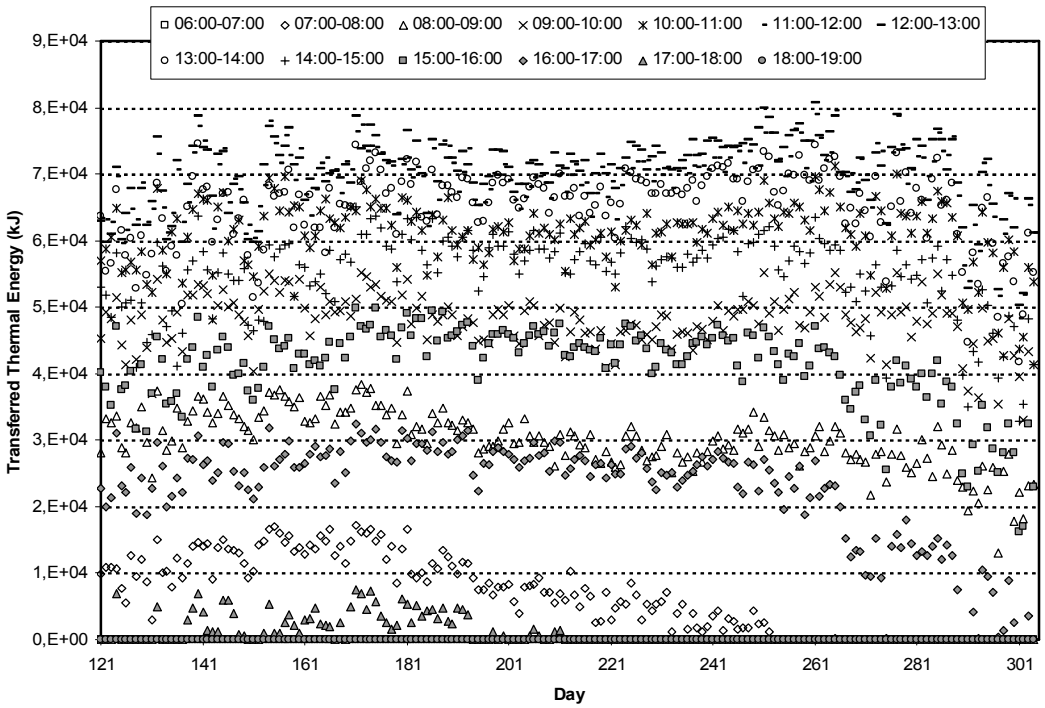

Figure 4.73. Variation of hourly thermal energy transferred to the regeneration air from solar energy during the summer season

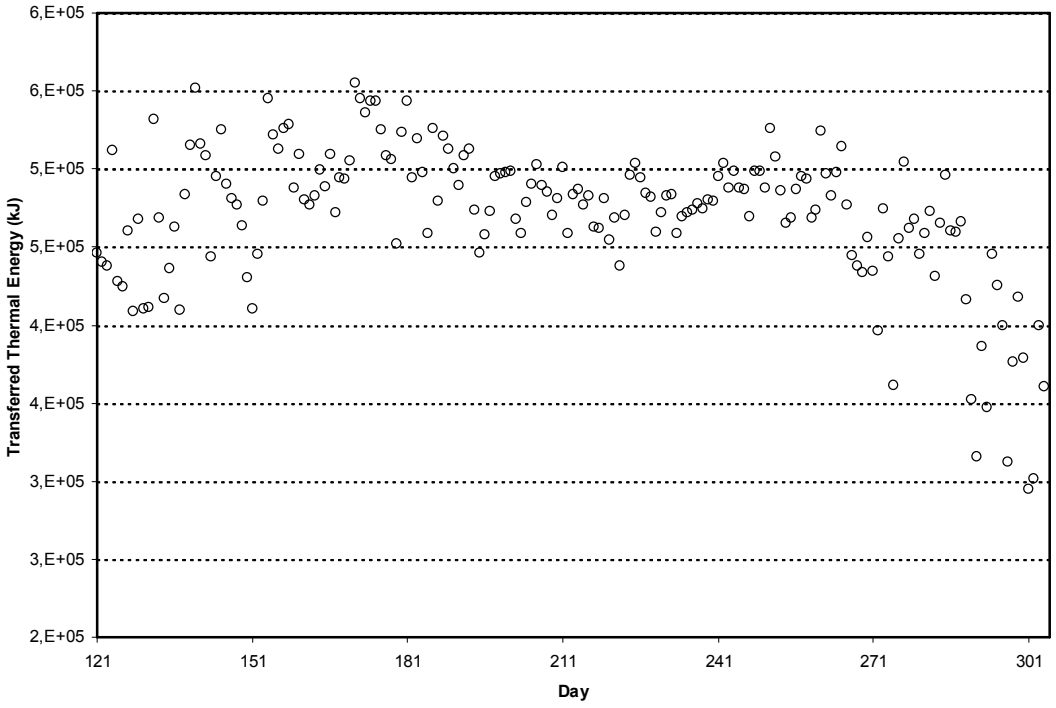

Figure 4.74. Variation of daily total thermal energy transferred to the regeneration air from solar energy during the summer season

The results obtained from all experiments (R/P=3/4, R/P=1) and the model were compared to determine the applicability of the solar energy in desiccant based air-conditioning system studied. The DMİ data that were measured during the day in which the experiments carried out was used in the calculations. Figure 4.75 shows effect of daily average ambient humidity ratio on daily total regeneration heat and daily (06:00-19:00) total thermal energy transfer from solar energy. As can be seen from the figure, the amount of daily total regeneration heat increases with the increase of ambient humidity ratio. However, daily total thermal energy transfer from solar energy does not change with ambient humidity ratio.

In the system, the ratio of daily total thermal energy transfer from solar energy to daily total regeneration heat (compensation ratio, CR) was calculated using Equation 4.9. Figure 4.76 shows variation of CR with daily average ambient humidity ratio. It is seen from the figure that CR is over 100% at low ambient humidity ratio values, and decreases with the increase of ambient humidity ratio. However even at the highest humidity ratio, it is possible to obtain about 40 percent of the regeneration air from the sun.

$$CR = \frac{Q_{reg,solar}}{Q_{reg}} \tag{4.9}$$

Comparison of coefficient of performance obtained from the experiments (COP_e) and the model (COP_m) is represented in Figure 4.77. The curve which was fitted (by using least square method) to the experimental and model COP data is also shown in Figure 4.77. As can be seen from figure, COP increases dramatically, if solar energy is used in the system. However it decreases with the increase of ambient humidity ratio. The equations of the curves (Eqn. 4.10-4.11) are given below:

$$COP_e=1.303-23.981* W_{a,da} \tag{4.10}$$

$$COP_m=5.328-228.68* * W_{a,da} \tag{4.11}$$

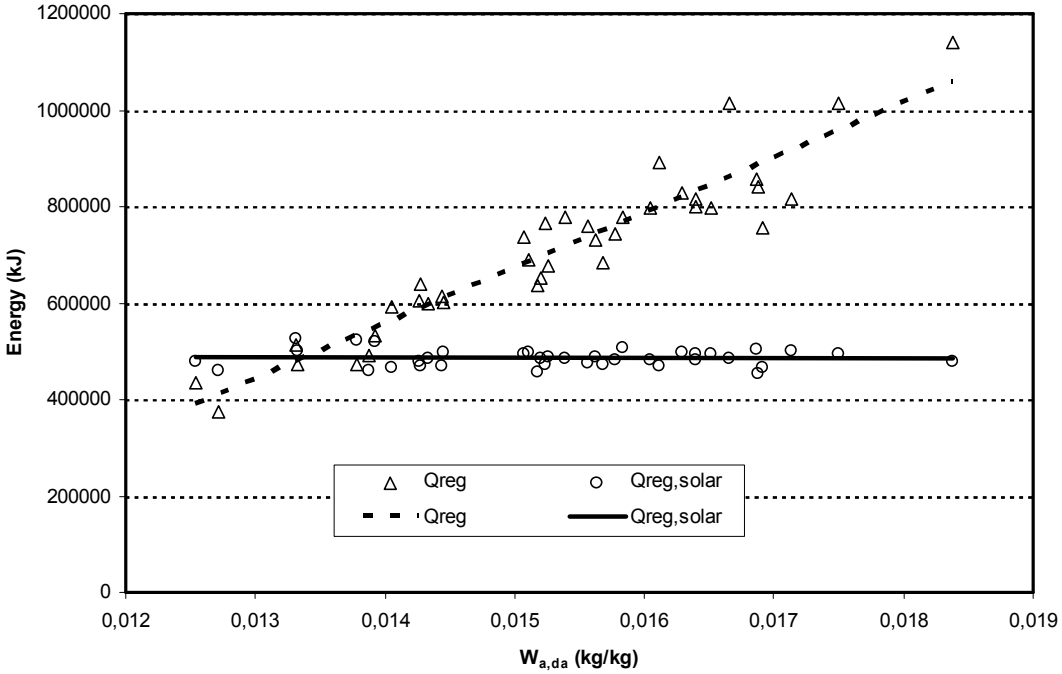

Figure 4.75. Effect of daily average ambient humidity ratio on daily total regeneration heat and daily (06:00-19:00) total thermal energy transfer due to solar energy

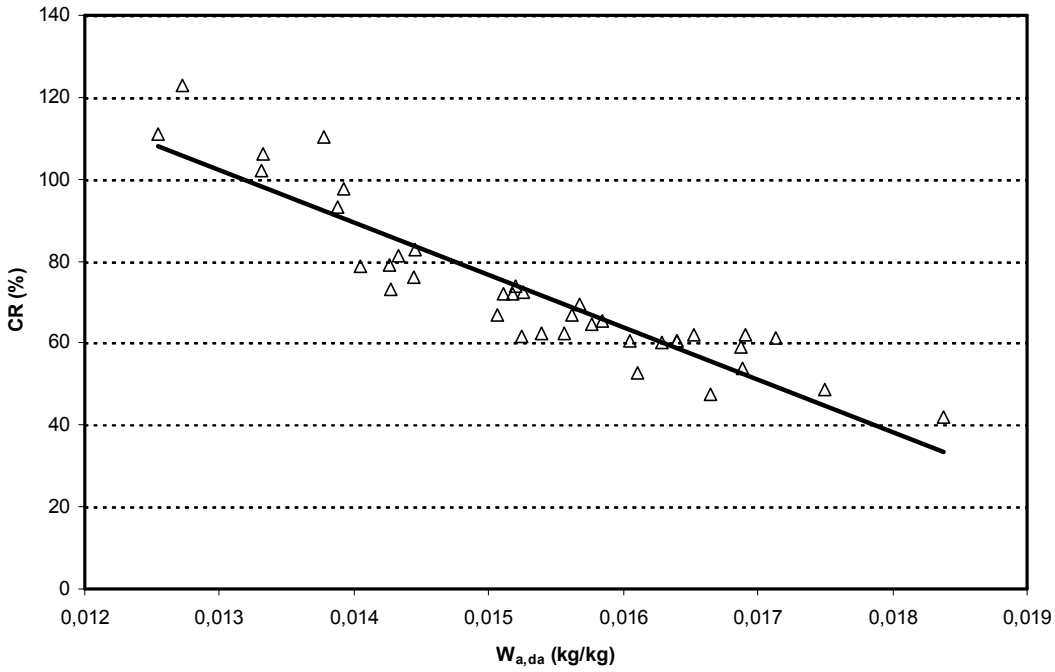

Figure 4.76. Variation of CR with daily average ambient humidity ratio

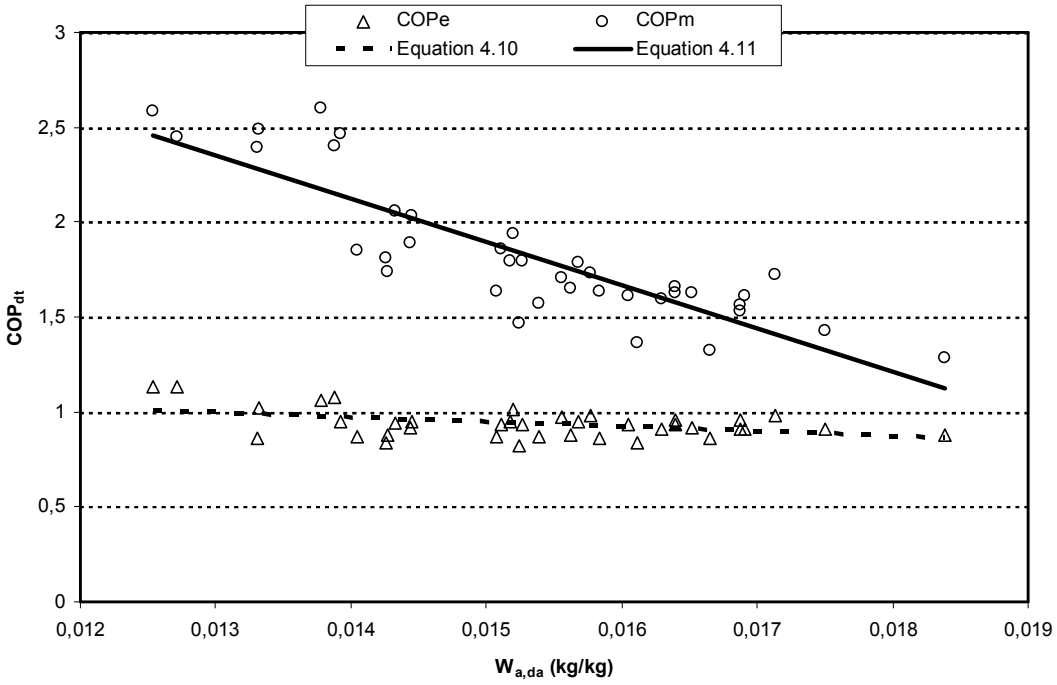

Figure 4.77. Comparison of coefficient of performance obtained from the experiments (COP_e) and the model (COP_m)

5. CONCLUSIONS AND RECOMMENDATIONS

5.1. Conclusions

In this study, a desiccant based air-conditioning system was designed, constructed and tested. The moisture of the fresh air was reduced passing it through a solid desiccant wheel and then its temperature was decreased by the "dry coil" of a vapor-compression cycle. To enhance the performance of the system, some technologies such as "pre-cooling with outdoor air", "waste cool recovery" and "pre-cooling of waste air with evaporative cooling" were utilized. Design parameters and suitability of the system suggested were investigated for the health care facilities in which hygiene is crucially important. It was aimed to increase the use of desiccant systems in Turkey in which this type of systems never used and not well known.

The most important component of the desiccant cooling system is the desiccant wheel. The performance data of the rotary desiccant wheel given by the manufacturers were evaluated in detail. It was found that F_d and F_r are functions of humidity ratio of the dehumidified (process) air and regeneration temperature. As a result, an equation that includes influence of both humidity ratio of outdoor air and regeneration temperature was obtained.

Performance of the system studied was analyzed using a computer program written. The climate data (dry bulb temperature and relative humidity) measured by The State Meteorological Affairs (DMİ) during 21 years for Adana, were used in the calculations. The analyses were made for 21st July and summer season. It was found that the amount of heat transferred in the heat exchanger 1, electric heater unit, and rotary regenerator at 07:00 and 21:00 hours is greater than at 14:00 h. If the daily period is considered, the amount of heat transfers in each heat exchanger at 07:00 h and 21:00 h are greater than at 14:00 h.

The results obtained from the experiments that were carried out with equal and different process and regeneration air flow rates were evaluated. It was found that there is no correlation between the ambient or regeneration temperature and daily average or daily total parameters (energy consumption, cooling effect, COP). It

was also seen that regeneration temperature set value has no considerable effect on daily average or daily total parameters. The main parameter that influences the performance of the system is ambient humidity (humidity ratio-relative humidity). Coefficient of performance of the system decreases with the increase of humidity. Daily total energy input to the system for the experiments with R/P=3/4 is higher, however daily total cooling capacity and daily average COP is lower than the experiments with R/P=1.

Applicability of the solar energy in desiccant based air- conditioning system studied was investigated. It was found that COP increases dramatically, if solar energy is used in the system.

5.2. Recommendations for Future Works

In the system studied, relative humidity of the air-conditioned room is adjusted by controlling the regeneration temperature with electric heaters. However regeneration temperature generally does not remain constant during the experiments according to the electric heaters start up and shut-down. Although the experiments are carried out at different regeneration temperature set values, they have no considerable effect on the daily total parameters (energy consumptions, cooling effect, COP) because of the automatic control strategy. To investigate the effect of regeneration temperature on the system, automatic control strategy can be changed in the future.

The desired blowing temperature of the fresh air is obtained in the cooling coil. In these types of systems, desired blowing temperature is generally obtained with evaporative coolers. Usage of evaporative cooler in the fresh air channel can be studied.

In the experiments two different mass flow rates were investigated. In the future, influence of different mass flow rates of regeneration air on the system can be investigated.

Although the increase in the regeneration air temperature due to solar energy assistance is calculated numerically using the model described above, effect of solar energy can be studied experimentally in the system.

During the past decade, there has been an increasing interest in using exergy as a potential analysis tool for design, analysis and performance evaluation of energy systems. Therefore exergy analysis can be applied to the desiccant cooling system in the future.

REFERENCES

AL-RABGHI OM, HITTLE DC., 2001. Energy simulation in buildings: overview and BLAST example. Energy Conversion & Management, Vol. 42, 1623–1635.

ANDO, K., KODAMA, A., HIROSE, T., GOTO, M., OKANO, H., 2005. Experimental study on a process design for adsorbtion desiccant cooling driven with a low-temperature heat. Adsorption, Vol. 11, pp. 631-636.

ARUNDEL, A.V., STERLING, E.M., BIGGING, J.H., STERLING, T.D., 1986. Indirect Health Effects of relative Humidity in indoor Environments, Env. Health Perspectives, Vol. 65, 351-361.

ASHRAE, 2000, Handbook of System and Equipment, American Society of Heating, Refrigerating and Air Conditioning Engineers, Inc, Atlanta, USA.

ASHRAE, 2001, Handbook of Fundamentals, American Society of Heating, Refrigerating and Air Conditioning Engineers, Inc, Atlanta, USA.

ASHRAE, 2003, Handbook of HVAC Applications, American Society of Heating, Refrigerating and Air Conditioning Engineers, Inc, Atlanta, USA.

BAYINDIRLIK ve İSKAN BAKANLIĞI, 1984. Güneşli Su Isıtıcıları. Teknik El Kitapları 3, Bayındırlık ve İskan Bakanlığı, Yapı işleri Genel Müdürlüğü.

BULUT, H., 2008, Adana İlinde Eğik Yüzeye Gelen Güneş Işınım Değerlerinin Belirlenmesi, Ç.Ü. Müh-Mim Fakültesi 30. yıl Sempozyumu, 556-561.

CEJUDO, J.M., MORENO, R., and CARRILLO, A., 2002. Physical and Neural Network Models of A Silica-Gel Desiccant Wheel, Energy and Building, Vol. 34, pp. 837-844.

CAMARGO, J.R., EBINUMA, C.D. and SILVEIRA, J.L., 2003. Thermoeconomic Analysis of An Evaporative Desiccant Air Conditioning System, Applied Thermal Engineering, Vol. 23, pp. 1537-1549.

CAMARGO, J.R., GODOY, E., EBINUMA, C.D.., 2005. An Evaporative and Desiccant Cooling System for Air Conditioning in Humid Climates, J. of the Braz. Soc. of Mech. Sci. & Eng., Vol. 17, pp. 243-247.

ÇARPINLIOĞLU, M.Ö. and YILDIRIM, M., 2005. A Methodology for The

Performance Evaluation of An Experimental Desiccant Cooling System, Int. Comm. in Heat and Mass Transfer, Vol. 32, pp. 1400-1410.

DAI, Y.J., WANG, R.Z. and XU, Y.X., 2002. Study of A Solar Powered Solid-Adsorption-Desiccant Cooling System Used for Grain Storage, Renewable Energy, Vol. 25, 417-430.

DAI, Y.J., WANG, R.Z., ZHANG, H.F. and YU, J.D., 2002. Use of Liquid Desiccant Cooling to Improve The Performance of Vapor Compression Air Conditioning, Applied Thermal Engineering, Vol. 21, pp. 1185-1202.

DAOU, K., WANG, R.Z., and XIA, Z.Z., 2004. Desiccant Cooling Air Conditioning: A Review, Renewable &Sustainable Energy Reviews, Vol. 10, pp. 1-23.

DCTRG (Desiccant Cooling Technology Resource Guide), 2000.

ELSAYED, SS., HAMAMOTO, Y., AKISAWA, A., KASHIWAGI, T., 2006. Analysis of an air cycle refrigerator driving air conditioning system integrated desiccant system, Int. Journal of Refrigeration, Vol. 29, pp. 219-228.

ELSAYED, S.S., MIYAZAKI, T., HAMAMOTO, Y., AKISAWA, A., KASHIWAGI, T., 2008. Performance analysis of air cycle refrigerator integrated desiccant system for cooling and dehumidifying warehouse, Int. J. Refrigeration, Vol. 31, pp. 189–196.

ENTERIA, N., YOSHINO, H., MOCHIDA, A., TAKAKI, R., SATAKE, A., YOSHIE, R., MITAMURA, T., BABA, S., 2009. Construction and initial operation of the combined solar thermal and electric desiccant cooling system. Solar Energy, Vol. 83, pp. 1300-1311.

ERNEST, L., MACFERRAN, FE., 1999. Equal area vs. Log-Tchebycheff, HPAC Engineering, pp. 25-31.

FERTELLİ, A., 2008, Air-conditioning system with ice thermal storage, PhD thesis, Çukurova University, Turkey.

GHADDAR, N., GHALI, K. and NAJM, A., 2003. Use of Desiccant Dehumidification to Improve Energy Utilization in Air-Conditioning System in Beirut, Int. Journal of Energy Research, Vol. 27, pp. 1317-1338.

GOOL, W.V., 1997. Energy Policy: Fairly Check Exact Spelling of Last Word, Tales

and Factualities, Dordrecht, Sayfa: 93-105.

GE, TS., DAİ, YJ., WANG, RZ., Lİ, Y., 2008. Experimental investigation on a one-rotor two-stage rotary desiccant cooling system. Energy, Vol. 33, pp. 1807-1815.

GE, T.S., LI, Y., WANG, R.Z. and DAI Y.J., 2009. Experimental Study on a Two-Stage Rotary Desiccant Cooling System, International Journal of Refrigeration, Vol. 32, pp. 498-508.

GE, T.S., ZIEGLER, F., WANG, R.Z. and WANG, H., 2010. Performance comparison between a solar driven rotary desiccant cooling system and conventional vapor compression system (performance study of desiccant cooling), Applied Thermal Engineering, Vol. 30, pp. 724-731.

HALLIDAY, S. P., BEGGS, C. B. and SLEIGH, P. A., 2002. The Use of Solar Desiccant Cooling in The UK: A Feasibility Study, Applied Thermal Engineering, Vol. 22, pp. 1327-1338.

HENNING, HM., 2007. Solar assisted air conditioning of buildings – an overview. Applied Thermal Engineering, Vol. 27, pp. 1734–1749.

HINES, AL., GHOSH, TK., LOYALKA, SK., WARDER, RC., 1992. Investigation of co-sorption of gases and vapors as a means to enhance indoor air quality-Phase 2: Removal of particulates and airborne micro-organisms by solid adsorbents and liquid desiccants. Report of Gas Research Institute, GRI-92/0157.5.

HIRUNLABH J., CHAROENWAT R., KHEDARI J. and TEEKASAP S., 2007. Feasibility Study of Desiccant Air-Conditioning System in Thailand, Building and Environment, Cilt 42, Sayfa: 572–577.

HOLMAN, JP., 1989, Experimental methods for engineers (5th edn.). McGraw Hill: New York, pp. 37-83.

JAIN, S., DHAR, PL., and KAUSHIK, SC., 1995. Evaluation of solid desiccant based evaporative cooling cycles for typical hot and humid climates. International Journal of Refrigeration , 18(5): 287-296.

JIA, C.X., DAI, Y.J., WU, J.Y., WANG, R.Z., 2006. Analysis on a hydric desiccant air-conditioning system, Applied Thermal Engineering, Vol. 26, pp. 2393-

2400.

JIA, C.X., DAI, Y.J., WU, J.Y., WANG, R.Z., 2007. Use of compound desiccant to develop high performance desiccant cooling system. Int. J. Refrig., Vol. 30, pp. 345-353.

JOUDI, KA., DHAIDAN, NS., 2001. Application of solar assisted heating and desiccant cooling systems for a domestic buildings, Energy Conversion & Management, Vol. 42, 995-1022.

KABEEL, A.E., 2007. Solar Powered Air Conditioning System Using Rotary Honeycomb Desiccant Wheel, Renewable Energy, 32/11,1842-1857.

KANOĞLU, M., ÇARPINLIOGLU, M.Ö. and YILDIRIM, M., 2004. Energy And Exergy Analyses of An Experimental Open-Cycle Desiccant Cooling System, Applied Thermal Engineering, Vol. 24, pp. 919-932.

KHALID, A., MAHMOOD, M., ASIF, M. ve MUNEER, T., 2009. Solar Assisted Pre-Cooled Hydrid Desiccant Cooling System for Pakistan, Renewable Energy, Cilt 34, Sayfa: 151-157.

KOVAK, B., 1997. Heimann, P.R., The Sanitizing Effects of Desiccant-Based Cooling, ASHRAE Journal, Vol. 39, pp. 60-64.

KREIDER J. F., VE RABL A., 1994. Heating and Cooling of Buildings, McGraw Hill.

LA, D., DAI, YJ., LI, Y., WANG, RZ., GE, TS., 2010, Technical development of rotary desiccant dehumidification and air conditioning: A review. Renewable and Sustainable Energy Reviews Vol. 14, pp. 130-147.

LIU, B.Y.H., JORDAN, R.C., 1961. Daily Insolation on Surfaces Tilted Towards the Equator, ASHRAE Journal, 3, 53-59.

LIU, B.Y.H., JORDAN, R.C., 1960. The Interrelationship and Characteristic Distribution of Direct, Diffuse and Total Solar Radiation, Solar Energy, 4, 1.

MAZZEI, P., MINICHIELLO, F., and PALMA, D., 2004. HVAC Dehumidification Systems for Thermal Comfort: A Critical Review, Applied Thermal Engineering, Vol. 25, pp. 677-707.

MINISTRY OF PUBLIC WORKS AND SETTLEMENTS, 1984, Güneşli Su Isıtıcıları. Teknik El Kitapları 3, Bayındırlık ve İskan Bakanlığı, Yapı işleri

Genel Müdürlüğü.

MMO, 2003. Hijyen İçin Alınacak Önlemler, http://www.mmoistanbul.org/yayin/cumartesisoylesileri/18/index.html.

NIA, FE., PAASSEN, DV., SAIDI, MH., 2006. Modeling and simulation of desiccant wheel for air conditioning. Energy and Buildings, Vol. 38(10), pp. 1230–1239.

NIU, J.L., ZHANG, L.Z. and ZUO, H.G., 2002. Energy Savings Potential of Chilled-Ceiling Combined With Desiccant Cooling in Hot and Humid Climates, Energy and Buildings, Vol. 24, pp. 487-495.

OLIVEIRA, A.C., AFONSO, C.F., RIFFAT, S.B. AND DOHERTY, P.S., 2000. Thermal Performance of A Novel Air Conditioning System Using A Liquid Desiccant, Applied Thermal Engineering, Vol. 20, pp. 1213-1223.

ORNL, 2000. Report on active Desiccant-Based Preconditioning Market Analysis and Product Development, ORNL/SUB/94-SV044/2.

PANARAS, G., MATHIOULAKIS, E., BELESSIOTIS, V., KYRIAKIS, N., 2010, Theoretical and experimental investigation of the performance of a desiccant air-conditioning system, Renewable Energy, Vol. 35, pp. 1368-1375.

PESARAN, A. A., PENNY, T. R. AND CZANDERNA, A. W., 1992. Desiccant cooling: state-of-the-art assessment, Technical Report No. NRE¸/TP-254-4147, National Renewable Energy Laboratory, Golden, CO.

PIETRUSCHKA, D., EICKER, U., HUBER, M. and SCHUMACHER, J., 2005. Experimental Performance Analysis and Modelling of Liquid Desiccant Cooling Systems for Air Conditioning in Residential Buildings, Int. Journal of Refrigeration, Vol. 29, pp. 1-15.

SUBRAMANYAM, N., MAIYA, M.P. and MURTHY, S.S., 2004. Application of Desiccant Wheel to Control Humidity in Air-Conditioning Systems, Applied Thermal Engineering, Vol. 24, pp. 2777-2788.

SUBRAMANYAM, N., MAIYA, M.P. and MURTHY, S.S., 2004. Parametric studies on a desiccant assisted air-conditioner, Applied Thermal Engineering, Vol. 24, pp. 2679-2689.

U.S. DEPARTMENT OF ENERGY (DOE), 2005. Advanced Desiccant Cooling and

Dehumidifcation Program, Desiccant Cooling and Dehumidification Bibliography, http://mfnl.xjtu.edu.cn /gov-doe-nrel/desiccantcool /bibliography2.html.

TR.NET WEBSITE, 2005. Hastane Enfeksiyonları ve Mrsa, Sağlık Bölümü, www.saglik.tr.net/genel_saglık_mrsa.shtml.

TURKISH INFECTION WEBSITE, 2005. Hastane İnfeksiyonları, http://www.infeksiyon.org/detail.Asp?Ctg=25&Article=390.

YILDIRIM, M., 2002, An experimental investigation on heat and mass transfer in a desiccant cooling system, PhD thesis, Gaziantep University, Turkey.

YILMAZ, A., BÜYÜKALACA, O., 1998. Nem Almalı (desisif) Soğutma Sistemleri, Tesisat Dergisi, Sayı 34, pp. 145-150.

YILMAZ T, ÖZGEREN M, GÜRÇINAR Y., 1995. Daily and yearly variation of humidity ratio. Proceedings of 10th National Thermal Science and Technique Conference, Ankara, Turkey.

YILMAZ T, BULUT H., 1996. Expression of daily and yearly variation of meteorological parameters with equations for Şanlıurfa. Proceedings of 4th National Congress on Cooling and Air-Conditioning Techniques, Adana, Turkey.

YUTONG, L., HONGXING, Y., 2008. Investigation on Solar Desiccant Dehumidification Process for Energy Conservation of Central Air-Conditioning Systems, Applied Thermal Engineering, Vol.28, Issue 10, Pages 1118-1126.

ZHANG, LZ., NIU, JL., 2003. A pre-cooling Munters environmental control desiccant cooling cycle in combination with chilled-ceiling panels, Energy, Vol. 28, pp. 275-292.

ZHANG, XJ., DAI, YJ., WANG, RZ., 2003. A simulation study of heat and mass transfer in a honeycombed rotary desiccant dehumidifier, Applied Thermal Engineering, Vol.23, pp. 989-1003.

ZHANG, XJ., SUMATHY, K., DAI, YJ., WANG, RZ., 2006. Dynamic hygroscopic effect of the composite material used in desiccant rotary wheel. Solar Energy, Vol. 80, pp. 1058-1061.

CURRICULUM VITAE

Ertaç HÜRDOĞAN was born in Cyprus, 1979. After being graduated from Kıbrıs Türk Maarif College, he enrolled in Mechanical Engineering Department of Çukurova University. He graduated from Çukurova University as a Mechanical Engineer in September 2000. He had obtained Master of Science degree from the Mechanical Engineer Department of Çukurova University in 2003. He had commenced the studies leading to the degree of Doctor of Philosophy in 2003 at the Department of Mechanical Engineering, Çukurova University. He has been working as a Research Assistant at the Mechanical Engineering Department of Çukurova University since 2002.

APPENDIX

APPENDIX-1. PREPARED COMPUTER PROGRAM FOR THE ANALYSES OF THE SYSTEM

```
C*****************************************************************
C****************** DESICCANT COOLING SYSTEM ***************
C********************** Version 5 (March 2007) ***********************
C*****************************************************************

C++++ Subroutine DW calculates properties of air stream ++++++++++++++++++++
C++++ when dry bulb and wet bulb temperatures of air are given +++++++++++++++

C++++ Subroutine DA calculates properties of air stream ++++++++++++++++++++
C++++ when dry bulb temperature and absolute humidity of air are given ++++++++

C++++ Subroutine WA calculates properties of air stream ++++++++++++++++++++
C++++ when wet bulb temperature and absolute humidity of air are given +++++++

C++++ Subroutine QD calculates properties of air stream ++++++++++++++++++++
C++++ when relative humidity and dry bulb temperature of air are known +++++++

      Program DesCool_5
      real mfresh1,mwaste8,mregen12,mregen14
      real mfresh3,mfresh4,mregen13,mregen17
      real mfresh5
      real nfan1,nfan3,nes1,nesj1,nes2,nesj2,ncona,ncon
      real nes5,nesj5

      write(*,*)
      write(*,*)'Enter air volume flow rate(m3/h)='
      read(*,*) Vfresh
      write(*,*)'Enter waste air volume flow rate(m3/h)='
      read(*,*) Vwaste
      write(*,*)'regenerate air volume flow rate(m3/h)='
      read(*,*) Vregen
      write(*,*)'Enter the regeneration temperature'
      read(*,*) tdb16

C########################## STATE 1 ################################

      write(*,*)'***************** State 1 ***************'
      write(*,*)'*****************************************'
      write(*,*)
      write(*,*)'Enter the dry bulb temperature in C:'
      read(*,*) tdb1
      write(*,*)'Enter the wet bulb temperature in C:'
      read(*,*) twb1

      call DW(tdb1,twb1,W1,tdp1,h1,Q1,d1,cp1)

      write(*,3)tdb1
      write(*,5)twb1
```

```
      write(*,7)W1
      write(*,9)tdp1
      write(*,11)h1
      write(*,13)Q1
      write(*,15)d1
      write(*,17)cp1
      write(*,*)
      read(*,*)

C########################## STATE 11 ################################

      write(*,*)'***************** State 11 ***************'
      write(*,*)'******************************************'
      write(*,*)'Properties of State 11 are equal to State 1'
      write(*,*)

      tdb11=tdb1
      twb11=twb1

      call DW(tdb11,twb11,W11,tdp11,h11,Q11,d11,cp11)

      write(*,3)tdb11
      write(*,5)twb11
      write(*,7)W11
      write(*,9)tdp11
      write(*,11)h11
      write(*,13)Q11
      write(*,15)d11
      write(*,17)cp11
      write(*,*)
      read(*,*)

C########################## STATE 2 ################################

      write(*,*)'***************** State 2 ***************'
      write(*,*)'******************************************'
      write(*,*)
      write(*,*)'Enter the power of Supply Fan in KW'
      read(*,*) Wfan
      write(*,*)'Enter the effectiveness of Supply Fan in %'
      read(*,*) nfan1

      TdbK1=tdb1+273.15
      Qgain=(1-(nfan1/100))*Wfan
      mfresh1=d1*(Vfresh/3600)

      TdbK2=(Qgain/cp1*mfresh1)+TdbK1
      tdb2=TdbK2-273.15

      W2=W1
      twbi=twb1

      call DA(tdb2,W2,twbi,twb2,tdp2,h2,Q2,d2,cp2)

      write(*,3)tdb2
```

```
      write(*,5)twb2
      write(*,7)W2
      write(*,9)tdp2
      write(*,11)h2
      write(*,13)Q2
      write(*,15)d2
      write(*,17)cp2
      write(*,*)
      read(*,*)

C########################## STATE 12 ################################

      write(*,*)'***************** State 12 ***************'
      write(*,*)'******************************************'
      write(*,*)
      write(*,*)'Enter the power of Regeneration Fan in KW;'
      read(*,*)Wfan3
      write(*,*)'Enter the effectiveness of Fan in %'
      read(*,*)nfan3

      TdbK11=tdb11+273.15
      Qgain3=(1-(nfan3/100))*Wfan3
      mregen11=d11*(Vregen/3600)

      TdbK12=(Qgain3/(cp11*mregen11))+TdbK11
      tdb12=TdbK12-273.15

      W12=W11
      twbi=twb11

      call DA(tdb12,W12,twbi,twb12,tdp12,h12,Q12,d12,cp12)

      write(*,3)tdb12
      write(*,5)twb12
      write(*,7)W12
      write(*,9)tdp12
      write(*,11)h12
      write(*,13)Q12
      write(*,15)d12
      write(*,17)cp12
      write(*,*)
      read(*,*)

C########################## STATE 7 ################################

      write(*,*)'***************** State 7 ***************'
      write(*,*)'******************************************'
      write(*,*)
      write(*,*)'Enter dry bulb temperature in air conditioned room'
      read(*,*)tdb7
      write(*,*)'Enter relative humidity in air conditioned room'
      read(*,*)Q7A

      Q7=Q7A/100
      twbi=twb2
```

```
      call QD(Q7,tdb7,W7,twbi,twb7,tdp7,h7,d7,cp7)

      write(*,3)tdb7
      write(*,5)twb7
      write(*,7)W7
      write(*,9)tdp7
      write(*,11)h7
      write(*,13)Q7
      write(*,15)d7
      write(*,17)cp7
      write(*,*)
      read(*,*)

C############################ STATE 6 ################################

      write(*,*)'***************** State 6 ***************'
      write(*,*)'****************************************'
      write(*,*)
      write(*,*)'Enter the sensible heat ratio in %'
      read(*,*) DIO
      write(*,*)'Enter the blowing temperature in C'
      read(*,*) tdb6

      W6=W7-((1.006/2531.7)*(tdb7-tdb6)*(1/(DIO-1)))
      twbi=twb5

      call DA(tdb6,W6,twbi,twb6,tdp6,h6,Q6,d6,cp6)

      write(*,3)tdb6
      write(*,5)twb6
      write(*,7)W6
      write(*,9)tdp6
      write(*,11)h6
      write(*,13)Q6
      write(*,15)d6
      write(*,17)cp6
      write(*,*)
      read(*,*)

C############################ STATE 3a ################################

      write(*,*)'***************** State 3a ***************'
      write(*,*)'****************************************'
      write(*,*)'*** Assuming dehumidification process is **'
      write(*,*)'*** at constant wet bulb temperature ******'
      write(*,*)

      W3a=W6
      twb3a=twb2

      call AW(W3a,twb3a,tdb3a,tdp3a,h3a,Q3a,d3a,cp3a)

      write(*,3)tdb3a
      write(*,5)twb3a
      write(*,7)W3a
```

```
      write(*,9)tdp3a
      write(*,11)h3a
      write(*,13)Q3a
      write(*,15)d3a
      write(*,17)cp3a
      write(*,*)
      read(*,*)

C############################ STATE 3 ###################################

      write(*,*)'***************** State 3 *****************'
      write(*,*)'******************************************'
      write(*,*)'******* Actual dehumidification process ***'
      write(*,*)

      W3=W6
      TdbK16=tdb16+273.15
      F1=(5.82*((W2*1000)**(-0.507))*(tdb16**0.652))
      F=F1/100

      twbi=twb2

      TdbK3a=tdb3a+273.15
      TdbK3=((F*TdbK2)-TdbK3a)/(F-1)
      tdb3=TdbK3-273.15

      call DA(tdb3,W3,twbi,twb3,tdp3,h3,Q3,d3,cp3)

      write(*,3)tdb3
      write(*,5)twb3
      write(*,7)W3
      write(*,9)tdp3
      write(*,11)h3
      write(*,13)Q3
      write(*,15)d3
      write(*,17)cp3
      write(*,*)
      read(*,*)

C############################ STATE 4 ###################################

      write(*,*)'***************** State 4 *****************'
      write(*,*)'******************************************'
      write(*,*)
      write(*,*)'Enter the effectiveness  of heat exchanger 1 in %'
      read(*,*) nes1
      nesj1=nes1/100

      W4=W3
      mregen12=(Vregen/3600)*d12
      mfresh3=(Vfresh/3600)*d3
      C1=cp3*mfresh3
      C2=cp12*mregen12
      TdbK3=273.15+tdb3
```

```
      if(C1.LT.C2) then
      TdbK4=TdbK3-nesj1*(C1/C2)*(TdbK3-TdbK12)
      else
      TdbK4=TdbK3-nesj1*(C2/C1)*(TdbK3-TdbK12)
      endif

      tdb4=TdbK4-273.15
      twbi=twb3

      call DA(tdb4,W4,twbi,twb4,tdp4,h4,Q4,d4,cp4)

      write(*,3)tdb4
      write(*,5)twb4
      write(*,7)W4
      write(*,9)tdp4
      write(*,11)h4
      write(*,13)Q4
      write(*,15)d4
      write(*,17)cp4
      write(*,*)
      read(*,*)

C########################## STATE 8 ################################

      write(*,*)'***************** State 8 ***************'
      write(*,*)'****************************************'
      write(*,*)
      write(*,*)'Enter the effectiveness of humidifier in %'
      read(*,*)ncona
      ncon=ncona/100

      h8=h7
      twb8=twb7
      TdbK7=tdb7+273.15
      TwbK7=twb7+273.15

      TdbK8=TdbK7-ncon*(TdbK7-TwbK7)
      tdb8=TdbK8-273.15

      call DW(tdb8,twb8,W8,tdp8,Q8,d8,cp8)

      write(*,3)tdb8
      write(*,5)twb8
      write(*,7)W8
      write(*,9)tdp8
      write(*,11)h8
      write(*,13)Q8
      write(*,15)d8
      write(*,17)cp8
      write(*,*)
      read(*,*)

C########################## STATE 5 ################################

      write(*,*)'***************** State 5 ***************'
```

```
write(*,*)'****************************************'
write(*,*)
write(*,*)'Enter the effectiveness of heat exchanger 2 in %'
read(*,*) nes2
nesj2=nes2/100
W5=W4
TdbK5=TdbK4-nesj2*(TdbK4-TdbK8)
tdb5=TdbK5-273.15

twbi=twb4

call DA(tdb5,W5,twbi,twb5,tdp5,h5,Q5,d5,cp5)

write(*,3)tdb5
write(*,5)twb5
write(*,7)W5
write(*,9)tdp5
write(*,11)h5
write(*,13)Q5
write(*,15)d5
write(*,17)cp5
write(*,*)
read(*,*)

C############################ STATE 9 ###################################

write(*,*)'**************** State 9 ***************'
write(*,*)'****************************************'
write(*,*)

W9=W8
mfresh4=d4*(Vfresh/3600)
mwaste8=d8*(Vwaste/3600)
C1a=mwaste8*cp8
C2a=mfresh4*cp4

if(C1a.LT.C2a) then
TdbK9=TdbK8-nesj2*(C1a/C2a)*(TdbK8-TdbK4)
else
TdbK9=TdbK8-nesj2*(C2a/C1a)*(TdbK8-TdbK4)
endif

tdb9=TdbK9-273.15
twbi=twb8

call DA(tdb9,W9,twbi,twb9,tdp9,h9,Q9,d9,cp9)

write(*,3)tdb9
write(*,5)twb9
write(*,7)W9
write(*,9)tdp9
write(*,11)h9
write(*,13)Q9
write(*,15)d9
write(*,17)cp9
```

```
      write(*,*)
      read(*,*)

C############################ STATE 13 ################################

      write(*,*)'***************** State 13 ***************'
      write(*,*)'******************************************'
      write(*,*)

      W13=W12
      mfresh3=d3*(Vfresh/3600)
      mregen12=d12*(Vregen/3600)
      C1b=mfresh3*cp3
      C2b=mregen12*cp12

      if(C1b.LT.C2b) then
      TdbK13=TdbK12-nesj1*(C1b/C2b)*(TdbK12-TdbK3)
      else
      TdbK13=TdbK12-nesj1*(C2b/C1b)*(TdbK12-TdbK3)
      endif

      tdb13=TdbK13-273.15
      twbi=twb12

      call DA(tdb13,W13,twbi,twb13,tdp13,h13,Q13,d13,cp13)

      write(*,3)tdb13
      write(*,5)twb13
      write(*,7)W13
      write(*,9)tdp13
      write(*,11)h13
      write(*,13)Q13
      write(*,15)d13
      write(*,17)cp13
      write(*,*)
      read(*,*)

C############################ STATE 16 ################################

      write(*,*)'***************** State 16 ***************'
      write(*,*)'******************************************'
      write(*,*)

      W16=W12
      TdbK16=tdb16+273.15
      twbi=twb12

      call DA(tdb16,W16,twbi,twb16,tdp16,h16,Q16,d16,cp16)

      write(*,3)tdb16
      write(*,5)twb16
      write(*,7)W16
      write(*,9)tdp16
      write(*,11)h16
      write(*,13)Q16
```

```
      write(*,15)d16
      write(*,17)cp16
      write(*,*)
      read(*,*)

C########################## STATE 17a ##############################

      write(*,*)'***************** State 17a ***************'
      write(*,*)'*********************************************'
      write(*,*)'*** Assuming reactivation process is *******'
      write(*,*)'*** at constant wet bulb temperature *******'
      write(*,*)

      TdbK3a=tdb3a+273.15
      TP=TdbK3a-TdbK2
      TdbK17a=TdbK16-TP
      tdb17a=TdbK17a-273.15
      twb17a=twb16

      call DW(tdb17a,twb17a,W17a,tdp17a,h17a,Q17a,d17a,cp17a)

      write(*,3)tdb17a
      write(*,5)twb17a
      write(*,7)W17a
      write(*,9)tdp17a
      write(*,11)h17a
      write(*,13)Q17a
      write(*,15)d17a
      write(*,17)cp17a
      write(*,*)
      read(*,*)

C########################## STATE 17 ##############################

      write(*,*)'***************** State 17 *********************'
      write(*,*)'************************************************'
      write(*,*)'*** Actual dehumidification process ************'
      write(*,*)

      W17=W17a
      TdbK17=((F*TdbK16)-TdbK17a)/(F-1)
      tdb17=TdbK17-273.15
      twbi=twb16

      call DA(tdb17,W17,twbi,twb17,tdp17,h17,Q17,d17,cp17)

      write(*,3)tdb17
      write(*,5)twb17
      write(*,7)W17
      write(*,9)tdp17
      write(*,11)h17
      write(*,13)Q17
      write(*,15)d17
      write(*,17)cp17
      write(*,*)
```

```
      read(*,*)

C########################## STATE 14 ################################
      write(*,*)'***************** State 14 ***************'
      write(*,*)'******************************************'
      write(*,*)
      write(*,*)'Enter the effectiveness of heat exchanger 5 in %'
      read(*,*) nes5
      nesj5=nes5/100
      W14=W13
      mregen13=d13*(Vregen/3600)
      mregen17=d17*(Vregen/3600)
      C1d=mregen13*cp13
      C2d=mregen17*cp17

      if(C1d.LT.C2d) then
      TdbK14=TdbK13-nesj5*(C1d/C2d)*(TdbK13-TdbK17)
      else
      TdbK14=TdbK13-nesj5*(C2d/C1d)*(TdbK13-TdbK17)
      endif

      tdb14=TdbK14-273.15
      write(*,*) tdb14
      twbi=twb13

      call DA(tdb14,W14,twbi,twb14,tdp14,h14,Q14,d14,cp14)

      write(*,3)tdb14
      write(*,5)twb14
      write(*,7)W14
      write(*,9)tdp14
      write(*,11)h14
      write(*,13)Q14
      write(*,15)d14
      write(*,17)cp14
      write(*,*)
      read(*,*)

C########################## STATE 18 ################################
      write(*,*)'***************** State 18 ***************'
      write(*,*)'******************************************'
      write(*,*)

      W18=W17
      mregen13=d13*(Vregen/3600)
      mregen17=d17*(Vregen/3600)
      C1c=mregen13*cp13
      C2c=mregen17*cp17

      if(C1c.LT.C2c) then
        TdbK18=TdbK17-nesj5*(C1c/C2c)*(TdbK17-TdbK13)
      else
        TdbK18=TdbK17-nesj5*(C2c/C1c)*(TdbK17-TdbK13)
      endif
```

```
      tdb18=TdbK18-273.15
      twbi=twb17

      call DA(tdb18,W18,twbi,twb18,tdp18,h18,Q18,d18,cp18)

      write(*,3)tdb18
      write(*,5)twb18
      write(*,7)W18
      write(*,9)tdp18
      write(*,11)h18
      write(*,13)Q18
      write(*,15)d18
      write(*,17)cp18
      write(*,*)
      read(*,*)

C######### Calculation of Heat Requirement for Process 14-16 #######

      write(*,*)'*********************************************'
      write(*,*)'*** Calculation of Heat For Process 14-16 ***'
      write(*,*)'*********************************************'

      mregen14=d14*(Vregen/3600)
      write(*,*) mregen14
      Qneed=mregen14*(h16-h14)

      write(*,19) Qneed
      read(*,*)

C######### Calculation of Heat Requirement for Process 5-6 #########

      write(*,*)'************************************************'
      write(*,*)'*** Calculation of Heat For Process 5-6 *********'
      write(*,*)'************************************************'

      mfresh5=d5*(Vfresh/3600)
      write(*,*) mfresh5
      Qnd=mfresh5*(h5-h6)

      write(*,19) Qnd
      read(*,*)

3     format(7x,'dry bulb temperature(C)  :',F9.4)
5     format(7x,'wet bulb temperature(C)  :',F9.4)
7     format(7x,'absolute humidity(kg/kg) :',F9.4)
9     format(7x,'dew point temperature(C) :',F9.4)
11    format(7x,'enthalpy(kj)             :',F9.4)
13    format(7x,'relative humidity(%)     :',F9.4)
15    format(7x,'density(kg/m3)           :',F9.4)
17    format(7x,'specific heat(kj/kg.K)   :',F9.4)
19    format(7x,'heat (kw)                              :',F9.4)

      End
```

```
C####################### SUBROUTINES ################################

      Subroutine DW(tdb,twb,W,tdp,h,Q,d,cp)

      real,parameter::PATM=101.325
      real,parameter::C8=-5800.2206
      real,parameter::C9=-5.516256
      real,parameter::C10=-0.048640239
      real,parameter::C11=0.000041764768
      real,parameter::C12=-0.000000014452093
      real,parameter::C13=6.5459673
      real,parameter::C14=6.54
      real,parameter::C15=14.526
      real,parameter::C16=0.7389
      real,parameter::C17=0.09486
      real,parameter::C18=0.4569

      TdbK=tdb+273.15
      TwbK=twb+273.15

      Pwsu1=((C8/TwbK)+C9+(C10*TwbK)+C11*(TwbK**2))
      Pwsu2=((C12*TwbK**3)+(C13*ALOG(TwbK)))
      Pwsu=EXP(Pwsu1+Pwsu2)
      Wsu=0.62198*(Pwsu/(PATM-Pwsu))
      W=((2501-2.381*twb)*Wsu-(tdb-twb))/(2501+1.805*tdb-4.186*twb)
      Pw=(PATM*W)/(0.62198+W)
      Z=ALOG(Pw)
      tdp=C14+C15*Z+C16*(Z**2)+C17*(Z**3)+C18*(Pw**0.1984)
      h=1.006*tdb+W*(2501+(1.805*tdb))
      Pws1=((C8/TdbK)+C9+(C10*TdbK)+C11*(TdbK**2))
      Pws2=(C12*(TdbK**3)+(C13*ALOG(TdbK)))
      Pws=EXP(Pws1+Pws2)
      Q=(Pw/Pws)*100
      d=(348.1*(PATM/(273+tdb)))/100
      cp=1.005+0.006*(TdbK/100)**1.73

      return
      end

C#####################################################################

      Subroutine DA(tdb,W,twbi,twb,tdp,h,Q,d,cp)

      real,parameter::PATM=101.325
      real,parameter::C8=-5800.2206
      real,parameter::C9=-5.516256
      real,parameter::C10=-0.048640239
      real,parameter::C11=0.000041764768
      real,parameter::C12=-0.000000014452093
      real,parameter::C13=6.5459673
      real,parameter::C14=6.54
      real,parameter::C15=14.526
      real,parameter::C16=0.7389
      real,parameter::C17=0.09486
      real,parameter::C18=0.4569
```

```
      twb=twbi
      TwbK=273.15+twb
      itr=0
20    continue
      itr=itr+1
      TwbK=twb+273.15
      Pwsu1=(C8/TwbK)+(C9+C10*TwbK)+(C11*(TwbK**2))
      Pwsu2=(C12*TwbK**3)+(C13*ALOG(TwbK))
      Pwsu=EXP(Pwsu1+Pwsu2)
      Wsu=0.62198*(Pwsu/(PATM-Pwsu))
      twby=(tdb+W*(2501+1.805*tdb)-2501*Wsu)/(4.186*W-2.381*Wsu+1)
      bhx=abs((twby-twb)/twby)
      if (bhx.LT.1E-4) GOTO 30
      twb=(0.9*twb+0.1*twby)
      if (itr>100) go to 30
      goto 20
30    continue

      twb=twby
      TdbK=tdb+273.15
      Pw=(PATM*W)/(0.62198+W)
      Z=ALOG(Pw)
      tdp=C14+C15*Z+C16*(Z**2)+C17*(Z**3)+C18*(Pw**0.1984)
      h=1.006*tdb+W*(2501+(1.805*tdb))
      Pws1=((C8/TdbK)+C9+(C10*TdbK)+C11*(TdbK**2))
      Pws2=(C12*(TdbK**3)+(C13*ALOG(TdbK)))
      Pws=EXP(Pws1+Pws2)
      Q=(Pw/Pws)*100
      d=(348.1*(PATM/(273+tdb)))/100
      cp=1.005+0.006*(TdbK/100)**1.73

      return
      end

C#####################################################################

      Subroutine AW(Wa,twba,tdba,tdpa,ha,Qa,da,cpa)

      real,parameter::PATM=101.325
      real,parameter::C8=-5800.2206
      real,parameter::C9=-5.516256
      real,parameter::C10=-0.048640239
      real,parameter::C11=0.000041764768
      real,parameter::C12=-0.000000014452093
      real,parameter::C13=6.5459673
      real,parameter::C14=6.54
      real,parameter::C15=14.526
      real,parameter::C16=0.7389
      real,parameter::C17=0.09486
      real,parameter::C18=0.4569

      TwbKa=twba+273.15
```

```
      Pwsu1=(C8/TwbKa)+(C9+C10*TwbKa)+(C11*TwbKa**2)
      Pwsu2=(C12*TwbKa**3)+(C13*ALOG(TwbKa))
      Pwsu=EXP(Pwsu1+Pwsu2)
      Wsua=0.62198*(Pwsu/(PATM-Pwsu))
      A=(Wsua*(2501-2.381*twba)+twba*(1+4.186*Wa)-2501*Wa)
      B=(1+1.805*Wa)
      tdba=A/B
      Pw=(PATM*Wa)/(0.62198+Wa)
      Z=ALOG(Pw)
      tdpa=C14+C15*Z+C16*(Z**2)+C17*(Z**3)+C18*(Pw**0.1984)
      ha=1.006*tdba+Wa*(2501+(1.805*tdba))
      TdbKa=tdba+273.15
      Pws1=((C8/TdbKa)+C9+(C10*TdbKa)+C11*(TdbKa**2))
      Pws2=(C12*(TdbKa**3)+(C13*ALOG(TdbKa)))
      Pws=EXP(Pws1+Pws2)
      Qa=(Pw/Pws)*100
      da=(348.1*(PATM/(273+tdba)))/100
      cpa=1.005+0.006*(TdbKa/100)**1.73

      return
      end

C#####################################################################

      Subroutine QD(Q,tdb,W,twbi,twb,tdp,h,d,cp)

      real,parameter::PATM=101.325
      real,parameter::C8=-5800.2206
      real,parameter::C9=-5.516256
      real,parameter::C10=-0.048640239
      real,parameter::C11=0.000041764768
      real,parameter::C12=-0.000000014452093
      real,parameter::C13=6.5459673
      real,parameter::C14=6.54
      real,parameter::C15=14.526
      real,parameter::C16=0.7389
      real,parameter::C17=0.09486
      real,parameter::C18=0.4569

      TdbK=tdb+273.15

      Pws1=((C8/TdbK)+C9+(C10*TdbK)+C11*(TdbK**2))
      Pws2=(C12*(TdbK**3)+(C13*ALOG(TdbK)))
      Pws=EXP(Pws1+Pws2)
      W=(Q*Pws*0.62198)/(PATM-(Q*Pws))
      h=1.006*tdb+W*(2501+(1.805*tdb))
      Pw=(PATM*W)/(0.62198+W)
      Z=ALOG(Pw)
      tdp=C14+C15*Z+C16*(Z**2)+C17*(Z**3)+C18*(Pw**0.1984)
      twb=twbi
      TwbK=273.15+twb

      itr=0
110   continue
      itr=itr+1
```

```
      TwbK=twb+273.15
      Pwsu1=((C8/TwbK)+C9+(C10*TwbK)+(C11*(TwbK**2)))
      Pwsu2=(C12*(TwbK**3)+(C13*(ALOG(TwbK))))
      Pwsu=EXP(Pwsu1+Pwsu2)
      Wsu=0.62198*(Pwsu/(PATM-Pwsu))
      A7=(tdb+W*(2501+1.805*tdb)-2501*Wsu)
      B7=(4.186*W-2.381*Wsu+1)
      twby=A7/B7
      bhxd=abs((twby-twb)/twby)
      if (bhxd.LT.1E-4) GOTO 120
      twb=(0.9*twb+0.1*twby)
      if (itr>100) go to 120
      goto 110
120   continue

      twb=twby
      d=(348.1*(PATM/(273+tdb)))/100
      cp=1.005+0.006*(TdbK/100)**1.73

      return
      end
```

APPENDIX-2. UNCERTAINTY CALCULATION PROCEDURE

The total uncertainty in the measurement of the volumetric flow rate of the air by using a pitot tube and the uncertainty arising in calculating the mass flow rate of this solution are given in the following. Besides this, the uncertainties in the other measured and calculated parameters are determined in a similar fashion.

The total uncertainty in the measurement of the volumetric flow rate $w_{\dot{V}}$ may be calculated as follows (Holman, McGraw Hill, 1989):

$$w_{\dot{V}} = (w^2_{sen} + w^2_{das} + w^2_{sl} + w^2_{td})^{1/2} \quad (A.1)$$

where w_{sen} is the uncertainty in the sensor reading (%),w_{das} is the uncertainty associated with the data acquisition system (%), w_{sl} is the uncertainty associated with the system leakages (%) and w_{td} uncertainty associated with the temperature differences (density differences) (%).

$$w_{\dot{V}} = (1^2 + 0.1^2 + 2.5^2 + 1^2)^{1/2} = 2.88\ \%$$

The uncertainties arising in calculating a result (w_R) due to several independent variables is given in Holman, McGraw Hill, 1989 as

$$w_R = \left[\left(\frac{\partial R}{\partial x_1} w_1 \right)^2 + \left(\frac{\partial R}{\partial x_2} w_2 \right)^2 + \ldots + \left(\frac{\partial R}{\partial x_n} w_n \right)^2 \right]^{1/2} \quad (A.2)$$

where the result R is a given function of the independent variables x_1; x_2; . . . ; x_n and w_1;w_2; . . . ;w_n are the uncertainties in the independent variables.

The uncertainty in calculating the mass flow rate $w_{\dot{m}}$ may be found as follows:

$$\dot{m} = \rho \dot{V}$$

$$w_{\dot{m}} = \left[\left(\frac{\partial \dot{m}}{\partial \rho} \right)^2 w_{\rho} + \left(\frac{\partial \dot{m}}{\partial \dot{V}} \right)^2 w_{\dot{V}} \right]^{1/2}$$

$$\left(\frac{\partial \dot{m}}{\partial \rho} \right) = \dot{V} \, , \left(\frac{\partial \dot{m}}{\partial \dot{V}} \right) = \rho$$

After algebraic manipulation we obtain:

$$\frac{w_{\dot{m}}}{\dot{m}} = \left[\left(\frac{w_{\rho}}{\rho} \right)^2 + \left(\frac{w_{\dot{V}}}{\dot{V}} \right)^2 \right]^{1/2}$$

Taking into account an uncertainty value of ±0.20% in the thermophysical properties and inserting the numerical values of uncertainty yields

$$\frac{w_{\dot{m}}}{\dot{m}} = \left[(0.2)^2 + (2.88)^2 \right]^{1/2} = 2.89 \, \%$$

APPENDIX-3. PREPARED COMPUTER PROGRAM FOR SOLAR ENERGY ANALYSES

```
C     ***********DEFINITIONS OF VARIABLES USED IN THE PROGRAM***********
C
C     DTA    : The difference between ambient temperature and inlet air temperature of the heat
C              exchanger (°C)
C     DTW    : The difference between the water temperature at the entrance and exit of the heat
C              exchanger (°C)
C     EHE    : Efficiency of heat exchanger
C     IGUN   : Day of year
C     F      : Total surface area of the collectors  (m2)
C     MA     : Mass flow rate of air (kg/s)
C     A,B,C  : Coefficient of 2nd degree equation used for collector efficiency
C     TA     : Ambient temperature (C) (DMİ data)
C     RA     : Ambient relative humidity (%) (DMİ data)
C     QS     : Total solar radiation  (W/m2) (DMİ data)
C     TM     : Mean water temperature at the entrance and exit of the collector (°C)
C     TAG    : Air temperature at the entrance of the heat exchanger (°C)
C     TAC    : Air temperature at the exit of the heat exchanger (°C)
C     TWG    : Water temperature at the entrance of the heat exchanger (°C)
C     TWC    : Water temperature at the exit of the heat exchanger (°C)
C     TWGY   : Water temperature at the entrance of the heat exchanger (C) (Last calculated value)
C     EC     : Efficiency of collector
C     QC     : The amount of heat transferred at the collectors  (W) (QC=QA=QW)
C     QA     : The amount of heat transferred at the heat exchanger (W)(air side)
C     QW     : The amount of heat transferred at the heat exchanger (W) (water side)
C     MW     : Mass flow rate of water (kg/s)
C     CA     : Air capacitance rate (W/kgC)(cp*m)
C     CW     : Water capacitance rate (W/kgC)(cp*m)
C     CMIN   : Minimum of the capacitance rates
C     QMAX   : The maximum possible heat transfer rate (W)
C     BH     : Relative error
C
C     ************************************************************************

      PROGRAM SOLAR ENERGY
      REAL MW,MA

      DIMENSION TAD(214),RAD (214),QSD(214)

      OPEN(1, FILE='ADANA SIC-NEM-ISINIM 18-19.txt', status='old')
      OPEN(2, FILE='SONUC-EZINC 18-19.txt', status='unknown')

      DTW=5.0
      EHE=0.6
      F=50.0
      MA=1.3
      A=-11.235
      B=-3.4165
      C=0.728
      IGUN=120
      DO 10 I=1,184
```

```
      READ(1,*)TAD(I),RAD(I),QSD(I)
10    CONTINUE

      WRITE(2,*)'IGUN  TA  RA  QS  TAG  TAC  TWG
     &  TWC  EC  QW'

      I=0
40    I=I+1

      TA=TAD(I)
      RA=RAD(I)
      QS=QSD(I)

      IGUN=IGUN+1

      TAG=TA+(-0.0129*RA**2+2.1143*RA-62.091)
      TWC=TAG
      TWG=TWC+DTW

      IF (QS.EQ.0) THEN
      EC=0
      BH=0

      GOTO 70
      ELSE
      GOTO 20
      ENDIF

20    TM=TWG-DTW/2

      X=(TM-TA)/QS

      EC=A*X**2+B*X+C

      QC=EC*F*QS

      QW=QC
      QA=QC

      MW=QW/(4180*DTW)

      TAC=QA/(MA*1005)+TAG

      CA=1005*MA
      CW=4180*MW

      IF (CA.LT.CW) THEN
      CMIN=CA
      ELSE
      CMIN=CW
      ENDIF

      QMAX=QA/EHE

      TWGY=QMAX/CMIN+TAG
```

```
        TWC=TWGY-DTW

        BH=ABS(TWGY-TWG)

70      IF (BH.LT.0.01) THEN

        IF (EC.LE.0) THEN
        TAC=TAG
        TWC=TAG
        TWGY=TAG
        EC=0
        QW=0
        ELSE
        GOTO 60
        ENDIF

60      WRITE(2,30)IGUN,TA,RA,QS,TAG,TAC,TWGY,TWC,EC,QW

30      FORMAT(I5,X,9(F6.2,2X))

        IF (I.EQ.184) GO TO 50
        GO TO 40

        ELSE

        TWG=TWGY
        GO TO 20

        ENDIF

50      CONTINUE

        STOP
        END
```